

Electronic Supporting Information

Molecular hydrides of divalent ytterbium supported by a macrocyclic ligand: synthesis, structure and olefin hydrofunctionalization catalysis

*Danny Schuhknecht, Khai-Nghi Truong, Thomas P. Spaniol, Laurent Maron and Jun Okuda**

1. Table of Contents

1.	Table of Contents.....	S2
2.	General Remarks	S5
3.	Synthetic Procedures	S6
3.1.	Synthesis of [Yb(SiPh ₃) ₂ (thf) ₄] (1)	S6
3.2.	¹ H, ¹³ C{ ¹ H} and ²⁹ Si{ ¹ H} HMBC NMR spectra of [Yb(SiPh ₃) ₂ (thf) ₄] (1).....	S7
3.3.	Synthesis of [(Me ₄ TACD)Yb(SiPh ₃) ₂] (2)	S9
3.4.	¹ H, ¹³ C{ ¹ H} and ²⁹ Si{ ¹ H} NMR spectra of [(Me ₄ TACD)Yb(SiPh ₃) ₂] (2)	S10
3.5.	VT NMR spectra of [(Me ₄ TACD)Yb(SiPh ₃) ₂] (2)	S11
3.6.	Molecular Structure of [(Me ₄ TACD)Yb(SiPh ₃) ₂] (2)	S11
3.7.	Synthesis of [(Me ₄ TACD) ₂ Yb ₂ (μ ₂ -H) ₃][SiPh ₃] (3)	S12
3.8.	¹ H, ¹³ C{ ¹ H} and ¹⁷¹ Yb NMR spectra of [(Me ₄ TACD) ₂ Yb ₂ (μ ₂ -H) ₃][SiPh ₃] (3)	S13
3.9.	Synthesis of [Yb(CH ₂ Ph) ₂] (4)	S15
3.10.	¹ H, ¹³ C{ ¹ H} and ¹⁷¹ Yb{ ¹ H} NMR spectra of [Yb(CH ₂ Ph) ₂] (4).....	S16
3.11.	IR spectrum of [Yb(CH ₂ Ph) ₂] (4).....	S17
3.12.	Synthesis of [(Me ₄ TACD)Yb(CH ₂ Ph) ₂] (5)	S18
3.13.	IR spectrum of [(Me ₄ TACD)Yb(CH ₂ Ph) ₂] (5)	S19
3.14.	Synthesis of [(Me ₄ TACD)Yb(η ⁶ -PhCH ₂)][B(C ₆ H ₃ -3,5-Me ₂) ₄] (6)	S20
3.15.	¹ H, ¹³ C{ ¹ H} and ¹¹ B{ ¹ H} NMR spectra of [(Me ₄ TACD)Yb(η ⁶ -PhCH ₂)][B(C ₆ H ₃ -3,5-Me ₂) ₄] (6)	S21
3.16.	IR Spectrum of [(Me ₄ TACD)Yb(η ⁶ -PhCH ₂)][B(C ₆ H ₃ -3,5-Me ₂) ₄] (6)	S23
3.17.	UV-Vis spectrum of [(Me ₄ TACD)Yb(η ⁶ -PhCH ₂)][B(C ₆ H ₃ -3,5-Me ₂) ₄] (6).	S23

3.18.	Synthesis of $[(\text{Me}_4\text{TACD})_2\text{Yb}_2(\mu_2\text{-H})_2(\text{thf})][\text{B}(\text{C}_6\text{H}_3\text{-3,5-Me}_2)_4]_2 \bullet 2.5\text{THF}$ (7).....	S24
3.19.	^1H , ^2H , $^{13}\text{C}\{\text{H}\}$ and $^{11}\text{B}\{\text{H}\}$ NMR spectra of $[(\text{Me}_4\text{TACD})_2\text{Yb}_2(\mu_2\text{-H})_2(\text{thf})][\text{B}(\text{C}_6\text{H}_3\text{-3,5-Me}_2)_4]_2 \bullet 2.5\text{THF}$ (7).....	S25
3.20.	UV-Vis spectrum of $[(\text{Me}_4\text{TACD})_2\text{Yb}_2(\mu_2\text{-H})_2(\text{thf})][\text{B}(\text{C}_6\text{H}_3\text{-3,5-Me}_2)_4]_2 \bullet 2.5\text{THF}$ (7).....	S27
3.21.	Kinetic studies on hydrogenolysis/deuterogenolysis of $[(\text{Me}_4\text{TACD})\text{Yb}(\eta^6\text{-PhCH}_2)][\text{B}(\text{C}_6\text{H}_3\text{-3,5-Me}_2)_4]$ (6)	S28
3.22.	IR Spectrum of $[(\text{Me}_4\text{TACD})_2\text{Yb}_2(\mu_2\text{-H})_2(\text{thf})][\text{B}(\text{C}_6\text{H}_3\text{-3,5-Me}_2)_4]_2 \bullet 2.5\text{THF}$ (7) ...	S29
3.23.	IR Spectrum of $[(\text{Me}_4\text{TACD})_2\text{Yb}_2(\mu_2\text{-D})_2(\text{thf})][\text{B}(\text{C}_6\text{H}_3\text{-3,5-Me}_2)_4]_2 \bullet 2.5\text{THF}$ ([D ₂]- 7).....	S29
3.24.	Synthesis of $[(\text{Me}_4\text{TACD})_2\text{Yb}_2(\mu_2\text{-H})_3][\text{B}(\text{C}_6\text{H}_3\text{-3,5-Me}_2)_4] \bullet \text{THF}$ (8)	S30
3.25.	^1H , ^2H , $^{13}\text{C}\{\text{H}\}$ and $^{11}\text{B}\{\text{H}\}$ NMR spectra of $[(\text{Me}_4\text{TACD})_2\text{Yb}_2(\mu_2\text{-H})_3][\text{B}(\text{C}_6\text{H}_3\text{-3,5-Me}_2)_4] \bullet \text{THF}$ (8)	S31
3.26.	UV-Vis Spectrum of $[(\text{Me}_4\text{TACD})_2\text{Yb}_2(\mu_2\text{-H})_3][\text{B}(\text{C}_6\text{H}_3\text{-3,5-Me}_2)_4] \bullet \text{THF}$ (8).....	S34
3.27.	IR Spectrum of $[(\text{Me}_4\text{TACD})_2\text{Yb}_2(\mu_2\text{-H})_3][\text{B}(\text{C}_6\text{H}_3\text{-3,5-Me}_2)_4] \bullet \text{THF}$ (8).	S35
3.28.	IR Spectrum of $[(\text{Me}_4\text{TACD})_2\text{Yb}_2(\mu_2\text{-D})_3][\text{B}(\text{C}_6\text{H}_3\text{-3,5-Me}_2)_4] \bullet \text{THF}$ ([D ₃]- 8).....	S35
3.29.	Synthesis of $[(\text{Me}_4\text{TACD})\text{Yb}(\text{thf})_2][\text{B}(\text{C}_6\text{H}_3\text{-3,5-Me}_2)_4]_2$ (9)	S36
3.30.	^1H , $^{13}\text{C}\{\text{H}\}$ and $^{11}\text{B}\{\text{H}\}$ NMR spectra of $[(\text{Me}_4\text{TACD})\text{Yb}(\text{thf})_2][\text{B}(\text{C}_6\text{H}_3\text{-3,5-Me}_2)_4]_2$ (9)	S37
3.31.	UV-Vis Spectrum of $[(\text{Me}_4\text{TACD})\text{Yb}(\text{thf})_2][\text{B}(\text{C}_6\text{H}_3\text{-3,5-Me}_2)_4]_2$ (9)	S38
3.32.	Deuterolysis of $[(\text{Me}_4\text{TACD})_2\text{Yb}_2(\mu_2\text{-H})_2(\text{thf})][\text{B}(\text{C}_6\text{H}_3\text{-3,5-Me}_2)_4]_2 \bullet 2.5\text{THF}$ (7)....	S39
3.33.	Deuterolysis of $[(\text{Me}_4\text{TACD})_2\text{Yb}_2(\mu_2\text{-H})_3][\text{B}(\text{C}_6\text{H}_3\text{-3,5-Me}_2)_4] \bullet \text{THF}$ (8)	S39
3.34.	Scrambling of 7 with $[(\text{Me}_4\text{TACD})_2\text{Ca}_2(\mu_2\text{-H})_2(\text{thf})_x][\text{B}(\text{C}_6\text{H}_3\text{-3,5-Me}_2)_4]_2$	S40
3.35.	Scrambling of 8 with $[(\text{Me}_4\text{TACD})_2\text{Ca}_2(\mu_2\text{-H})_3(\text{thf})_x][\text{B}(\text{C}_6\text{H}_3\text{-3,5-Me}_2)_4]$	S41
4.	Catalysis.....	S43

4.1.	Typical NMR spectra of catalytic hydrosilylation	S44
5.	X-Ray Crystallography	S46
6.	Computational Details	S47
7.	References.....	S57

2. General Remarks

All operations were performed under an inert atmosphere of dry argon using standard Schlenk line or glovebox techniques. $[D_8]THF$ was distilled under argon from sodium/benzophenone ketyl prior to use. THF and *n*-pentane were purified using a MB SPS-800 solvent purification system. Hydrogen (99.999%) and deuterium (99.8%) were purchased from Praxair-Westfalen AG. 1H , 2H , $^{11}B\{^1H\}$, $^{13}C\{^1H\}$, $^{29}Si\{^1H\}$, and ^{171}Yb NMR spectra were recorded on a *Bruker Avance II 400* or a *Bruker Avance III HD 400* spectrometer at 25 °C in J. Young-type NMR tubes. Chemical shifts for 1H , 2H and $^{13}C\{^1H\}$ spectra were referenced internally using the residual solvent resonance and are reported relative to tetramethylsilane. $^{11}B\{^1H\}$, $^{29}Si\{^1H\}$ and ^{171}Yb were referenced externally to $BF_3(OEt_2)$, tetramethylsilane and $[Yb(\eta^5-C_5Me_5)_2(thf)_2]^{S1}$, respectively. The resonances in the 1H and $^{13}C\{^1H\}$ NMR spectra were assigned on the basis of two-dimensional NMR experiments (COSY, HSQC, HMBC). Elemental analyses were performed on an *Elementar vario EL* instrument. In several instances, the results were not satisfactory, possibly due to incomplete combustion. IR spectra were measured as KBr pellets using an *Nicolet AVATAR 360* FT-IR spectrometer. Abbreviations for IR spectra were used as follows: w (weak), m (medium), s (strong). UV-Vis measurements were performed on an *Agilent Technologies Cary 60* UV-Vis spectrophotometer. GC-MS spectra were recorded on a *Shimadzu GCMS-QP2010 Plus* instrument. Helium was used as the carrier gas at 58 kPa. The column used was an *FS-Supreme-5ms* with 30 m length. The method used was as follows: initial oven temperature 60 °C; initial hold time 2 min; rate 10 °C/min; final oven temperature 250 °C; final time 5 min. $[KSiPh_3(thf)]^{S2}$ $[KCH_2Ph]^{S3}$ $[YbI_2(thf)_3]^{S4}$ 1,4,7,10-tetramethyl-1,4,7,10-tetraazacyclododecane (Me_4TACD)^{S5} and $[NEt_3H][B(C_6H_3-3,5-Me_2)_4]^{S6}$ were prepared according to literature procedures.

3. Synthetic Procedures

3.1. Synthesis of $[\text{Yb}(\text{SiPh}_3)_2(\text{thf})_4]$ (**1**)

Method A

To a stirred suspension of Ybl_3 (111 mg, 0.2 mmol) in THF (2 mL) was added dropwise at room temperature a solution of $[\text{KSiPh}_3(\text{thf})]$ (222 mg, 0.6 mmol) in THF (3 mL). After stirring for 4 h, the precipitate was filtered off and the orange solution was concentrated to 3 mL. The resulting suspension was filtered again, layered with *n*-pentane (3 mL) and stored at –30 °C. The resulting orange solid was recrystallized twice from THF/ *n*-pentane. The crystals were washed with *n*-pentane (3 x 2 mL) and dried under reduced pressure to give $[\text{Yb}(\text{SiPh}_3)_2(\text{thf})_4]$ (**1**) as orange microcrystals (33 mg, 34 µmol); yield: 17%.

Method B

To a stirred suspension of $[\text{Ybl}_2(\text{thf})_3]$ (1.55 g, 2.40 mmol) in THF (10 mL) was added dropwise at room temperature a solution of $[\text{KSiPh}_3(\text{thf})]$ (1.78 g, 4.80 mmol) in THF (10 mL). After stirring for 2 h, the precipitate was filtered off and the deep red solution was concentrated under reduced pressure to 5 mL. The solution was layered with *n*-pentane (5 mL) and stored at –30 °C. After 16 h, orange microcrystals formed. The supernatant was decanted off, the crystals were washed with *n*-pentane (3 x 2 mL) and dried under reduced pressure to give $[\text{Yb}(\text{SiPh}_3)_2(\text{thf})_4]$ (**1**) as orange microcrystals (1.65 g, 1.68 mmol); yield: 70%.

^1H NMR (400 MHz, $[\text{D}_8]\text{THF}$, 25 °C): δ = 1.75 – 1.80 (m, 16 H, THF), 3.60 – 3.64 (m, 16 H, THF), 6.98 – 6.93 (m, 6 H, *para*-Ph), 7.06 – 7.00 (m, 12 H, *meta*-Ph), 7.41 – 7.36 (m, 12 H, *ortho*-Ph) ppm.

$^{13}\text{C}\{\text{H}\}$ NMR (101 MHz, $[\text{D}_8]\text{THF}$, 25 °C): δ = 26.44 (THF), 68.30 (THF), 125.51 (*para*-Ph), 127.32 (*meta*-Ph), 137.11 (*ortho*-Ph), 154.10 (*ipso*-Ph) ppm.

$^{29}\text{Si}\{\text{H}\}$ NMR (80 MHz, $[\text{D}_8]\text{THF}$, 25 °C): δ = 4 ppm.

Anal. calc. for $\text{C}_{52}\text{H}_{62}\text{O}_4\text{Si}_2\text{Yb}$ (980.29 g mol^{–1}): C, 63.71; H, 6.38. Found: C, 63.41; H, 6.36%.

3.2. ^1H , $^{13}\text{C}\{^1\text{H}\}$ and $^{29}\text{Si}\{^1\text{H}\}$ HMBC NMR spectra of $[\text{Yb}(\text{SiPh}_3)_2(\text{thf})_4]$ (**1**)

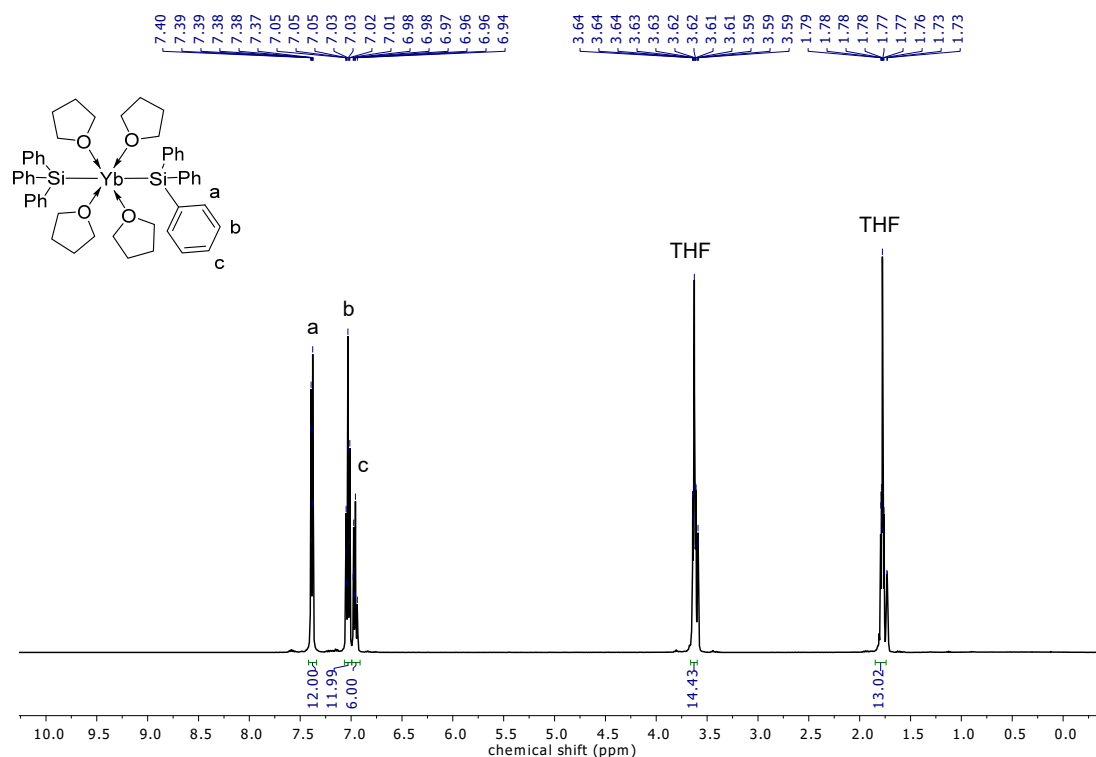


Fig. S1. ^1H NMR spectrum (400 MHz, $[\text{D}_8]\text{THF}$, 25 °C) of $[\text{Yb}(\text{SiPh}_3)_2(\text{thf})_4]$ (**1**).

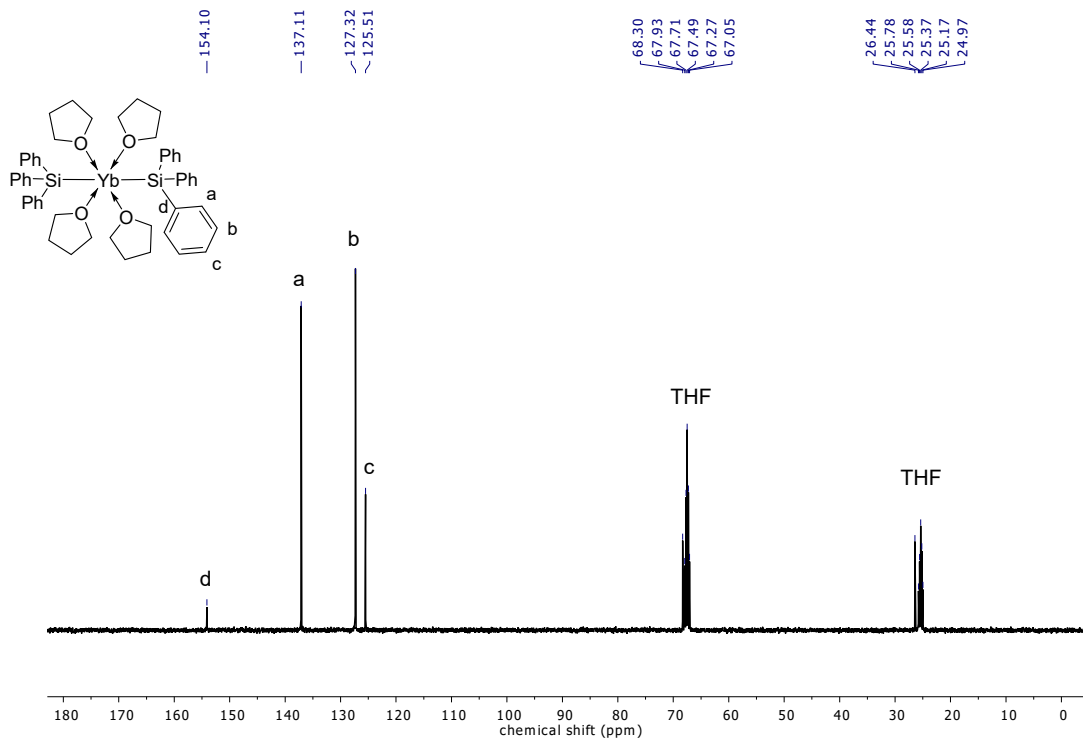


Fig. S2. $^{13}\text{C}\{^1\text{H}\}$ NMR spectrum (101 MHz, $[\text{D}_8]\text{THF}$, 25 °C) of $[\text{Yb}(\text{SiPh}_3)_2(\text{thf})_4]$ (**1**).

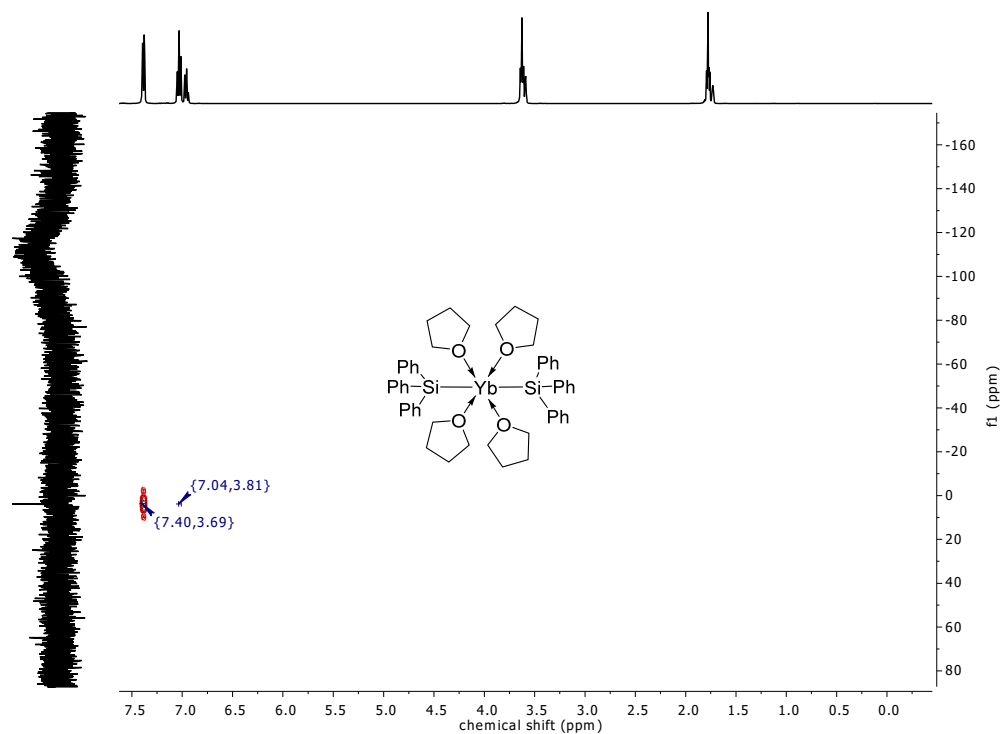


Fig. S3. $^{29}\text{Si}\{\text{H}\}$ HMBC NMR spectrum (80 MHz, $[\text{D}_8]\text{THF}$, 25 °C) of $[\text{Yb}(\text{SiPh}_3)_2(\text{thf})_4]$ (**1**).

3.3. Synthesis of [(Me₄TACD)Yb(SiPh₃)₂] (**2**)

To a stirred solution of [Yb(SiPh₃)₂(thf)₄] (**1**) (100 mg, 0.1 mmol) in THF (2 mL) was added dropwise at room temperature Me₄TACD (23 mg, 0.1 mmol). After 5 min, the solution was layered with *n*-pentane (2 mL) and stored at -30 °C. Orange microcrystals grew after 16 h. The solvent was decanted off, the crystals were washed with *n*-pentane (3 x 2 mL) and dried under reduced pressure to give [(Me₄TACD)Yb(SiPh₃)₂] (**2**) as red microcrystals (85 mg, 93 µmol); yield: 93%.

Single crystals of **2** were grown from a concentrated THF solution at -30°C.

¹H NMR (400.13 MHz, [D₈]THF, 25 °C): δ = 2.18 (s, 6 H, NCH_{3,free}), 2.31 – 2.34 (br, 4 H, NCH_{2,coord.}), 2.46 (s, 6 H, NCH_{3,coord.}), 2.50 (s, NCH_{2,free}), 6.79 – 7.08 (m, 18 H, *para-/meta*-Ph), 7.33 – 7.43 (m, 12 H, *ortho*-Ph) ppm.

¹³C{¹H} NMR (101 MHz, [D₈]THF, 25 °C): δ = 44.60 (NCH₃), 45.77 (NCH₃), 55.05 (br, NCH₂), 56.67 (NCH₂), 125.29 (*para*-Ph), 127.20 (*meta*-Ph), 137.54 (*ortho*-Ph), 154.24 (*ipso*-Ph) ppm.

Anal. calc. for C₄₈H₅₈N₄Si₂Yb (920.24 g mol⁻¹): C, 62.65; H, 6.35; N, 6.09. Found: C, 62.51; H, 6.47; N, 6.48%.

3.4. ^1H , $^{13}\text{C}\{^1\text{H}\}$ and $^{29}\text{Si}\{^1\text{H}\}$ NMR spectra of $[(\text{Me}_4\text{TACD})\text{Yb}(\text{SiPh}_3)_2]$ (**2**)

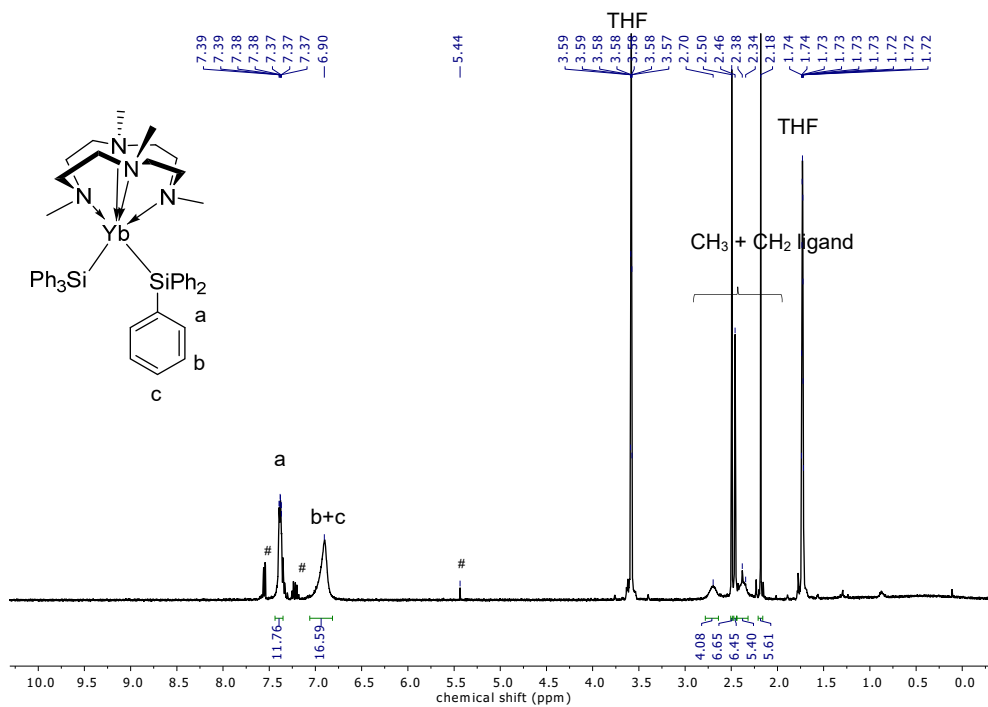


Fig. S4. ^1H NMR spectrum (400 MHz, $[\text{D}_8]\text{THF}$, 25 °C) of $[(\text{Me}_4\text{TACD})\text{Yb}(\text{SiPh}_3)_2]$ (**2**) (# = decomposition products).

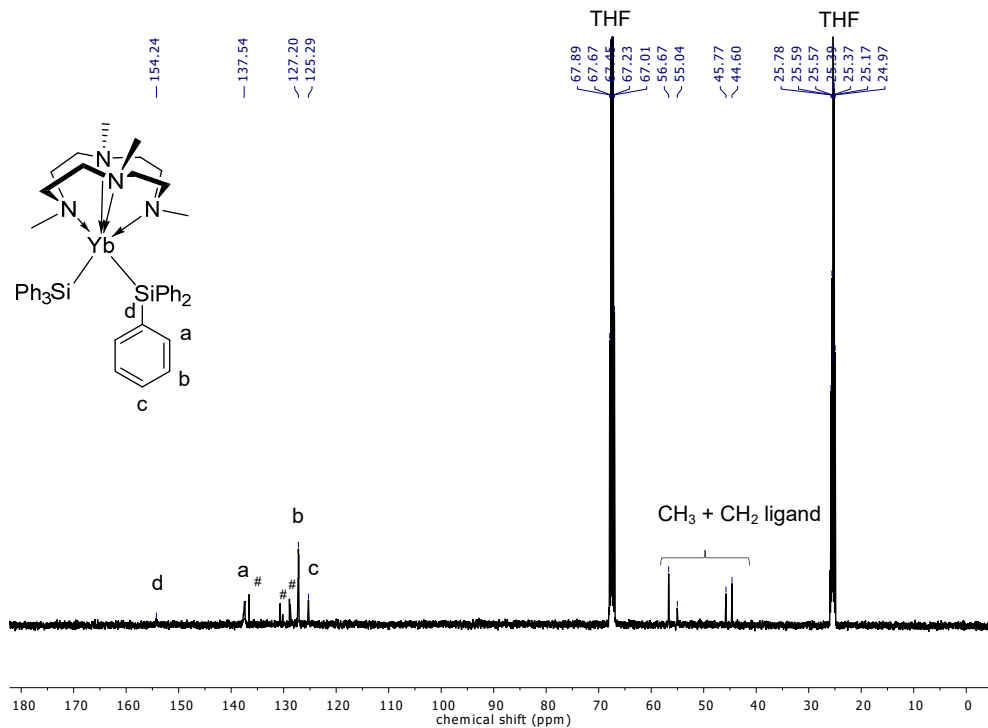


Fig. S5. $^{13}\text{C}\{^1\text{H}\}$ NMR spectrum (101 MHz, $[\text{D}_8]\text{THF}$, 25 °C) of $[(\text{Me}_4\text{TACD})\text{Yb}(\text{SiPh}_3)_2]$ (**2**) (# = decomposition products).

3.5. VT NMR spectra of $[(\text{Me}_4\text{TACD})\text{Yb}(\text{SiPh}_3)_2]$ (**2**)

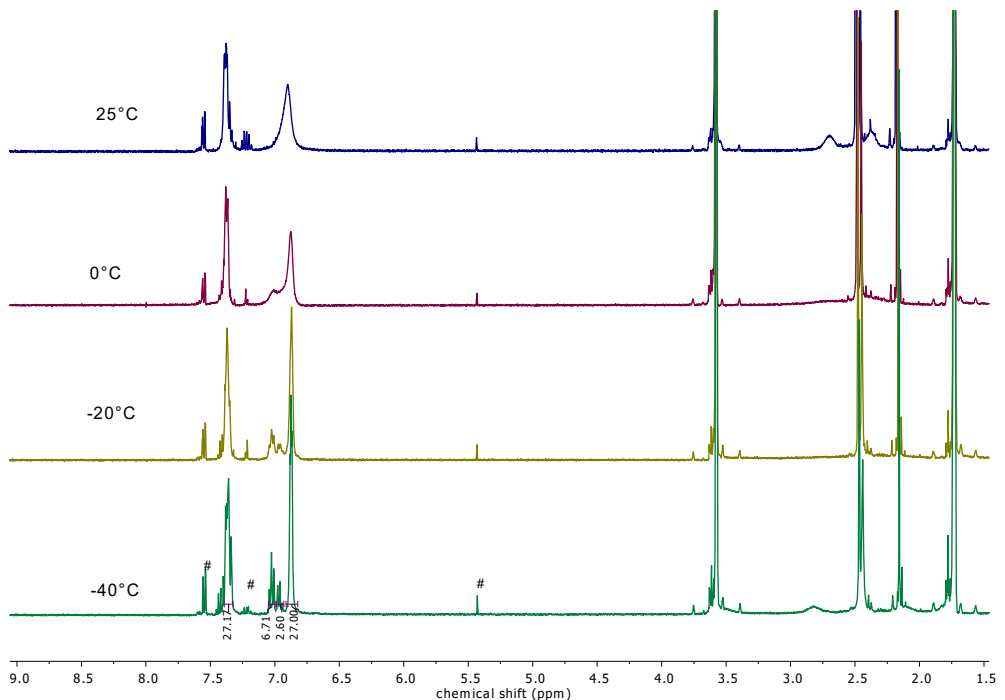


Fig. S6. VT NMR spectra (400 MHz, $[\text{D}_8]\text{THF}$) of $[(\text{Me}_4\text{TACD})\text{Yb}(\text{SiPh}_3)_2]$ (**2**) (# = decomposition products).

3.6. Molecular Structure of $[(\text{Me}_4\text{TACD})\text{Yb}(\text{SiPh}_3)_2]$ (**2**)

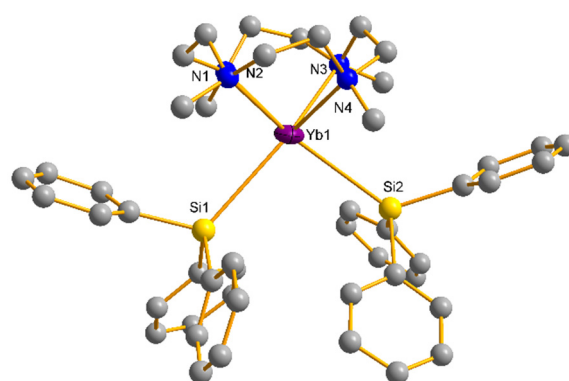


Fig. S7. Molecular structure of **2** in the crystal. Displacement parameters of Yb1 are shown at 50% probability; the hydrogen atoms are omitted for clarity. Selected interatomic distances [Å] and angles [°]: Yb1–N1 2.734(12), Yb1–N2 2.583(14), Yb1–N3 2.717(14), Yb1–N4 2.496(11), Yb1–Si1 3.278(5), Yb1–Si2 3.247(4), Si1–Yb1–Si2 96.78(11).

3.7. Synthesis of $[(\text{Me}_4\text{TACD})_2\text{Yb}_2(\mu_2\text{-H})_3][\text{SiPh}_3]$ (**3**)

Method A

In a glass autoclave, a stirred solution of $[(\text{Me}_4\text{TACD})\text{Yb}(\text{SiPh}_3)_2]$ (**2**) (92 mg, 0.1 mmol) in THF (4 mL) was charged with H_2 . After 5 min, the solution was filtered, layered with *n*-pentane (5 mL) and stored at -30°C . After 16 h, black microcrystals formed. The supernatant was decanted off, the crystals were washed with *n*-pentane (3 x 2 mL) and dried under reduced pressure to give $[(\text{Me}_4\text{TACD})_2\text{Yb}_2(\mu_2\text{-H})_3][\text{SiPh}_3]$ (**3**) as black microcrystals (35 mg, 33 μmol); yield: 66%.

Method B

To a stirred solution of $[\text{Yb}(\text{SiPh}_3)_2(\text{thf})_4]$ (**1**) (490 mg, 0.5 mmol) in THF (10 mL) was added dropwise at room temperature a solution of Me_4TACD (115 mg, 0.5 mmol) in THF (10 mL) in a glass autoclave. After 5 min, the autoclave was charged with H_2 . After 15 min, the solution was filtered, concentrated to 10 mL, layered with *n*-pentane (10 mL) and stored at -30°C . After 16 h, black microcrystals formed. The supernatant was decanted off, the crystals were washed with *n*-pentane (3 x 5 mL) and dried under reduced pressure to give $[(\text{Me}_4\text{TACD})_2\text{Yb}_2(\mu_2\text{-H})_3][\text{SiPh}_3]$ (**3**) as black microcrystals (137 mg, 0.13 mmol); yield: 52%.

^1H NMR (400 MHz, $[\text{D}_8]\text{THF}$, 25 °C): δ = 2.15 – 2.47 (br, 16 H, NCH_2), 2.60 (s, 24 H, NCH_3), 2.66 – 3.06 (br, 16 H, NCH_2), 6.69 – 6.80 (m, 3 H, *para*-Ph), 6.81 – 6.96 (m, 6 H, *meta*-Ph), 7.26 – 7.46 (m, 6 H, *ortho*-Ph), 7.52 (3 H, $^1J_{\text{YbH}} = 300$ Hz, YbH) ppm.

$^{13}\text{C}\{\text{H}\}$ NMR (101 MHz, $[\text{D}_8]\text{THF}$, 25 °C): δ = 45.90 (NCH_3), 54.63 (NCH_2), 123.51 (*para*-Ph), 126.58 (*meta*-Ph), 137.24 (*ortho*-Ph), 159.58 (*ipso*-Ph) ppm.

^{171}Yb NMR (71 MHz, $[\text{D}_8]\text{THF}$, 25 °C): δ = 992 ($^1J_{\text{YbH}} = 300$ Hz) ppm.

Anal. calc. for $\text{C}_{42}\text{H}_{74}\text{N}_8\text{SiYb}_2$ (1065.30 g mol $^{-1}$): C, 47.35; H, 7.00; N, 10.52. Found: C, 43.56; H, 6.93; N, 10.26%.

3.8. ^1H , $^{13}\text{C}\{^1\text{H}\}$ and ^{171}Yb NMR spectra of $[(\text{Me}_4\text{TACD})_2\text{Yb}_2(\mu_2\text{-H})_3][\text{SiPh}_3]$ (**3**)

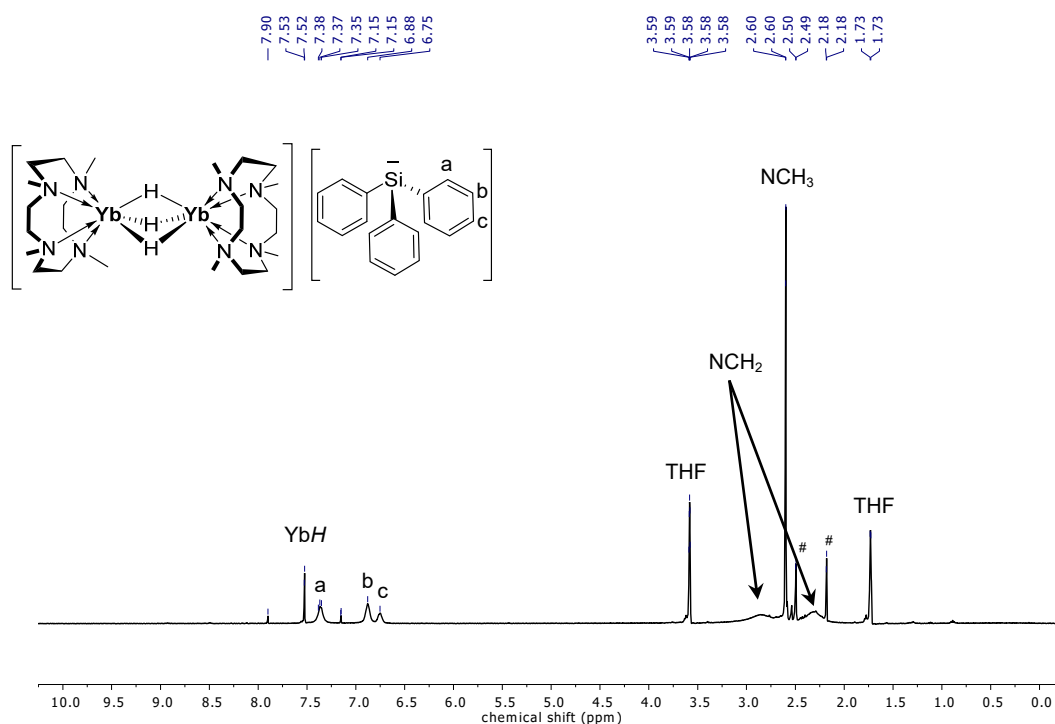


Fig. S8. ^1H NMR spectrum (400 MHz, $[\text{D}_8]\text{THF}$, 25 °C) of $[(\text{Me}_4\text{TACD})_2\text{Yb}_2(\mu_2\text{-H})_3][\text{SiPh}_3]$ (**3**) (# = free Me₄TACD)

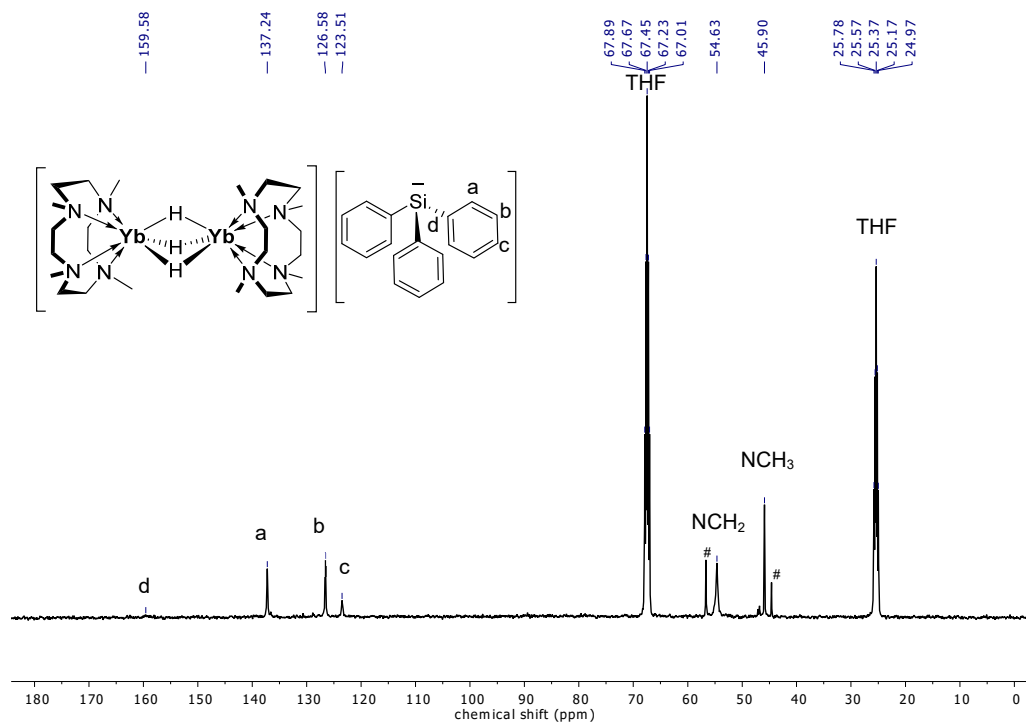


Fig. S9. $^{13}\text{C}\{^1\text{H}\}$ NMR spectrum (101 MHz, $[\text{D}_8]\text{THF}$, 25 °C) of $[(\text{Me}_4\text{TACD})_2\text{Yb}_2(\mu_2\text{-H})_3][\text{SiPh}_3]$ (**3**) (# = free Me₄TACD).

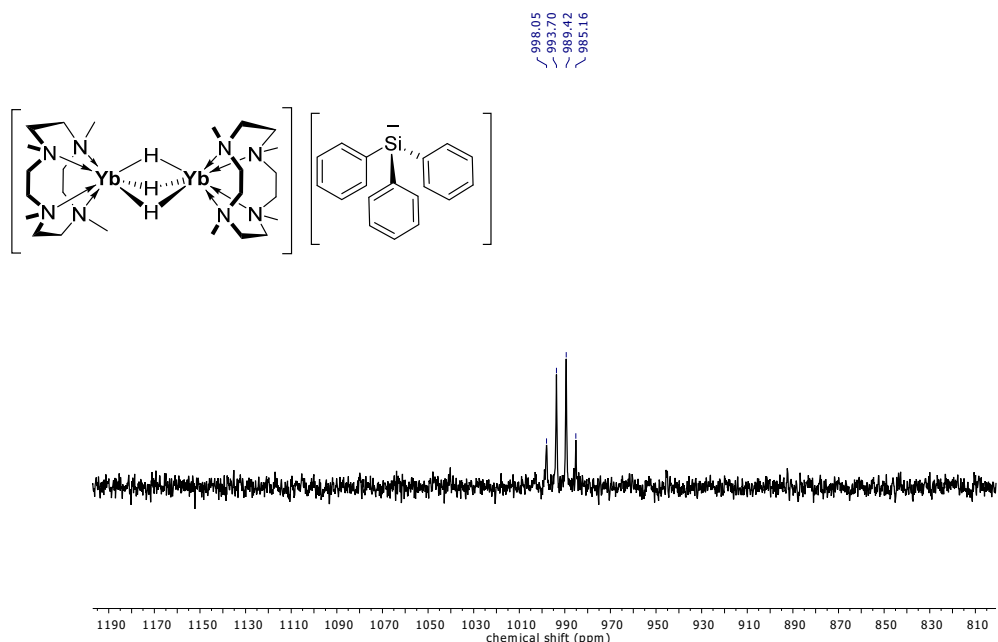


Fig. S10. ^{171}Yb NMR spectrum (71 MHz, $[\text{D}_8]\text{THF}$, 25 °C) of $[(\text{Me}_4\text{TACD})_2\text{Yb}_2(\mu_2\text{-H})_3][\text{SiPh}_3]$ (**3**).

3.9. Synthesis of $[Yb(CH_2Ph)_2]$ (**4**)

To a solution of $[YbI_2(\text{thf})_3]$ (643 mg, 1.00 mmol) in THF (10 mL) was added dropwise a solution of $[KCH_2\text{Ph}]$ (260 mg, 2.00 mmol) in THF (5 mL) at 25 °C. After 1 h, the solution turned dark green and the precipitate was removed by centrifugation. The mother liquor was decanted off, filtered and the solvents were removed under vacuum. The resulting oil was triturated with toluene (3 x 5 mL) to give a black amorphous solid (283 mg, 80 μmol); yield: 80%.

^1H NMR (400 MHz, $[\text{D}_8]\text{THF}$, 25 °C): δ 1.58 (s, $^1J_{\text{CH}} = 126$ Hz, 4 H, PhCH_2), 5.72 – 5.79 (m, 2 H, *para*-Ph), 6.29 – 6.38 (m, 4 H, *meta*-Ph), 6.46 – 6.56 (m, 4 H, *ortho*-Ph) ppm.

$^{13}\text{C}\{\text{H}\}$ NMR (101 MHz, $[\text{D}_8]\text{THF}$, 25 °C): δ 48.02 (PhCH_2), 109.18 (*para*-Ph), 119.38 (*ortho*-Ph), 128.60 (*meta*-Ph), 159.90 (*ipso*-Ph) ppm.

^{171}Yb NMR (71 MHz, $[\text{D}_8]\text{THF}$, 25 °C): δ = 562 ppm.

Anal. calc. for $\text{C}_{14}\text{H}_{14}\text{Yb}$ (355.32 g mol⁻¹): C, 47.32; H, 3.97. Found: C, 45.08; H, 4.06%.

IR (KBr): $\tilde{\nu} = 3029$ (w), 2921 (w), 2850 (m), 1578 (s), 1475 (m), 1451 (m), 1243 (m), 1171 (w), 1144 (w), 1059 (w), 985 (w), 863 (w), 769 (w), 730 (s), 694 (m), 511 (w) cm⁻¹.

3.10. ^1H , $^{13}\text{C}\{^1\text{H}\}$ and $^{171}\text{Yb}\{^1\text{H}\}$ NMR spectra of $[\text{Yb}(\text{CH}_2\text{Ph})_2]$ (**4**)

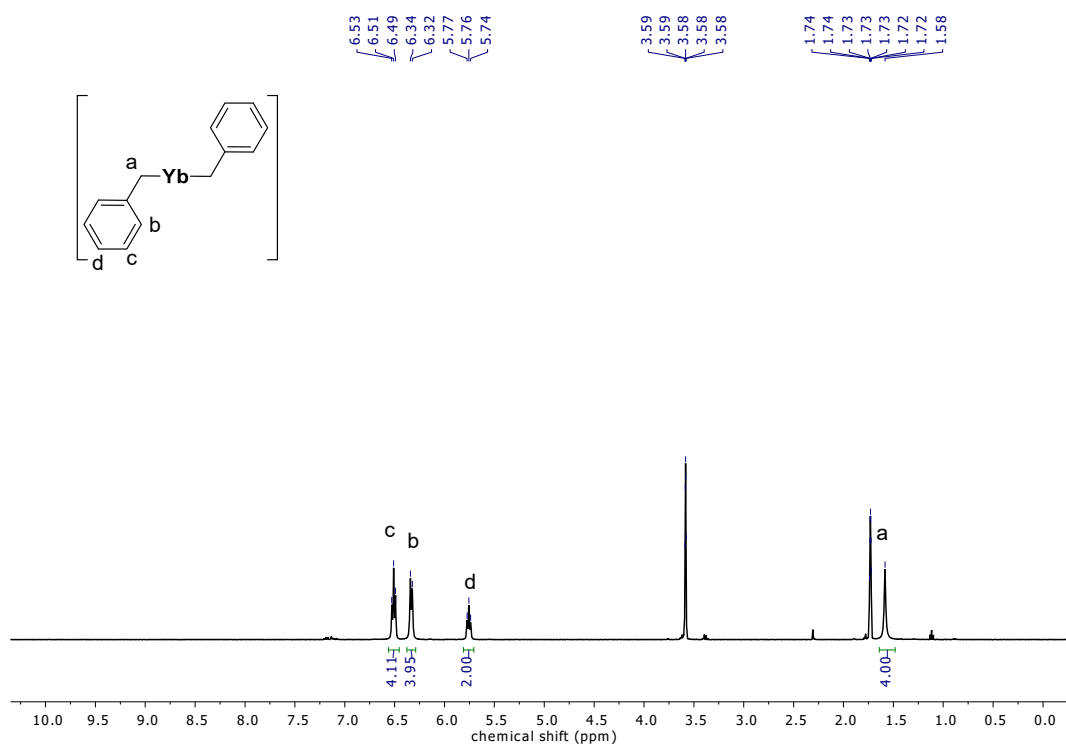


Fig. S11. ^1H NMR spectrum (400 MHz, $[\text{D}_8]\text{THF}$, 25 °C) of $[\text{Yb}(\text{CH}_2\text{Ph})_2]$ (**4**).

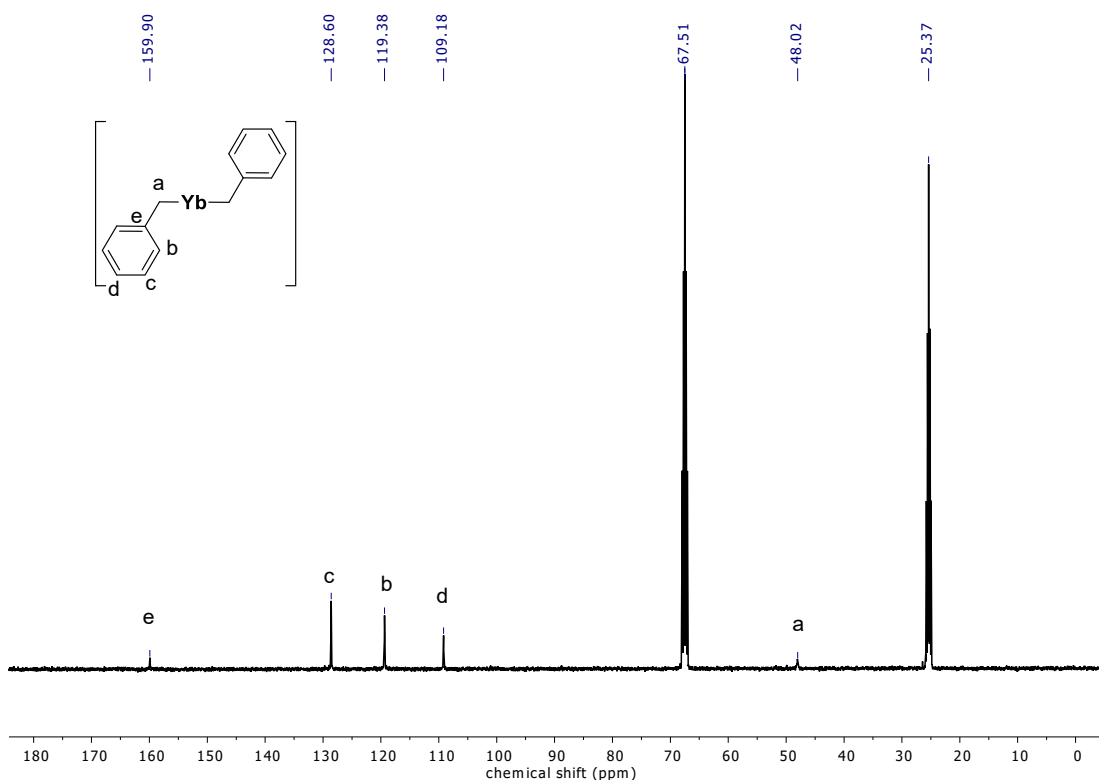


Fig. S12. $^{13}\text{C}\{^1\text{H}\}$ NMR spectrum (101 MHz, $[\text{D}_8]\text{THF}$, 25 °C) of $[\text{Yb}(\text{CH}_2\text{Ph})_2]$ (**4**).

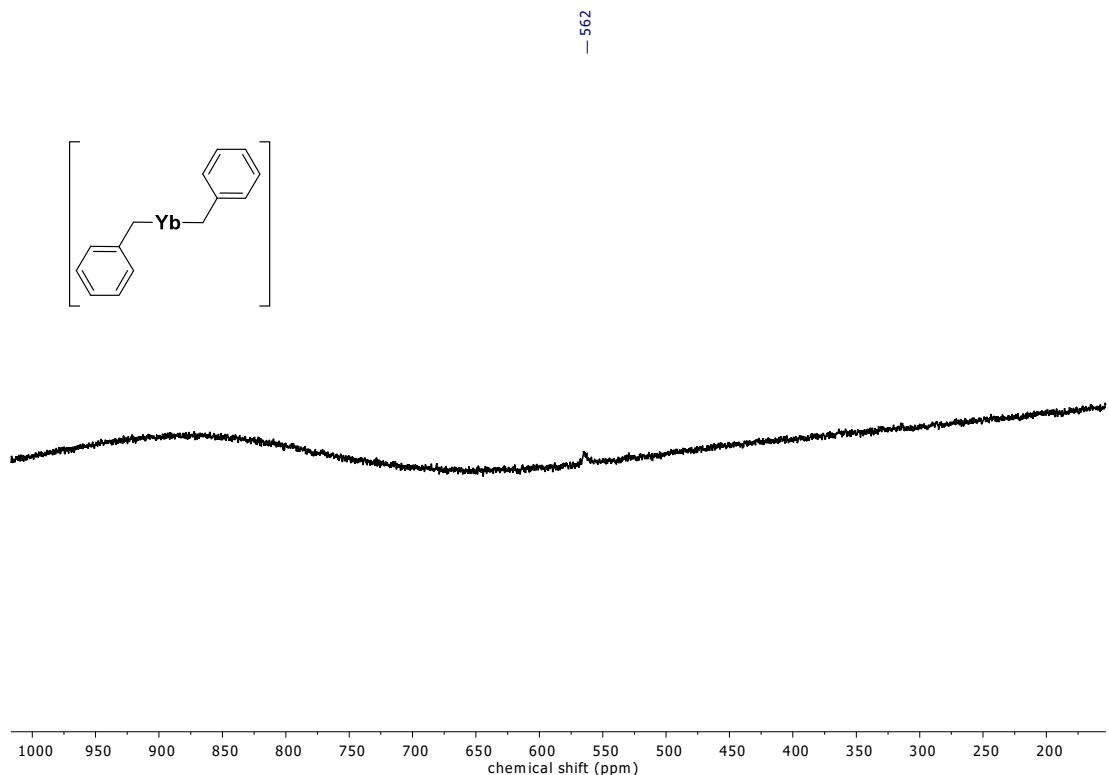


Fig. S13. $^{171}\text{Yb}\{^1\text{H}\}$ NMR spectrum (71 MHz, $[\text{D}_8]\text{THF}$, 25 °C) of $[\text{Yb}(\text{CH}_2\text{Ph})_2]$ (**4**).

3.11. IR spectrum of $[\text{Yb}(\text{CH}_2\text{Ph})_2]$ (**4**)

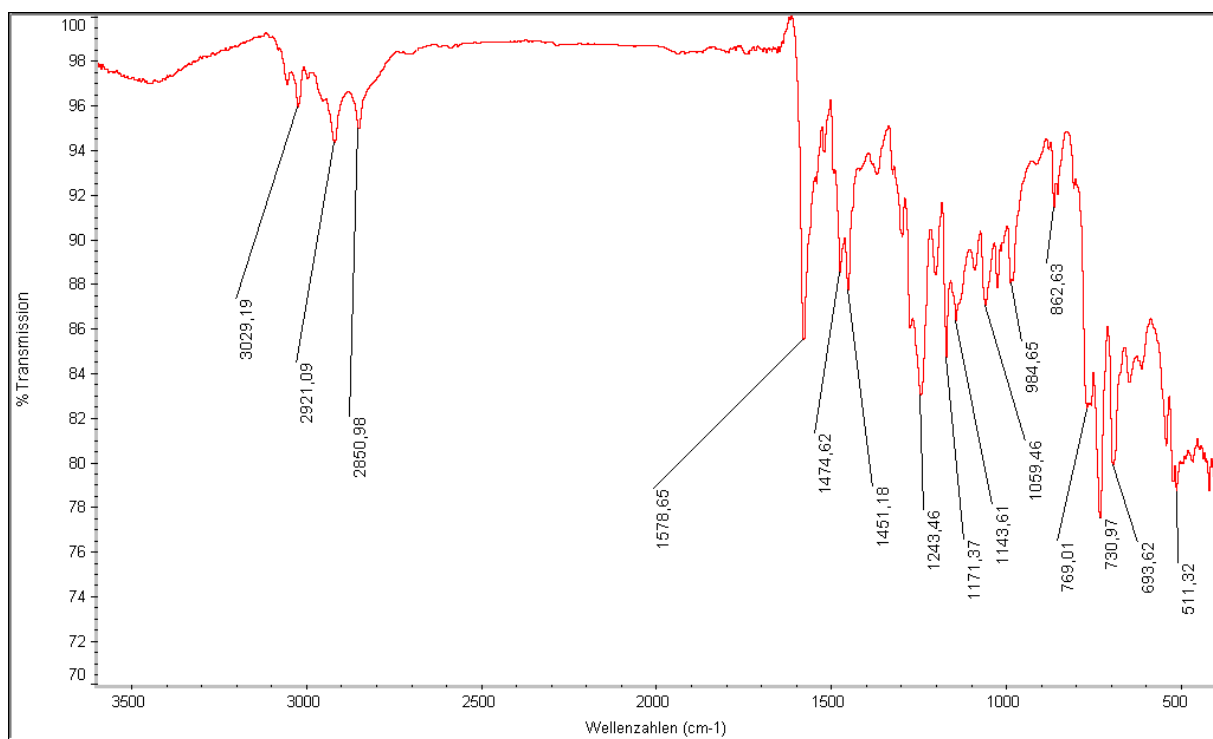


Fig. S14. IR spectrum (KBr) of $[\text{Yb}(\text{CH}_2\text{Ph})_2]$ (**4**).

3.12. Synthesis of $[(\text{Me}_4\text{TACD})\text{Yb}(\text{CH}_2\text{Ph})_2]$ (**5**)

Method A

To a solution of $[\text{Yb}(\text{CH}_2\text{Ph})_2]$ (**4**) (200 mg, 0.56 mmol) in THF (3 mL), a solution of Me_4TACD (128 mg, 0.56 mmol) in THF (1 mL) was added dropwise at room temperature. After 60 min at -30°C , a red precipitate formed. The supernatant was decanted off and the precipitate was washed with cold THF (2 mL) and *n*-pentane (3 x 2 mL). The solvents were removed under vacuum to give $[(\text{Me}_4\text{TACD})\text{Yb}(\text{CH}_2\text{Ph})_2]$ (**5**) as a red powder (314 mg, 0.54 mmol); yield: 94%.

Method B

To a stirred suspension of $[\text{YbI}_2(\text{thf})_3]$ (1.29 g, 2.00 mmol) in THF (5 mL) was added dropwise a solution of $[\text{KCH}_2\text{Ph}]$ (520 mg, 4 mmol) in THF (10 mL) at room temperature. The deep red solution was stirred for 90 min and the precipitate was removed by filtration. To the solution was added dropwise at room temperature Me_4TACD (460 mg, 2.00 mmol) in THF (5 mL). After 60 min at -30°C , a red precipitate formed. The supernatant was decanted off and the precipitate was washed with cold THF (3 mL) and *n*-pentane (3 x 3 mL). The solvents were removed under vacuum, giving $[(\text{Me}_4\text{TACD})\text{Yb}(\text{CH}_2\text{Ph})_2]$ (**5**) as a red powder (899 mg, 1.54 mmol); yield: 77%.

Insolubility in aliphatic and aromatic hydrocarbons as well as in ethereal solvents precluded recording NMR spectra.

Anal. calc. for $\text{C}_{26}\text{H}_{42}\text{N}_4\text{Yb}$ (583.70 g mol⁻¹): C, 53.50; H, 7.25; N, 9.60. Found: C, 53.39; H, 7.20; N, 9.92%.

IR (KBr): $\tilde{\nu} = 3029$ (w), 2921 (w), 2850 (w), 1578 (s), 1475 (m), 1451 (m), 1243 (m), 1171 (w), 1144 (w), 1059 (w), 985 (w), 862 (w), 769 (w), 730 (m), 693 (m), 511 (w) cm⁻¹.

3.13. IR spectrum of $[(\text{Me}_4\text{TACD})\text{Yb}(\text{CH}_2\text{Ph})_2]$ (**5**)

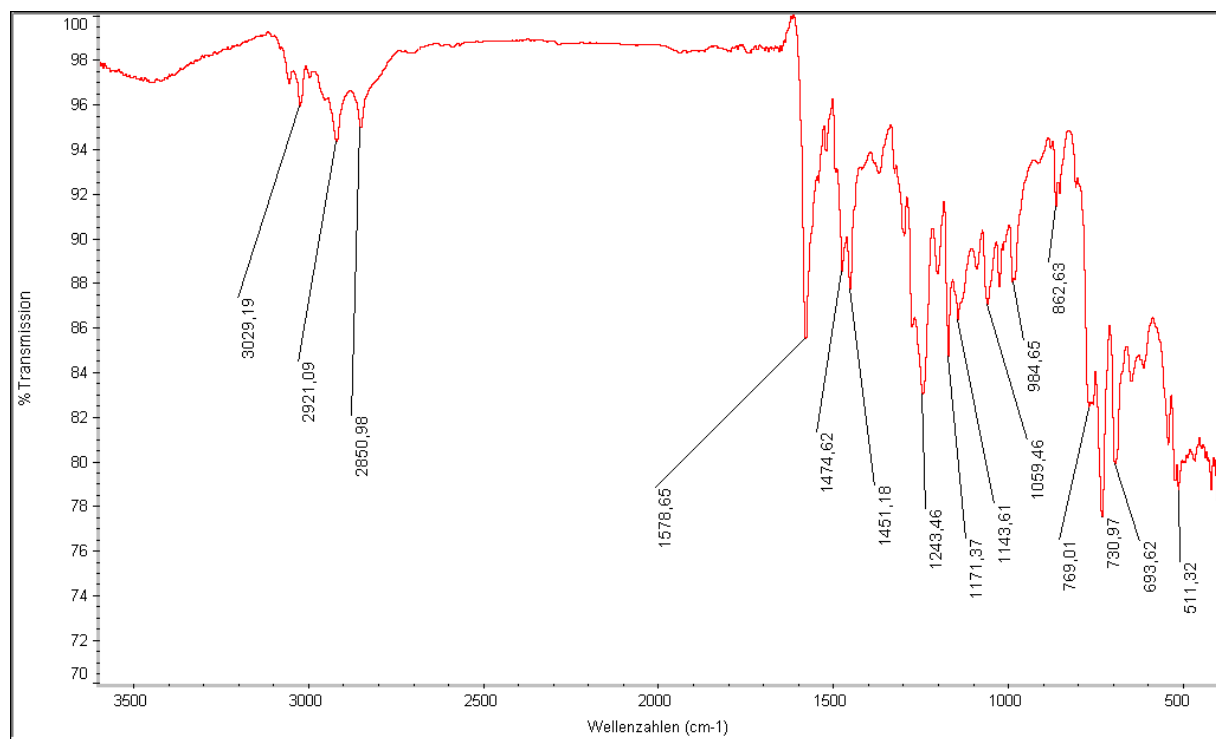


Fig. S15. IR spectrum (KBr) of $[(\text{Me}_4\text{TACD})\text{Yb}(\text{CH}_2\text{Ph})_2]$ (**5**).

3.14. Synthesis of $[(\text{Me}_4\text{TACD})\text{Yb}(\eta^6\text{-PhCH}_2)][\text{B}(\text{C}_6\text{H}_3\text{-3,5-Me}_2)_4]$ (**6**)

To a stirred suspension of $[(\text{Me}_4\text{TACD})\text{Yb}(\text{CH}_2\text{Ph})_2]$ (**5**) (584 mg, 1.00 mmol) in THF (5 mL) was added dropwise a solution of $[\text{NEt}_3]\text{H}[\text{B}(\text{C}_6\text{H}_3\text{-3,5-Me}_2)_4]$ (533 mg, 1.00 mmol) in THF (5 mL) at room temperature. The red solution was filtered, concentrated to 5 mL, layered with *n*-pentane (5 mL), and stored at –30 °C. After 24 h, a purple precipitate formed. The supernatant was decanted off and the solid was washed with *n*-pentane (3 x 2 mL). After removing all volatiles under vacuum, $[(\text{Me}_4\text{TACD})\text{Yb}(\eta^6\text{-PhCH}_2)][\text{B}(\text{C}_6\text{H}_3\text{-3,5-Me}_2)_4]$ (**6**) was isolated as a purple powder (857 mg, 0.93 mmol); yield: 93%.

Single crystals of $[(\text{Me}_4\text{TACD})\text{Yb}(\eta^6\text{-PhCH}_2)][\text{B}(\text{C}_6\text{H}_3\text{-3,5-Me}_2)_4]$ (**6**) were grown from a concentrated THF solution at –30 °C.

^1H NMR (400 MHz, $[\text{D}_8]\text{THF}$, 25 °C): δ 2.10 (s, 24 H, Ar-CH₃), 2.13 – 2.37 (m + s, 20 H, NCH₂ + NCH₃), 2.37 – 2.62 (m + s ($^1\text{J}_{\text{CH}} = 148$ Hz), 10 H, NCH₂ + PhCH₂), 5.12 – 5.15 (m, 1 H, *para*-Ph), 5.68 – 5.71 (m, 2 H, *ortho*-Ph), 6.34 – 6.38 (m, 6 H, *meta*-Ph + *para*-C₆H₃), 6.98 – 7.00 (m, 8 H, *ortho*-C₆H₃) ppm.

$^{13}\text{C}\{\text{H}\}$ NMR (101 MHz, $[\text{D}_8]\text{THF}$, 25 °C): δ = 22.40 (Ar-CH₃), 44.64 (NCH₃), 54.05 (br, NCH₂), 65.64 (PhCH₂), 97.15 (*para*-Ph), 112.01 (*ortho*-Ph), 123.64 (*para*-C₆H₃), 132.54 (*meta*-Ph), 132.99 (q, $^3\text{J}_{\text{BH}} = 2.7$ Hz, *meta*-C₆H₃), 135.54 (*ortho*-C₆H₃), 149.48 (*ipso*-Ph), 165.73 (q, $^1\text{J}_{\text{BC}} = 49.3$ Hz, *ipso*-C₆H₃) ppm.

$^{11}\text{B}\{\text{H}\}$ NMR (128 MHz, $[\text{D}_8]\text{THF}$, 25 °C): δ = –7.02 ppm.

Anal. calc. for C₅₁H₇₁N₄BYb (924.02 g mol^{–1}): C, 66.29; H, 7.75; N, 6.06. Found: C, 65.33; H, 7.83; N, 6.06%.

IR (KBr): $\tilde{\nu}$ = 2999 (m), 2907 (s), 2853 (s), 1587 (s), 1574 (s), 1462 (s), 1358 (w), 1300 (m) 1268 (w), 1144 (m), 1078 (w), 1018 (w), 968 (m), 837 (m), 735 (m), 645 (w), 579 (w) cm^{–1}.

UV-Vis (THF, 25 °C): λ_{max} (ε , mol L^{–1} cm^{–1}) = 330 (4330); 360 (4450); 370 (4700); 430 nm (760).

3.15. ^1H , $^{13}\text{C}\{^1\text{H}\}$ and $^{11}\text{B}\{^1\text{H}\}$ NMR spectra of $[(\text{Me}_4\text{TACD})\text{Yb}(\eta^6\text{-PhCH}_2)][\text{B}(\text{C}_6\text{H}_3\text{-3,5-Me}_2)_4]$ (**6**)

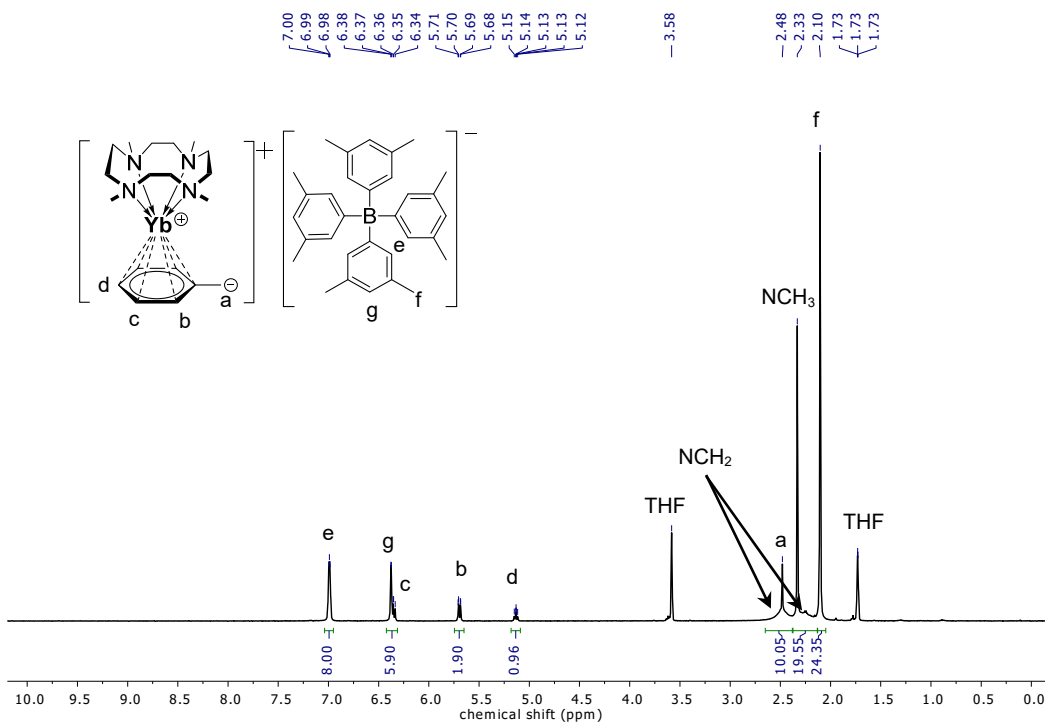


Fig. S16. ^1H NMR spectrum (400 MHz, $[\text{D}_8]\text{THF}$, 25 °C) of $[(\text{Me}_4\text{TACD})\text{Yb}(\eta^6\text{-PhCH}_2)][\text{B}(\text{C}_6\text{H}_3\text{-3,5-Me}_2)_4]$ (**6**).

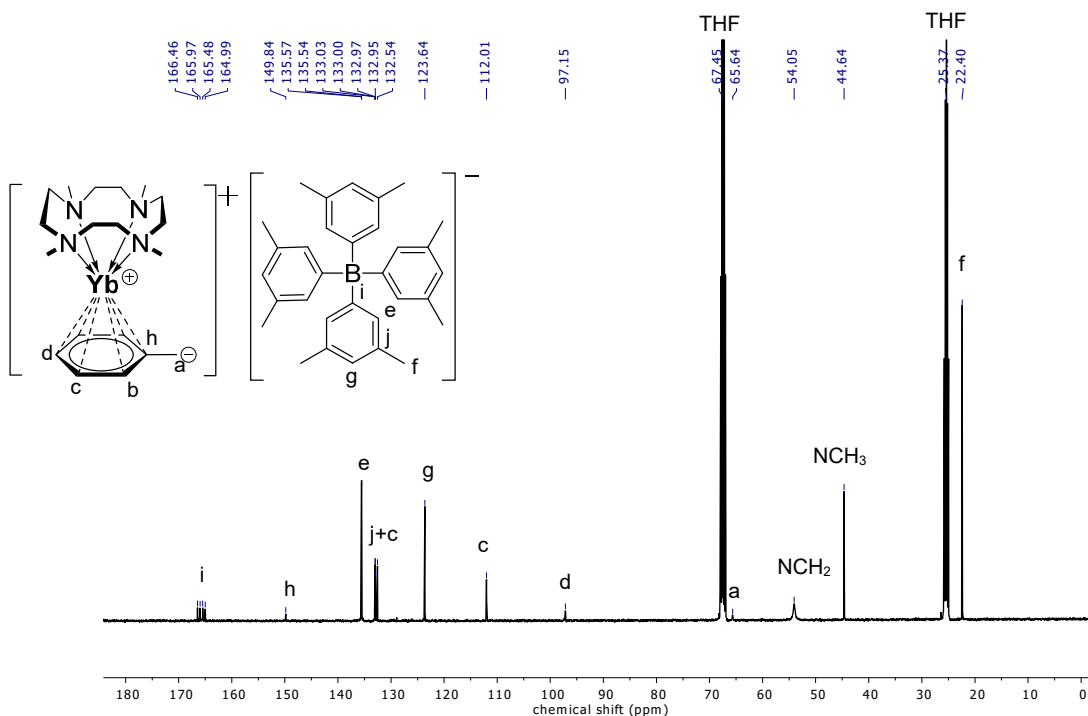


Fig. S17. $^{13}\text{C}\{^1\text{H}\}$ NMR spectrum (101 MHz, $[\text{D}_8]\text{THF}$, 25 °C) of $[(\text{Me}_4\text{TACD})\text{Yb}(\eta^6\text{-PhCH}_2)][\text{B}(\text{C}_6\text{H}_3\text{-3,5-Me}_2)_4]$ (**6**).

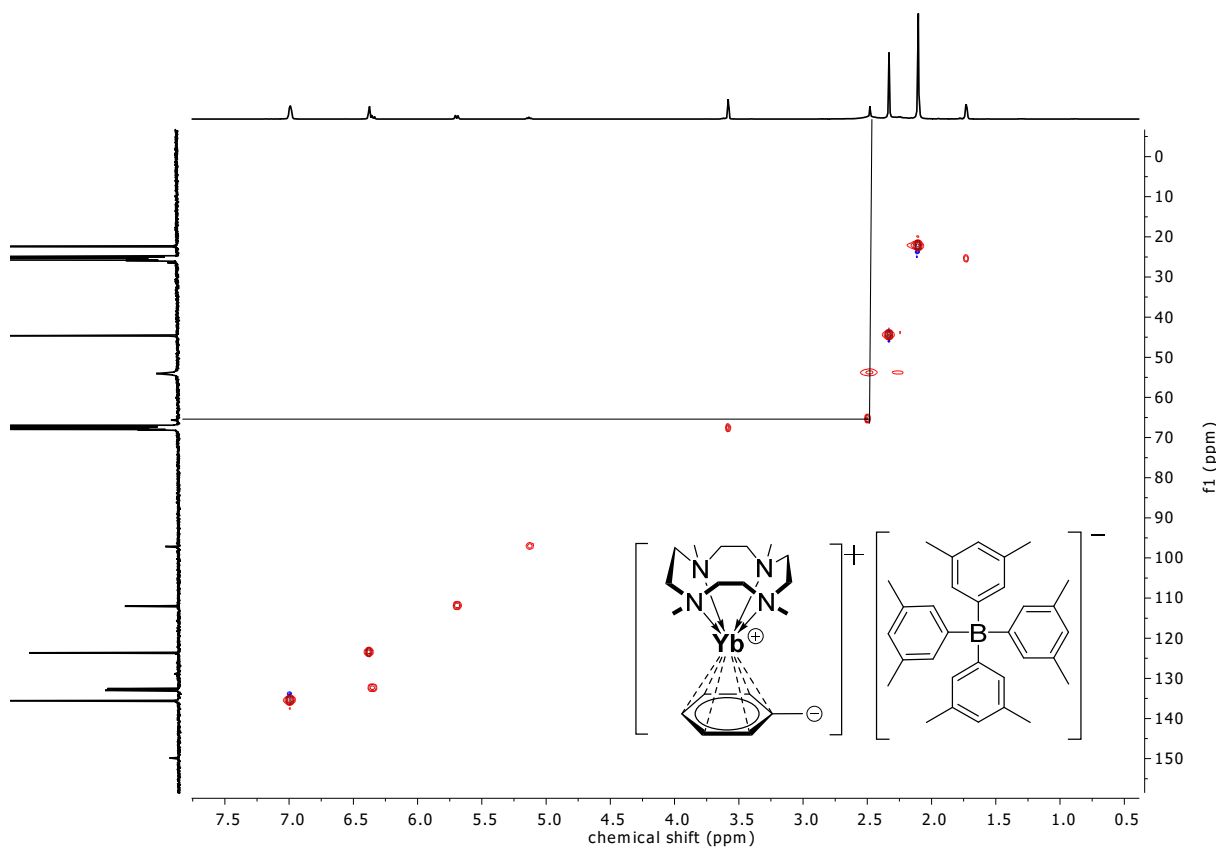


Fig. S18. ^1H - ^{13}C -HSQC spectrum ($[\text{D}_8]\text{THF}$, 25 °C) of $[(\text{Me}_4\text{TACD})\text{Yb}(\eta^6\text{-PhCH}_2)][\text{B}(\text{C}_6\text{H}_3\text{-3,5-Me}_2)_4]$ (**6**).

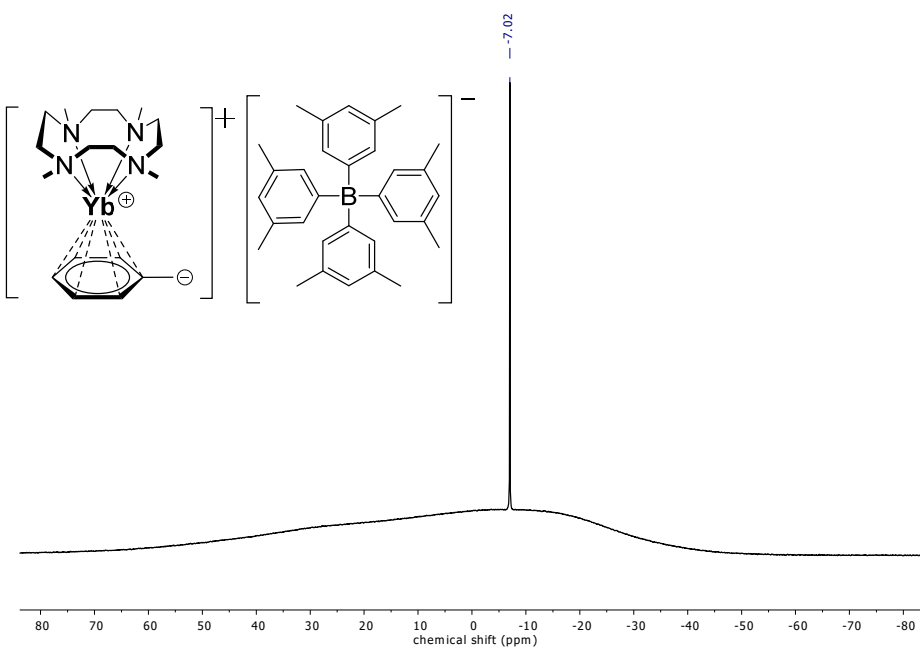


Fig. S19. $^{11}\text{B}\{^1\text{H}\}$ spectrum (128 MHz, $[\text{D}_8]\text{THF}$, 25 °C) of $[(\text{Me}_4\text{TACD})\text{Yb}(\eta^6\text{-PhCH}_2)][\text{B}(\text{C}_6\text{H}_3\text{-3,5-Me}_2)_4]$ (**6**).

3.16. IR Spectrum of $[(\text{Me}_4\text{TACD})\text{Yb}(\eta^6\text{-PhCH}_2)]\text{[B(C}_6\text{H}_3\text{-3,5-Me}_2)_4]$ (**6**)

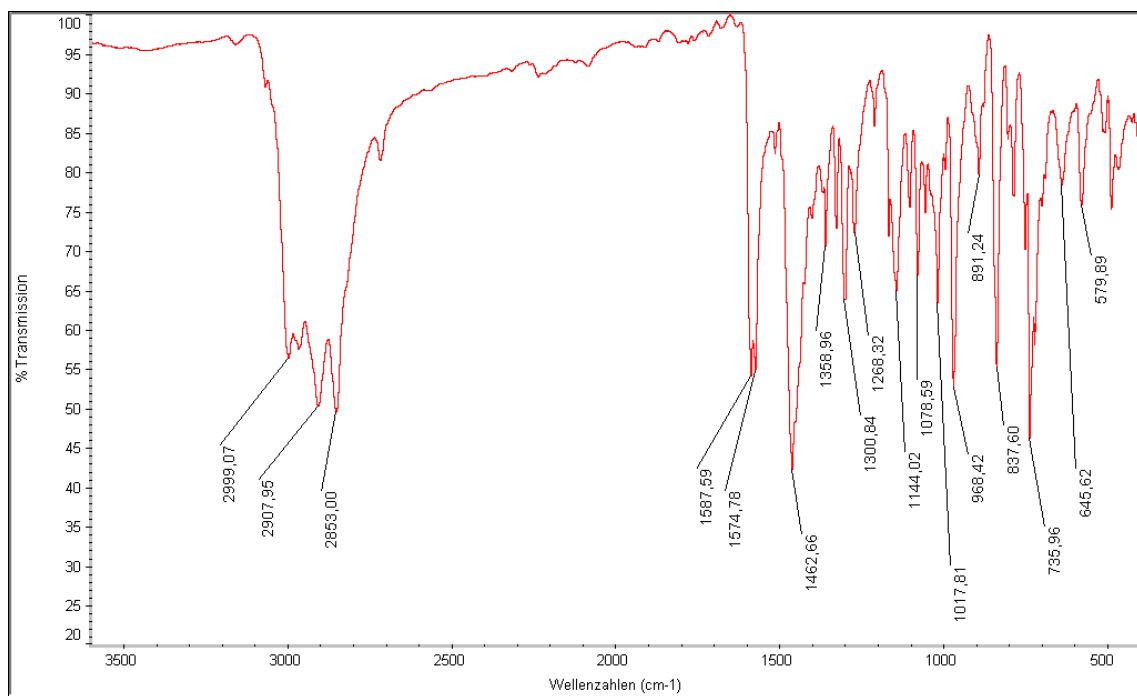


Fig. S20. IR spectrum (KBr) of $[(\text{Me}_4\text{TACD})\text{Yb}(\eta^6\text{-PhCH}_2)]\text{[B(C}_6\text{H}_3\text{-3,5-Me}_2)_4]$ (**6**)

3.17. UV-Vis spectrum of $[(\text{Me}_4\text{TACD})\text{Yb}(\eta^6\text{-PhCH}_2)]\text{[B(C}_6\text{H}_3\text{-3,5-Me}_2)_4]$ (**6**).

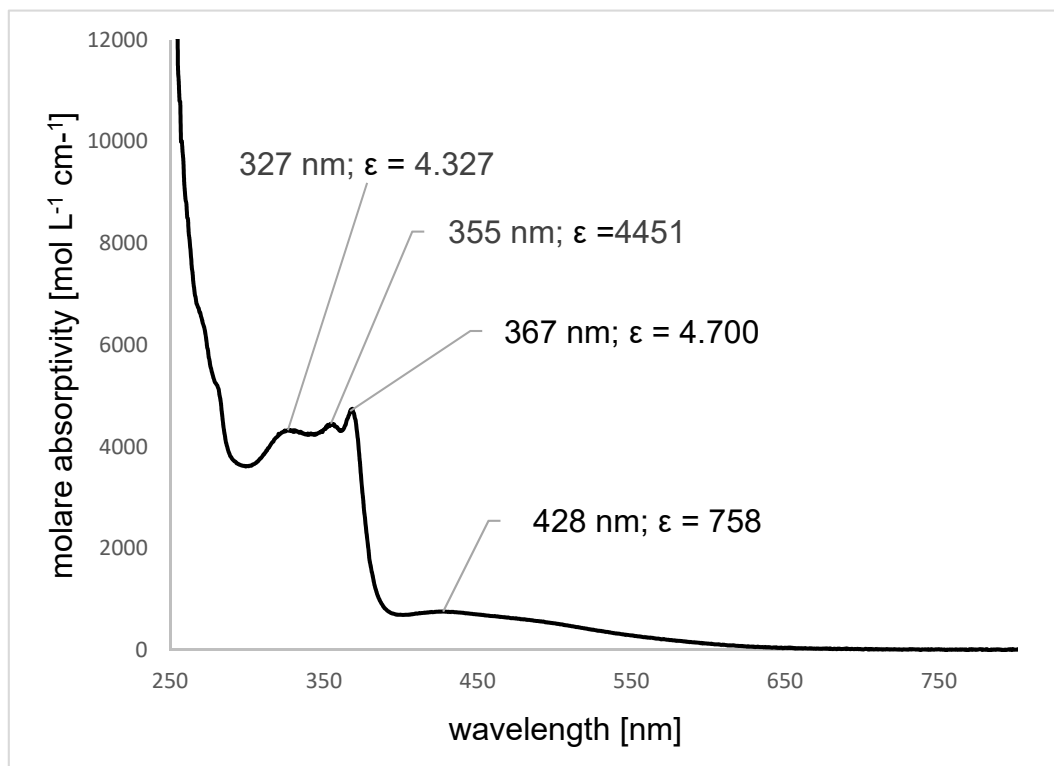


Fig. S21. UV-Vis spectrum (THF, 25 °C) of $[(\text{Me}_4\text{TACD})\text{Yb}(\eta^6\text{-PhCH}_2)]\text{[B(C}_6\text{H}_3\text{-3,5-Me}_2)_4]$ (**6**).

3.18. Synthesis of $[(\text{Me}_4\text{TACD})_2\text{Yb}_2(\mu_2\text{-H})_2(\text{thf})][\text{B}(\text{C}_6\text{H}_3\text{-3,5-Me}_2)_4]_2 \bullet 2.5\text{THF}$ (7)

In a glass autoclave, $[(\text{Me}_4\text{TACD})\text{Yb}(\eta^6\text{-PhCH}_2)][\text{B}(\text{C}_6\text{H}_3\text{-3,5-Me}_2)_4]$ (**6**) (92 mg, 0.1 mmol) was dissolved in THF (5 mL). The red solution was degassed, charged with H_2 (1 bar) and stirred for 45 min. The solution was filtered, the volume of the reaction mixture reduced to ca. 2 mL and the solution was stored at -30°C . After 16 h, red crystals formed. The supernatant was decanted off, the crystals were washed with *n*-pentane (3 x 1 mL) and dried under reduced pressure to give $[(\text{Me}_4\text{TACD})_2\text{Yb}_2(\mu_2\text{-H})_2(\text{thf})][\text{B}(\text{C}_6\text{H}_3\text{-3,5-Me}_2)_4]_2 \bullet 2.5\text{THF}$ (**7**) (84 mg, 44 μmol); yield: 88%.

Crystals suitable for single crystal XRD were grown from a concentrated THF solution. $[(\text{Me}_4\text{TACD})_2\text{Yb}_2(\mu_2\text{-D})_2(\text{thf})][\text{B}(\text{C}_6\text{H}_3\text{-3,5-Me}_2)_4]_2 \bullet 2.5\text{THF}$ (**[D₂]-7**) was prepared using D₂ in an analogous manner.

¹H NMR (400 MHz, [D₈]THF, 25 °C): δ = 1.75 – 1.80 (m, 12 H, THF), 2.10 (s, 48 H, Ar-CH₃), 2.15 – 2.30 (br, 16 H, NCH₂), 2.34 (s, 24 H, NCH₃), 2.40 – 2.60 (br, 16 H, NCH₂), 3.60 – 3.65 (m, 12 H, THF), 6.33 – 6.38 (m, 8 H, *para*-C₆H₃), 6.92 – 7.00 (m, 16 H, *ortho*-C₆H₃), 9.00 (s, ¹J_{YbH} = 364 Hz, YbH) ppm.

²H NMR (61 MHz, THF, 25 °C): δ = 9.08 (t, ¹J_{YbD} = 56 Hz, YbD) ppm.

¹³C{¹H} NMR (101 MHz, [D₈]THF, 25 °C): δ = 22.44 (Ar-CH₃), 26.43 (THF), 44.70 (NCH₃), 54.15 (NCH₂), 123.60 (*para*-C₆H₃), 132.90 (q, ³J_{BC} = 2.7 Hz, *meta*-C₆H₃), 135.55 (*ortho*-C₆H₃), 165.67 (q, ¹J_{BC} = 49.4 Hz, *ipso*-C₆H₃) ppm.

¹¹B{¹H} NMR (128 MHz, [D₈]THF, 25 °C): δ = –8.84 ppm.

Anal. calc. for C₁₀₂H₁₅₈N₈BO_{3.5}Yb₂ (1920.17 g mol^{–1}): C, 63.80; H, 8.29; N, 5.84. Found: C, 60.89; H, 7.72; N, 6.18%.

IR (**7**, KBr): $\tilde{\nu}$ = 3001 (m), 2969 (s), 2910 (s), 2855 (s), 1575 (s), 1464 (s), 1354 (w), 1301 (m) 1275 (w), 1144 (m), 1058 (w), 1021 (w), 970 (m), 896 (w), 839 (m), 784 (w), 730 (s), 694 (w), 582 (m), 541 (w), 483 (w), 458 (w) cm^{–1}.

IR (**[D₂]-7**, KBr): $\tilde{\nu}$ = 3001 (m), 2970 (s), 2910 (s), 2855 (s), 1575 (s), 1464 (s), 1354 (w), 1301 (m), 1275 (w), 1144 (m), 1058 (w), 1021 (w), 970 (m), 898 (w), 839 (m), 784 (w), 731 (s), 583 (m), 507 (w), 484 (w), 458 (w) cm^{–1}.

UV-Vis (THF, 25 °C): λ_{max} (ε , mol L^{–1} cm^{–1}) = 320 (2310); 494 nm (1020).

3.19. ^1H , ^2H , $^{13}\text{C}\{^1\text{H}\}$ and $^{11}\text{B}\{^1\text{H}\}$ NMR spectra of $[(\text{Me}_4\text{TACD})_2\text{Yb}_2(\mu_2-\text{H})_2(\text{thf})][\text{B}(\text{C}_6\text{H}_3-3,5-\text{Me}_2)_4]_2 \bullet 2.5\text{THF}$ (**7**)

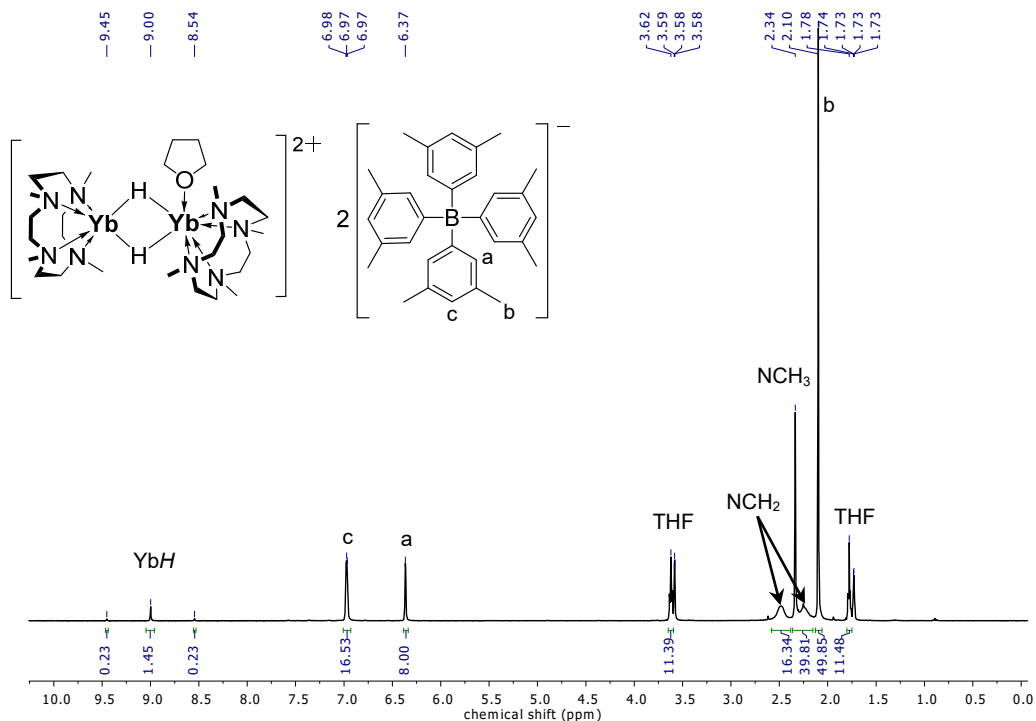


Fig. S22. ^1H NMR spectrum (400 MHz, $[\text{D}_8]\text{THF}$, 25 °C) of $[(\text{Me}_4\text{TACD})_2\text{Yb}_2(\mu_2-\text{H})_2(\text{thf})][\text{B}(\text{C}_6\text{H}_3-3,5-\text{Me}_2)_4]_2 \bullet 2.5\text{THF}$ (**7**).

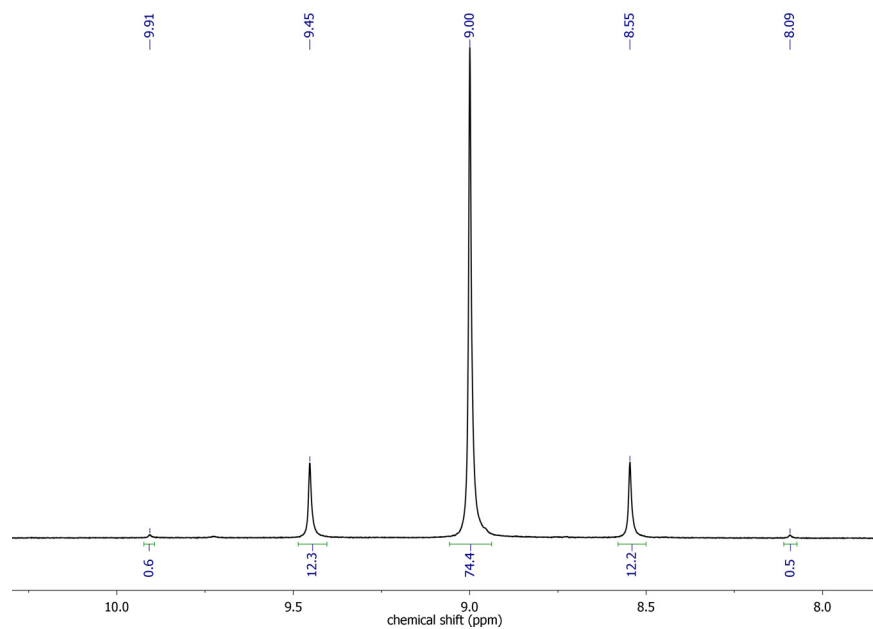


Fig. S23. ^1H NMR spectrum (400 MHz, $[\text{D}_8]\text{THF}$, 25 °C) of $[(\text{Me}_4\text{TACD})_2\text{Yb}_2(\mu_2-\text{H})_2(\text{thf})][\text{B}(\text{C}_6\text{H}_3-3,5-\text{Me}_2)_4]_2 \bullet 2.5\text{THF}$ (**7**) in the region of 8.0–10.0 ppm.

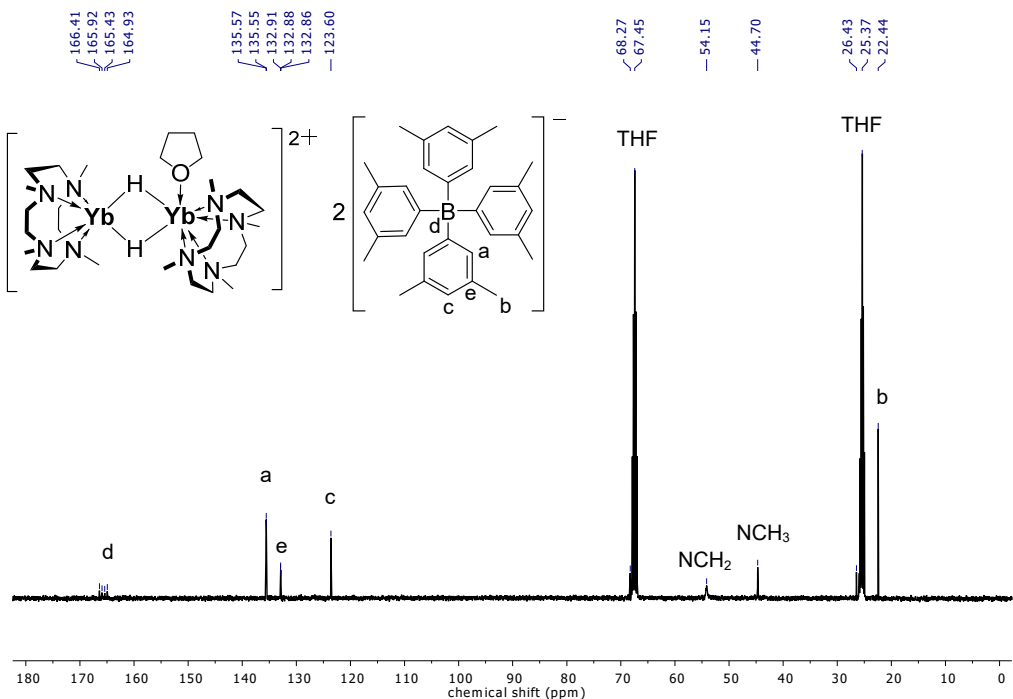


Fig. S24. ¹³C{¹H} NMR spectrum (101 MHz, [D₈]THF, 25 °C) of [(Me₄TACD)₂Yb₂(μ₂-H)₂(thf)][B(C₆H₃-3,5-Me₂)₄]₂•2.5THF (**7**).

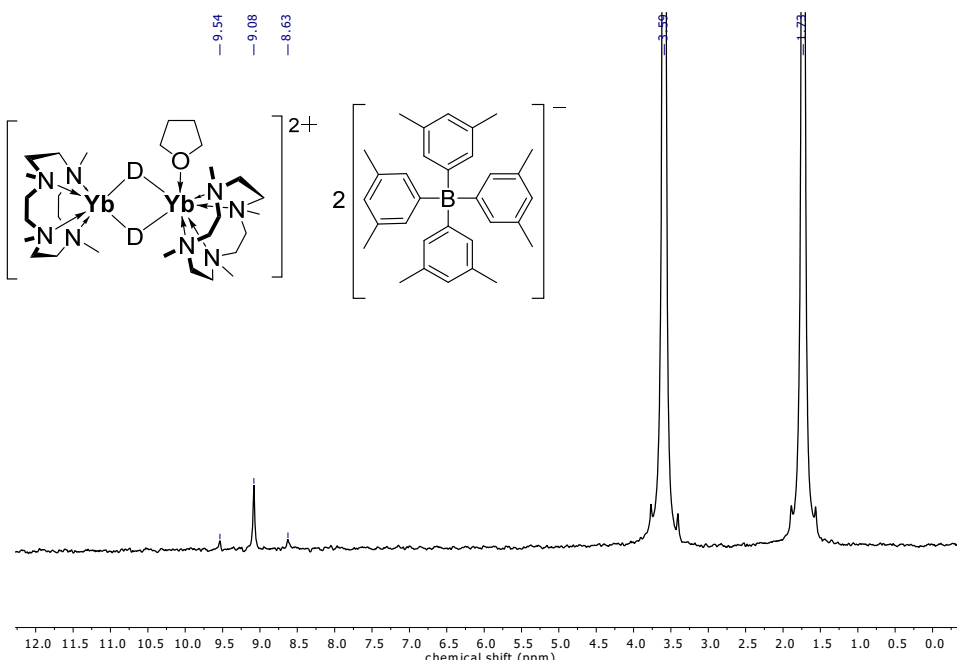


Fig. S25. ²H NMR spectrum (61 MHz, THF, 25 °C) of [(Me₄TACD)₂Yb₂(μ₂-D)₂(thf)][B(C₆H₃-3,5-Me₂)₄]₂•2.5THF ([D₂]-**7**).

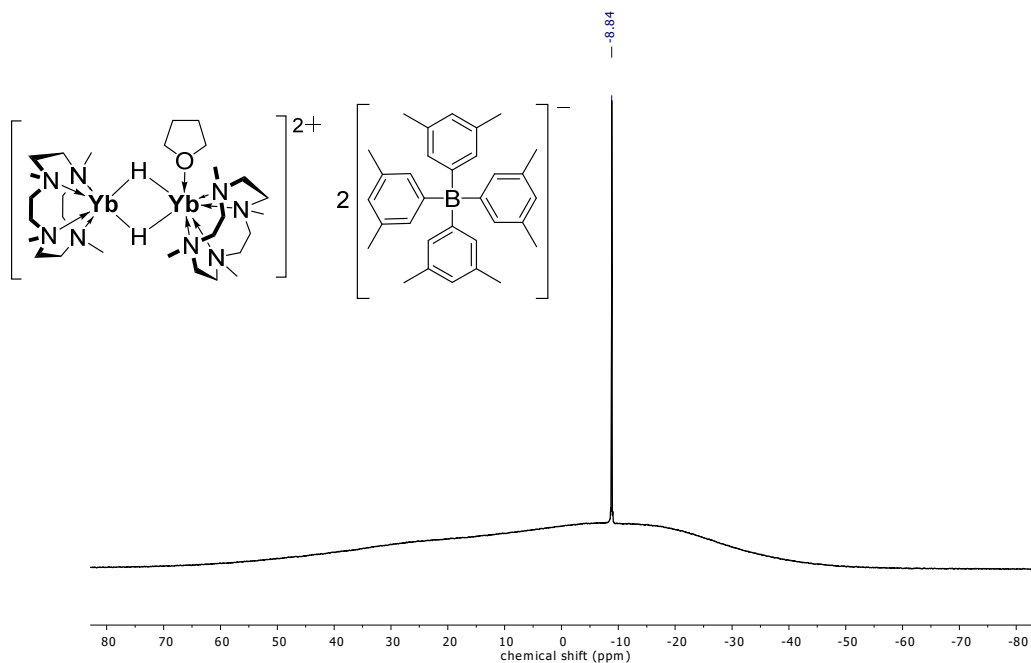


Fig. S26. $^{11}\text{B}\{^1\text{H}\}$ NMR spectrum (128 MHz, $[\text{D}_8]\text{THF}$, 25 °C) of $[(\text{Me}_4\text{TACD})_2\text{Yb}_2(\mu_2-\text{H})_2(\text{thf})][\text{B}(\text{C}_6\text{H}_3-3,5-\text{Me}_2)_4]_2 \cdot 2.5\text{THF}$ (**7**).

3.20. UV-Vis spectrum of $[(\text{Me}_4\text{TACD})_2\text{Yb}_2(\mu_2-\text{H})_2(\text{thf})][\text{B}(\text{C}_6\text{H}_3-3,5-\text{Me}_2)_4]_2 \cdot 2.5\text{THF}$ (**7**)

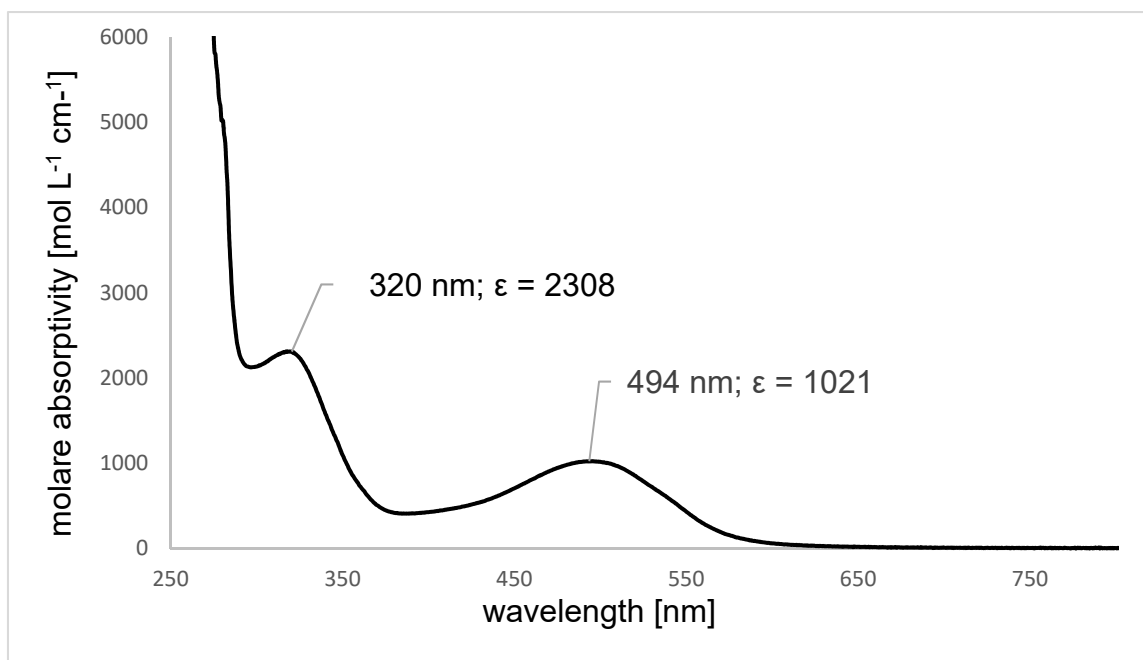


Fig. S27. UV-Vis spectrum (THF, 25 °C) of $[(\text{Me}_4\text{TACD})_2\text{Yb}_2(\mu_2-\text{H})_2(\text{thf})][\text{B}(\text{C}_6\text{H}_3-3,5-\text{Me}_2)_4]_2 \cdot 2.5\text{THF}$ (**7**).

3.21. Kinetic studies on hydrogenolysis/deuterogenolysis of
[(Me₄TACD)Yb(η⁶-PhCH₂)][B(C₆H₃-3,5-Me₂)₄] (**6**)

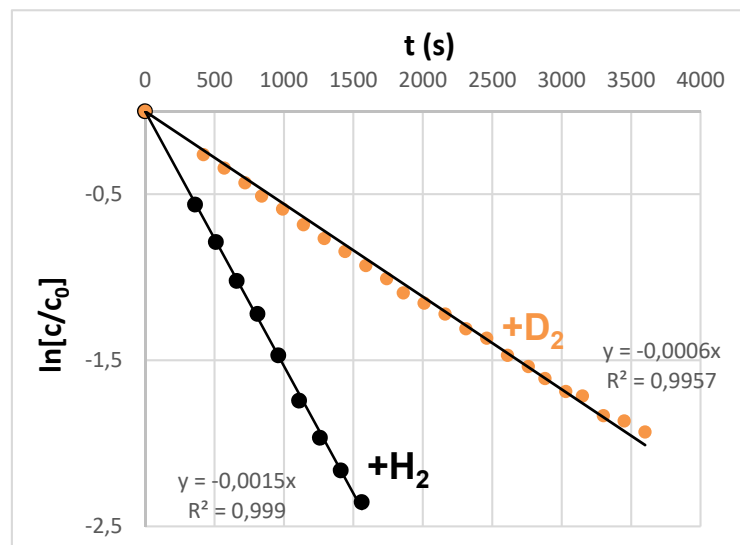


Fig. S28. Pseudo first-order plot for the hydrogenolysis/deuterogenolysis of
[(Me₄TACD)Yb(η⁶-PhCH₂)][B(C₆H₃-3,5-Me₂)₄] (**6**).

3.22. IR Spectrum of $[(\text{Me}_4\text{TACD})_2\text{Yb}_2(\mu_2-\text{H})_2(\text{thf})][\text{B}(\text{C}_6\text{H}_3-3,5-\text{Me}_2)_4]_2 \bullet 2.5\text{THF}$ (**7**)

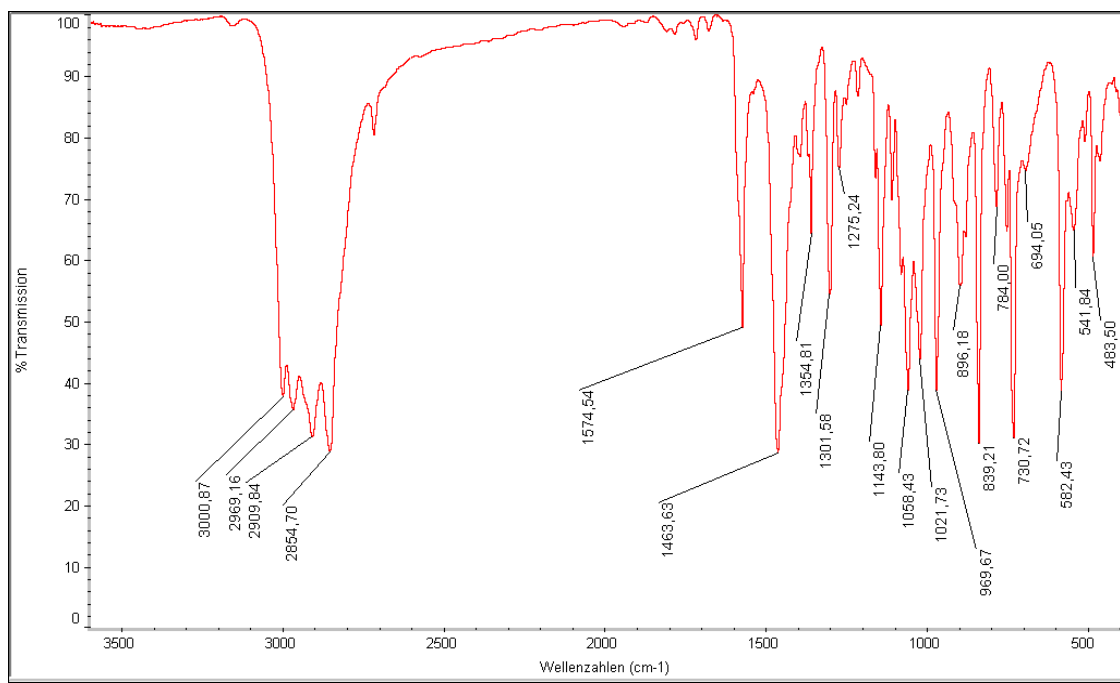


Fig. S29. IR spectrum (KBr) of $[(\text{Me}_4\text{TACD})_2\text{Yb}_2(\mu_2-\text{H})_2(\text{thf})][\text{B}(\text{C}_6\text{H}_3-3,5-\text{Me}_2)_4]_2 \bullet 2.5\text{THF}$ (**7**).

3.23. IR Spectrum of $[(\text{Me}_4\text{TACD})_2\text{Yb}_2(\mu_2-\text{D})_2(\text{thf})][\text{B}(\text{C}_6\text{H}_3-3,5-\text{Me}_2)_4]_2 \bullet 2.5\text{THF}$ (**[D₂]-7**)

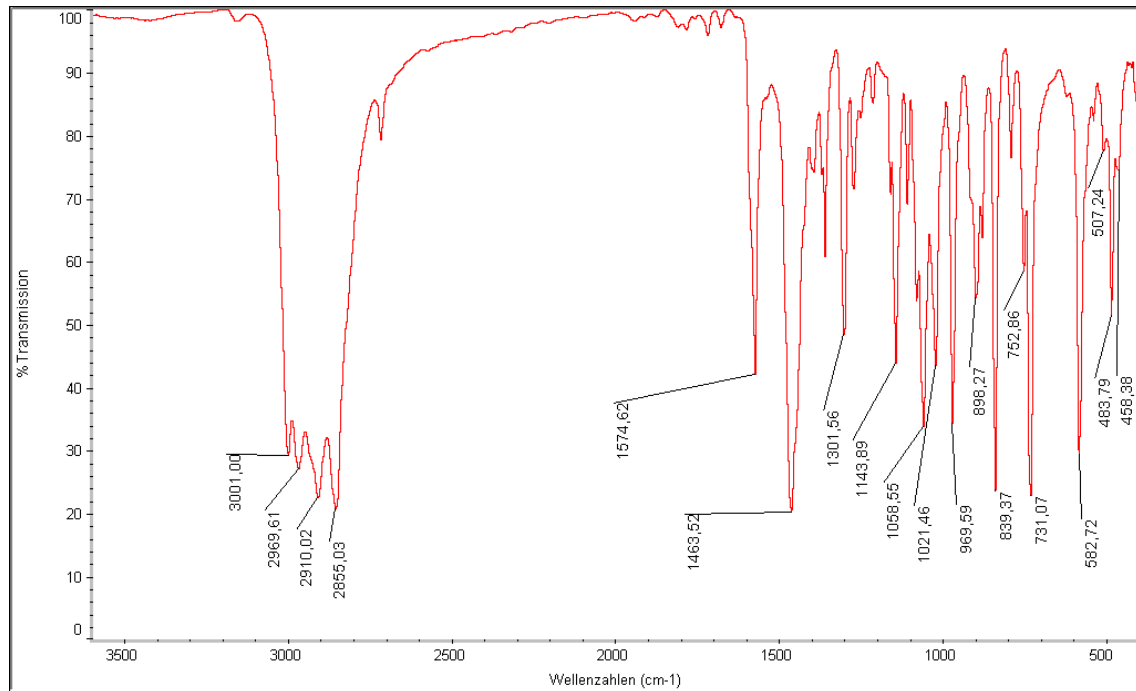


Fig. S30. IR spectrum (KBr) of $[(\text{Me}_4\text{TACD})_2\text{Yb}_2(\mu_2-\text{D})_2(\text{thf})][\text{B}(\text{C}_6\text{H}_3-3,5-\text{Me}_2)_4]_2 \bullet 2.5\text{THF}$ (**[D₂]-7**).

3.24. Synthesis of $[(\text{Me}_4\text{TACD})_2\text{Yb}_2(\mu_2\text{-H})_3][\text{B}(\text{C}_6\text{H}_3\text{-3,5-Me}_2)_4]\bullet\text{THF}$ (**8**)

In a glass autoclave, to a suspension of $[(\text{Me}_4\text{TACD})\text{Yb}(\text{CH}_2\text{Ph})_2]$ (**5**) (58 mg, 0.1 mmol) in THF (2 mL) was added dropwise a solution of $[(\text{Me}_4\text{TACD})\text{Yb}(\eta^6\text{-PhCH}_2)][\text{B}(\text{C}_6\text{H}_3\text{-3,5-Me}_2)_4]$ (**6**) (92 mg, 0.1 mmol) in THF (3 mL) at room temperature. The suspension was degassed, charged with H_2 (1 bar) and stirred for 2 h. The volume of the reaction mixture was reduced to 2 mL, the solution filtered, layered with *n*-pentane (5 mL) and stored at –30 °C. After 16 h, violet microcrystals formed. The supernatant was decanted off and the crystals were washed with *n*-pentane (3 x 2 mL). After drying *in vacuo*, $[(\text{Me}_4\text{TACD})_2\text{Yb}_2(\mu_2\text{-H})_3][\text{B}(\text{C}_6\text{H}_3\text{-3,5-Me}_2)_4]\bullet\text{THF}$ (**8**) was isolated as violet microcrystals (114 mg, 92 µmol); yield: 92%.

$[(\text{Me}_4\text{TACD})_2\text{Yb}_2(\mu_2\text{-D})_3][\text{B}(\text{C}_6\text{H}_3\text{-3,5-Me}_2)_4]\bullet\text{THF}$ (**[D₃]-8**) was prepared analogously using D₂.

¹H NMR (400 MHz, [D₈]THF, 25 °C): δ = 1.75 – 1.80 (m, 4 H, THF), 2.07 (s, 24 H, Ar-CH₃), 2.15 – 2.47 (br, 16 H, NCH₂), 2.47 – 2.73 (s + br, 40 H, NCH₃ + NCH₂), 3.60 – 3.64 (m, 4 H, THF), 6.31 – 6.36 (m, 4 H, *para*-C₆H₃), 6.93 – 6.99 (m, 8 H, *ortho*-C₆H₃), 7.54 (s, ¹J_{YbH} = 301 Hz, YbH) ppm.

²H NMR (61 MHz, THF, 25 °C): δ = 7.62 (s, ¹J_{YbD} = 28 Hz, YbD) ppm.

¹³C{¹H} NMR (101 MHz, [D₈]THF, 25 °C): δ = 22.44 (Ar-CH₃), 26.30 (THF), 45.81 (NCH₃), 54.20 (NCH₂), 68.27 (THF), 123.46 (*para*-C₆H₃), 132.75 (q, ³J_{BC} = 2.8 Hz, *meta*-C₆H₃), 135.56 (*ortho*-C₆H₃), 165.74 (q, ¹J_{BC} = 49.3 Hz, *ipso*-C₆H₃) ppm.

¹¹B{¹H} NMR (128 MHz, [D₈]THF, 25 °C): δ = –6.90 ppm.

¹⁷¹Yb NMR (71 MHz, [D₈]THF, 25 °C): δ = 990 (q, ¹J_{YbH} = 300 Hz, YbH) ppm.

Anal. calc. for C₅₆H₉₅N₈BYb₂ (1237.35 g mol^{–1}): C, 54.36; H, 7.74; N, 9.06. Found: C, 54.25; H, 7.66; N, 8.87%.

IR (**8**, KBr): $\tilde{\nu}$ = 2971 (s), 2908 (s), 2852 (s), 1575 (s), 1460 (s), 1359 (w), 1301 (m), 1272 (w), 1147 (m), 1084 (w), 1062 (w), 1026 (m), 970 (m), 902 (w), 839 (m), 792 (w), 754 (w), 754 (w), 736 (m), 581 (m), 503 (w), 465 (w) cm^{–1}.

IR (**[D₃]-8**, KBr): $\tilde{\nu}$ = 2972 (s), 2906 (s), 2851 (s), 1573 (s), 1460 (s), 1355 (w), 1300 (m), 1264 (w), 1146 (m), 1086 (w), 1062 (w), 1027 (m), 970 (m), 902 (w), 838 (m), 792 (w), 753 (w), 735 (m), 663 (w), 580 (m), 504 (w), 462 (w) cm^{–1}.

UV-Vis (THF, 25 °C): λ_{max} (ϵ , mol L^{–1} cm^{–1}) = 349 nm (2295); λ = 569 nm (1000).

3.25. ^1H , ^2H , $^{13}\text{C}\{^1\text{H}\}$ and $^{11}\text{B}\{^1\text{H}\}$ NMR spectra of
 $[(\text{Me}_4\text{TACD})_2\text{Yb}_2(\mu_2\text{-H})_3][\text{B}(\text{C}_6\text{H}_3\text{-3,5-Me}_2)_4]\bullet\text{THF}$ (**8**)

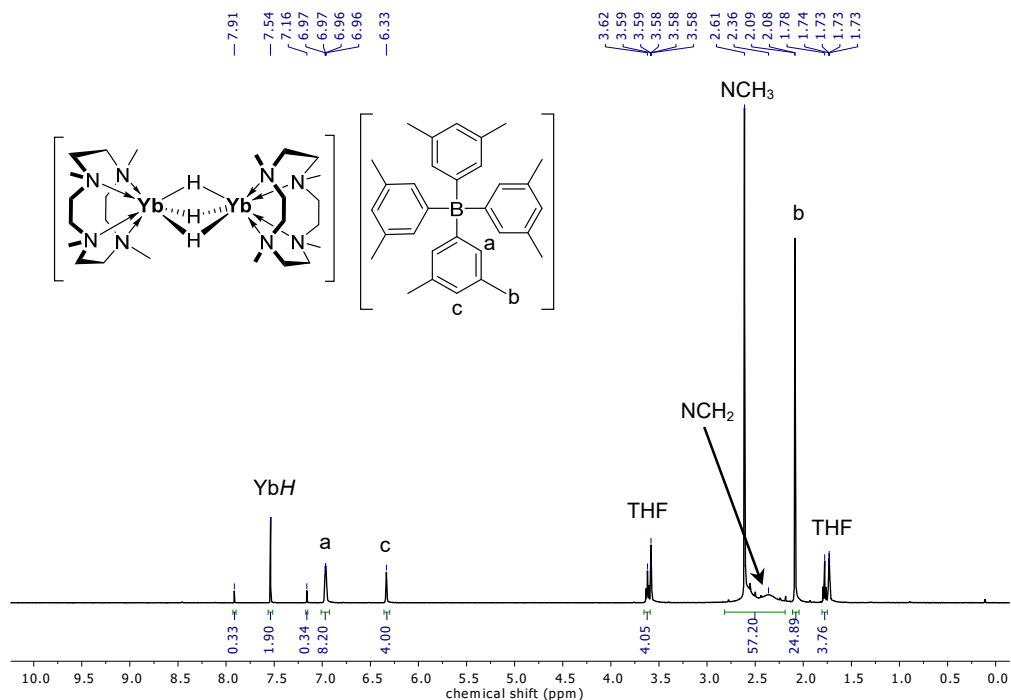


Fig. S31. ^1H NMR spectrum (400 MHz, $[\text{D}_8]\text{THF}$, 25 °C) of
 $[(\text{Me}_4\text{TACD})_2\text{Yb}_2(\mu_2\text{-H})_3][\text{B}(\text{C}_6\text{H}_3\text{-3,5-Me}_2)_4]\bullet\text{THF}$ (**8**).

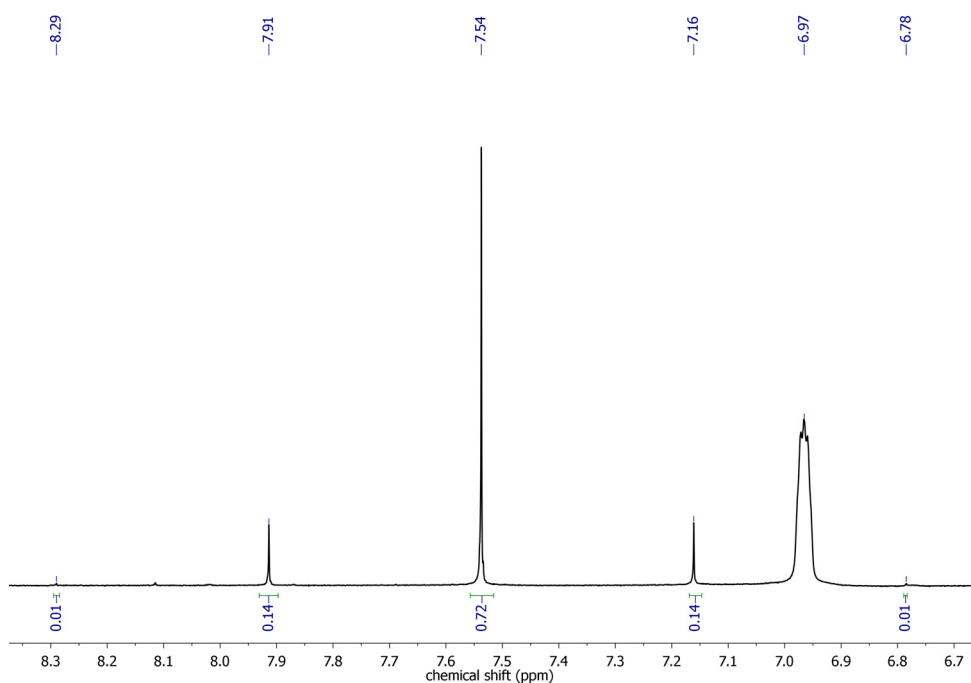


Fig. S32. ^1H NMR spectrum (400 MHz, $[\text{D}_8]\text{THF}$, 25 °C) of
 $[(\text{Me}_4\text{TACD})_2\text{Yb}_2(\mu_2\text{-H})_3][\text{B}(\text{C}_6\text{H}_3\text{-3,5-Me}_2)_4]\bullet\text{THF}$ (**8**) in the region of 6.7–8.4 ppm.

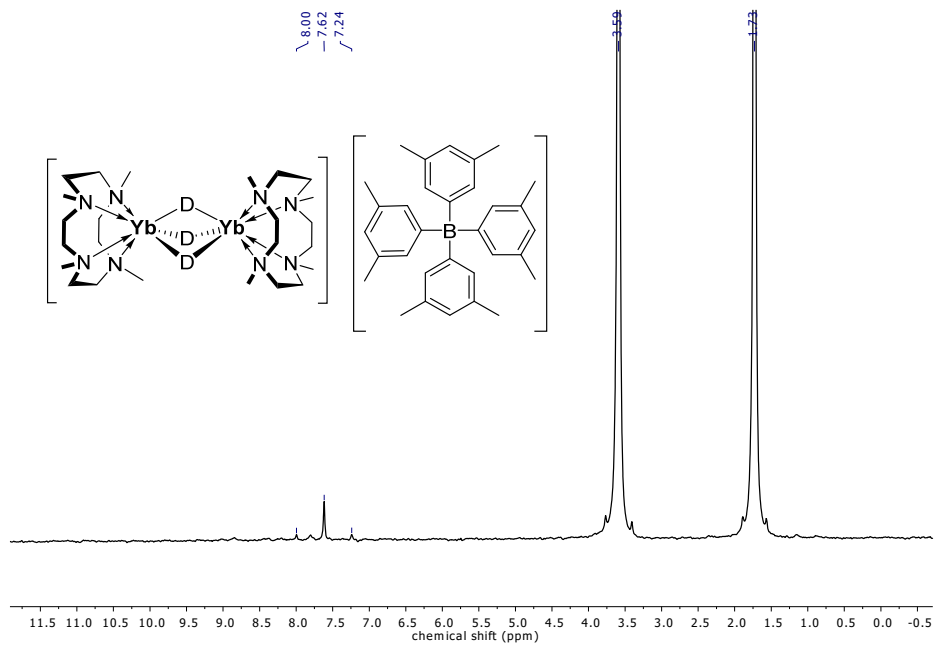


Fig. S33. ^2H NMR spectrum (61 MHz, THF, 25 °C) of $[(\text{Me}_4\text{TACD})_2\text{Yb}_2(\mu_2-\text{D})_3][\text{B}(\text{C}_6\text{H}_3-3,5-\text{Me}_2)_4]\bullet\text{THF}$ (D_3 -8).

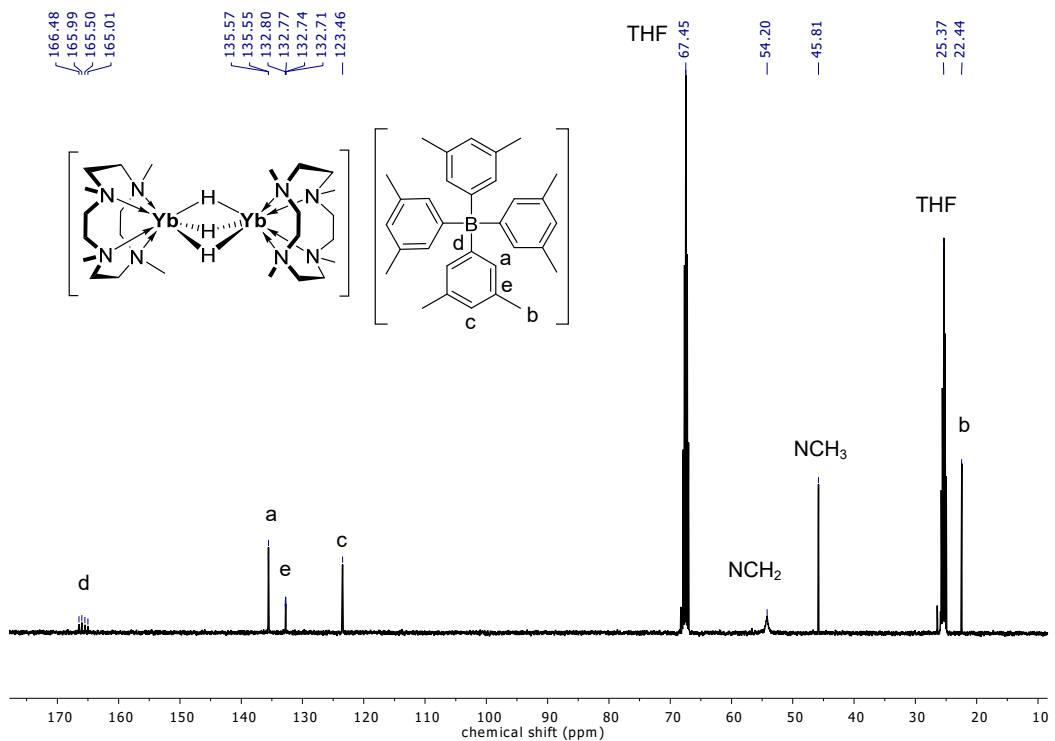


Fig. S34. $^{13}\text{C}\{\text{H}\}$ NMR spectrum (101 MHz, $[\text{D}_8]\text{THF}$, 25 °C) of $[(\text{Me}_4\text{TACD})_2\text{Yb}_2(\mu_2-\text{H})_3][\text{B}(\text{C}_6\text{H}_3-3,5-\text{Me}_2)_4]\bullet\text{THF}$ (8).

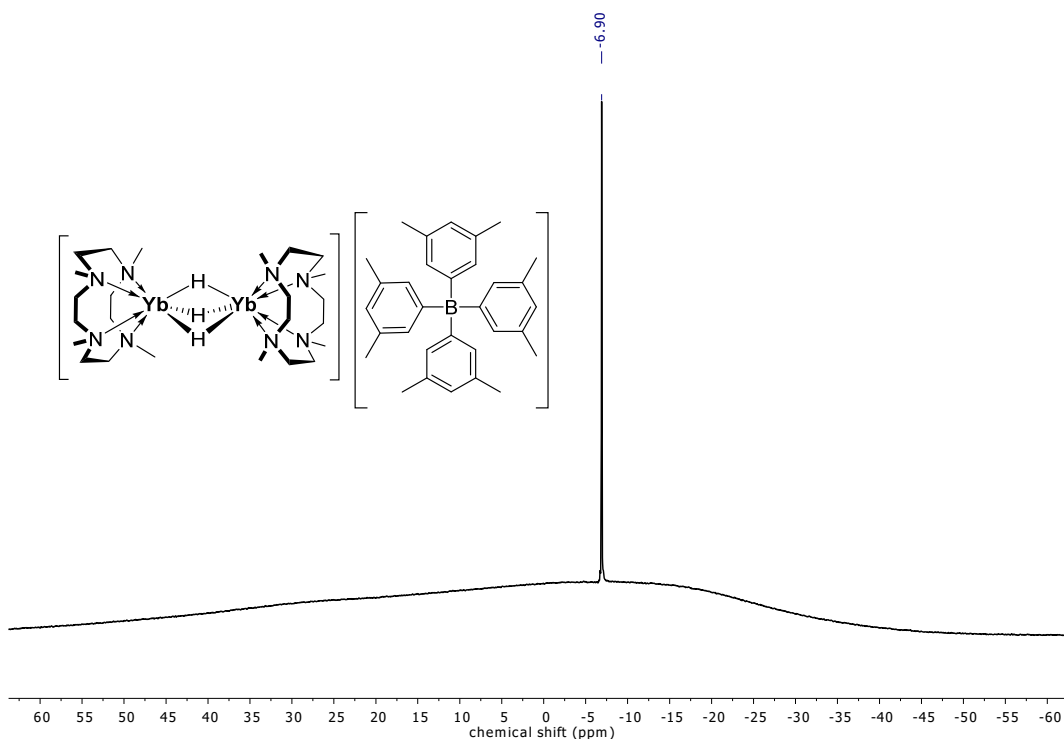


Fig. S35. $^{11}\text{B}\{^1\text{H}\}$ NMR spectrum (128 MHz, $[\text{D}_8]\text{THF}$, 25 °C) of $[(\text{Me}_4\text{TACD})_2\text{Yb}_2(\mu_2\text{-H})_3][\text{B}(\text{C}_6\text{H}_3-3,5\text{-Me}_2)_4]\bullet\text{THF}$ (**8**).

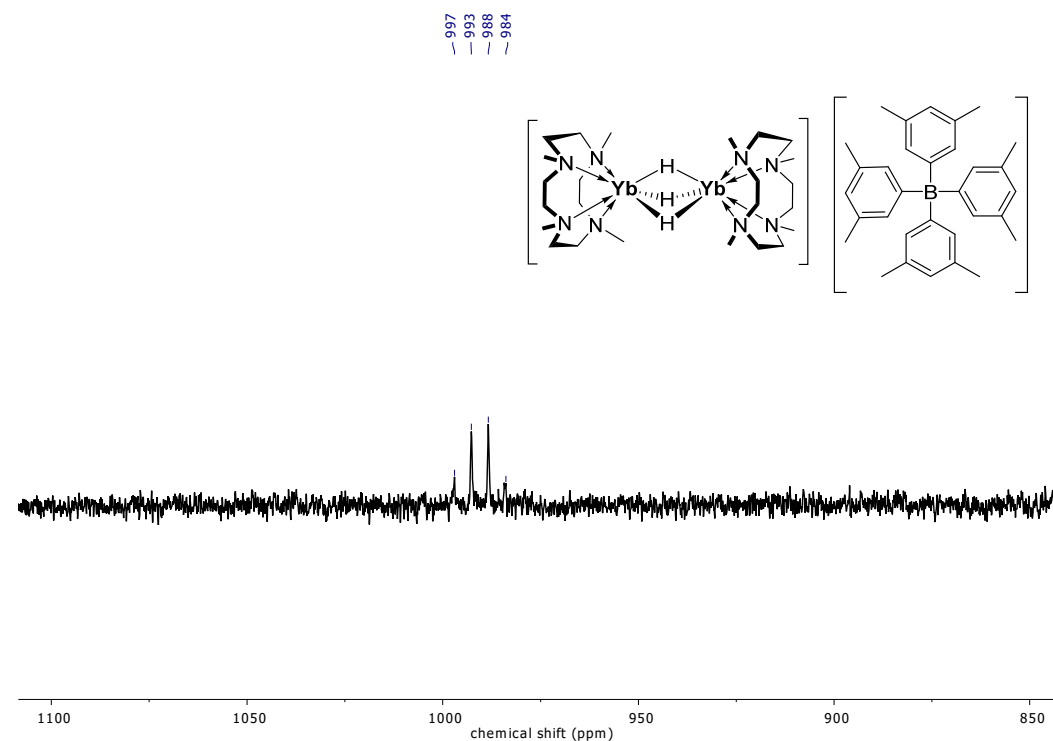


Fig. S36. ^{171}Yb NMR spectrum (71 MHz, $[\text{D}_8]\text{THF}$, 25 °C) of $[(\text{Me}_4\text{TACD})_2\text{Yb}_2(\mu_2\text{-H})_3][\text{B}(\text{C}_6\text{H}_3-3,5\text{-Me}_2)_4]\bullet\text{THF}$ (**8**).

3.26. UV-Vis Spectrum of $[(\text{Me}_4\text{TACD})_2\text{Yb}_2(\mu_2\text{-H})_3][\text{B}(\text{C}_6\text{H}_3\text{-3,5-Me}_2)_4]\bullet\text{THF}$ (**8**)

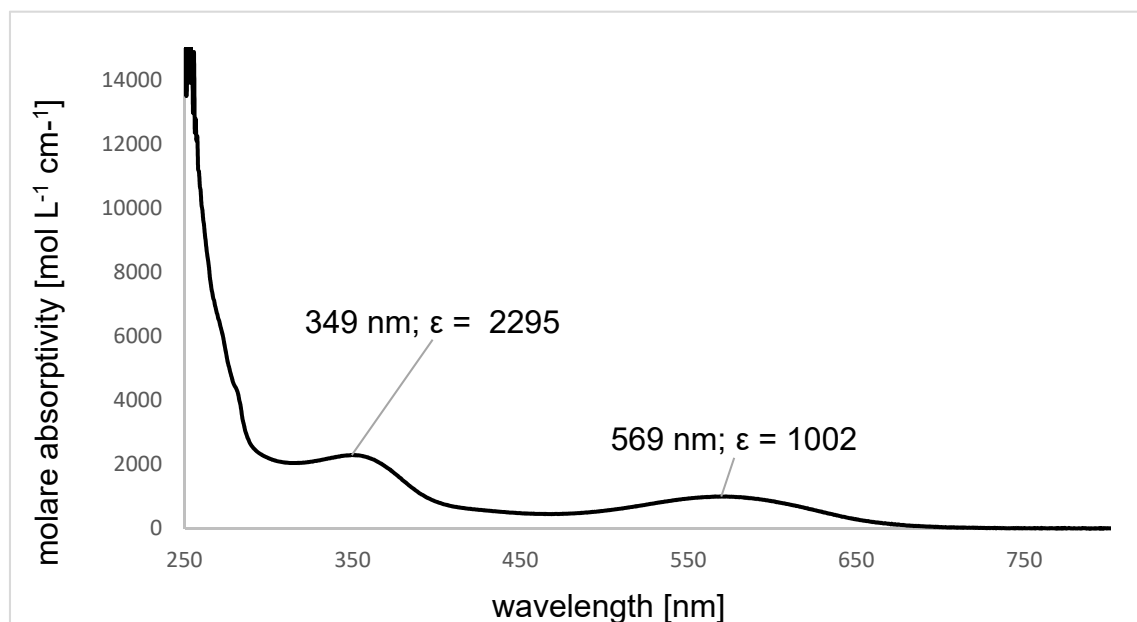


Fig. S37. UV-Vis spectrum (THF, 25 °C) of $[(\text{Me}_4\text{TACD})_2\text{Yb}_2(\mu_2\text{-H})_3][\text{B}(\text{C}_6\text{H}_3\text{-3,5-Me}_2)_4]\bullet\text{THF}$ (**8**).

3.27. IR Spectrum of $[(\text{Me}_4\text{TACD})_2\text{Yb}_2(\mu_2\text{-H})_3][\text{B}(\text{C}_6\text{H}_3\text{-3,5-Me}_2)_4]\bullet\text{THF}$ (**8**).

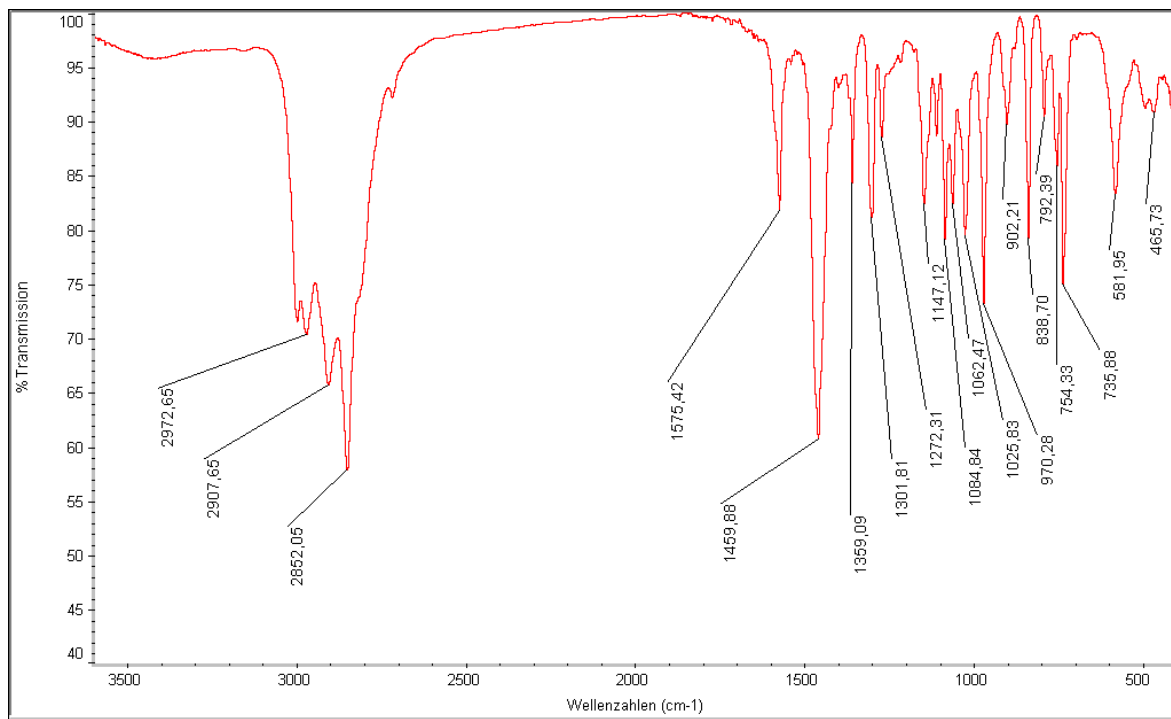


Fig. S38. IR spectrum (KBr) of $[(\text{Me}_4\text{TACD})_2\text{Yb}_2(\mu_2\text{-H})_3][\text{B}(\text{C}_6\text{H}_3\text{-3,5-Me}_2)_4]\bullet\text{THF}$ (**8**).

3.28. IR Spectrum of $[(\text{Me}_4\text{TACD})_2\text{Yb}_2(\mu_2\text{-D})_3][\text{B}(\text{C}_6\text{H}_3\text{-3,5-Me}_2)_4]\bullet\text{THF}$ (**[D₃]-8**).

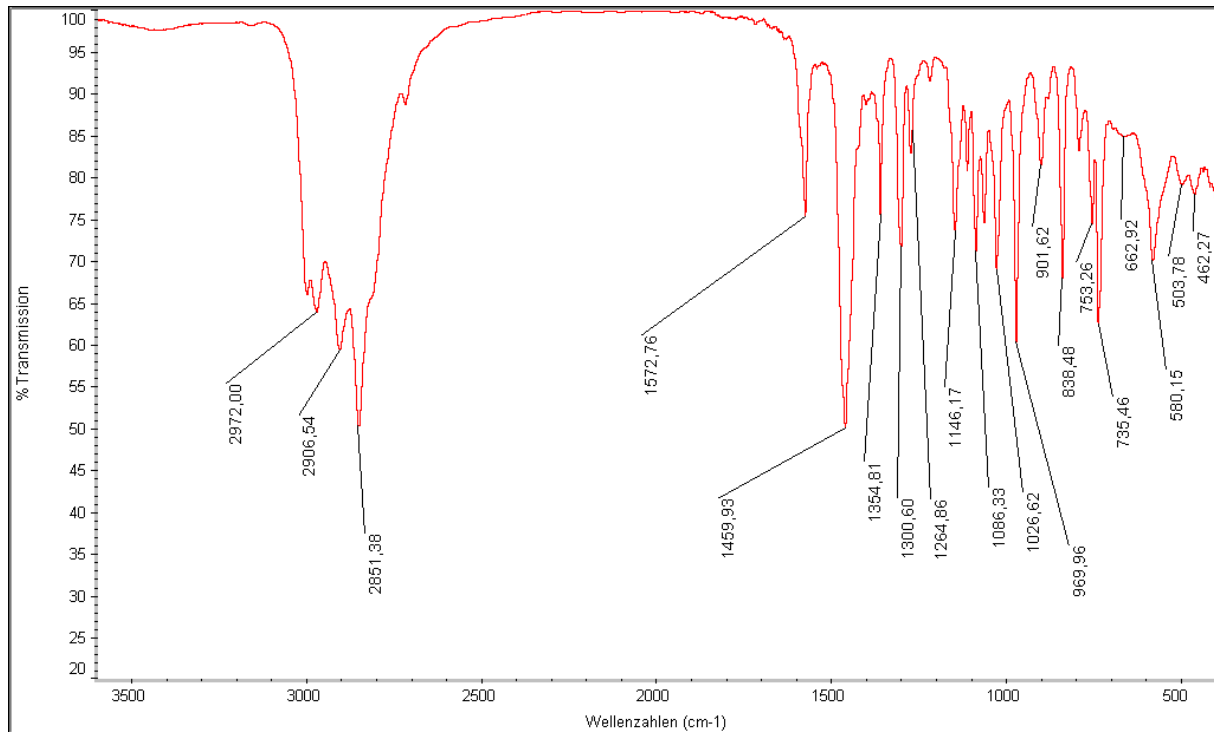


Fig. S39. IR spectrum of $[(\text{Me}_4\text{TACD})_2\text{Yb}_2(\mu_2\text{-D})_3][\text{B}(\text{C}_6\text{H}_3\text{-3,5-Me}_2)_4]\bullet\text{THF}$ (**[D₃]-8**).

3.29. Synthesis of $[(\text{Me}_4\text{TACD})\text{Yb}(\text{thf})_2][\text{B}(\text{C}_6\text{H}_3\text{-3,5-Me}_2)_4]_2$ (**9**)

To a stirred suspension of $[(\text{Me}_4\text{TACD})\text{Yb}(\text{CH}_2\text{Ph})_2]$ (**5**) (58 mg, 0.1 mmol) in THF (2 mL) was added dropwise a solution of $[\text{NEt}_3\text{H}][\text{B}(\text{C}_6\text{H}_3\text{-3,5-Me}_2)_4]$ (106 mg, 0.2 mmol) in THF (5 mL) at room temperature. After 5 min, the yellow solution was filtered, its volume reduced to 3 mL and layered with *n*-pentane (5 mL). After 16 h, yellow microcrystals formed. The solution was decanted off, the crystals were washed with *n*-pentane (3 x 2 mL) and dried under reduced pressure to give $[(\text{Me}_4\text{TACD})\text{Yb}(\text{thf})_2][\text{B}(\text{C}_6\text{H}_3\text{-3,5-Me}_2)_4]_2$ (**9**) as yellow microcrystals (126 mg, 89 μmol); yield: 89%.

^1H NMR (400 MHz, $[\text{D}_8]\text{THF}$, 25 °C): δ = 1.75 – 1.80 (m, 8 H, THF), 2.00 – 2.65 (br, 76 H, $\text{NCH}_3 + \text{NCH}_2 + \text{Ar-CH}_3$), 3.60 – 3.64 (m, 8 H, THF), 6.35 – 6.45 (m, 8 H, *para-C₆H₃*), 6.95 – 7.05 (m, 16 H, *ortho-C₆H₃*) ppm.

$^{13}\text{C}\{\text{H}\}$ NMR (101 MHz, $[\text{D}_8]\text{THF}$, 25 °C): δ = 22.41 (Ar-CH₃), 26.44 (THF), 44.88 (NCH₃), 54.12 (br, NCH₂), 68.28 (THF), 123.61 (*para-C₆H₃*), 133.02 (q, $^3J_{\text{BC}} = 3.0$ Hz, *meta-C₆H₃*), 135.52 (*ortho-C₆H₃*), 165.68 (q, $^1J_{\text{BC}} = 49.5$ Hz, *ipso-C₆H₃*) ppm.

$^{11}\text{B}\{\text{H}\}$ NMR (128 MHz, $[\text{D}_8]\text{THF}$, 25 °C): δ = –6.99 ppm.

Anal. calc. for $\text{C}_{84}\text{H}_{116}\text{N}_4\text{B}_2\text{O}_2\text{Yb}$ (1408.50 g mol^{–1}): C, 71.63; H, 8.30; N, 3.98. Found: C, 67.00; H, 7.70; N, 4.05%.

3.30. ^1H , $^{13}\text{C}\{^1\text{H}\}$ and $^{11}\text{B}\{^1\text{H}\}$ NMR spectra of $[(\text{Me}_4\text{TACD})\text{Yb}(\text{thf})_2][\text{B}(\text{C}_6\text{H}_3\text{-3,5-Me}_2)_4]_2$ (**9**)

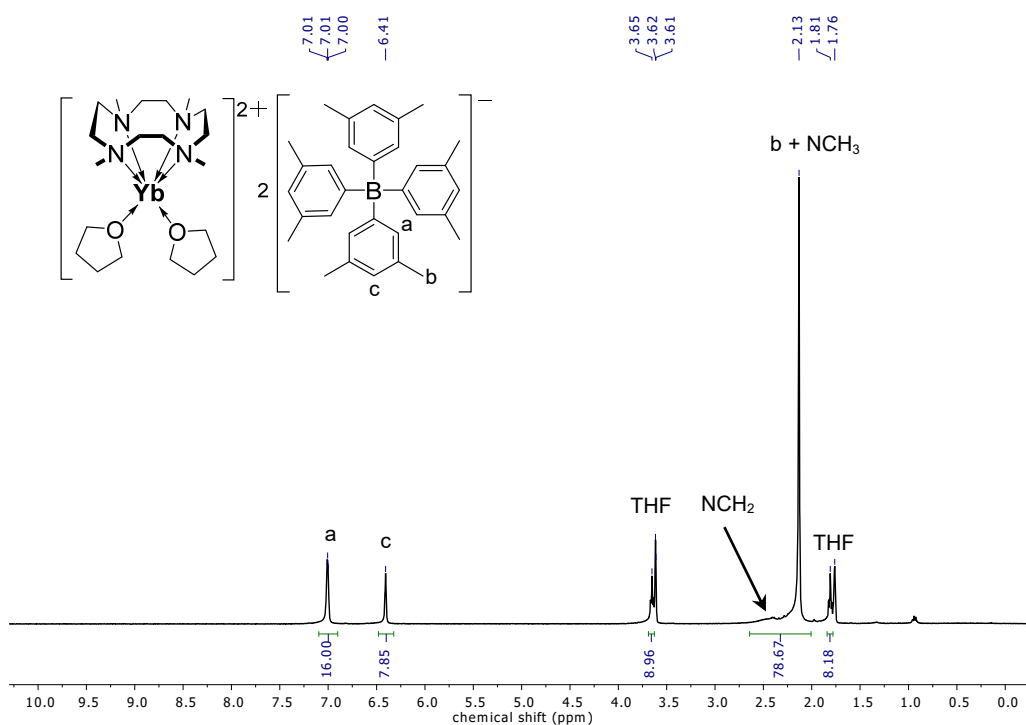


Fig. S40. ^1H NMR spectrum (400 MHz, $[\text{D}_8]\text{THF}$, 25 °C) of $[(\text{Me}_4\text{TACD})\text{Yb}(\text{thf})_2][\text{B}(\text{C}_6\text{H}_3\text{-3,5-Me}_2)_4]_2$ (**9**).

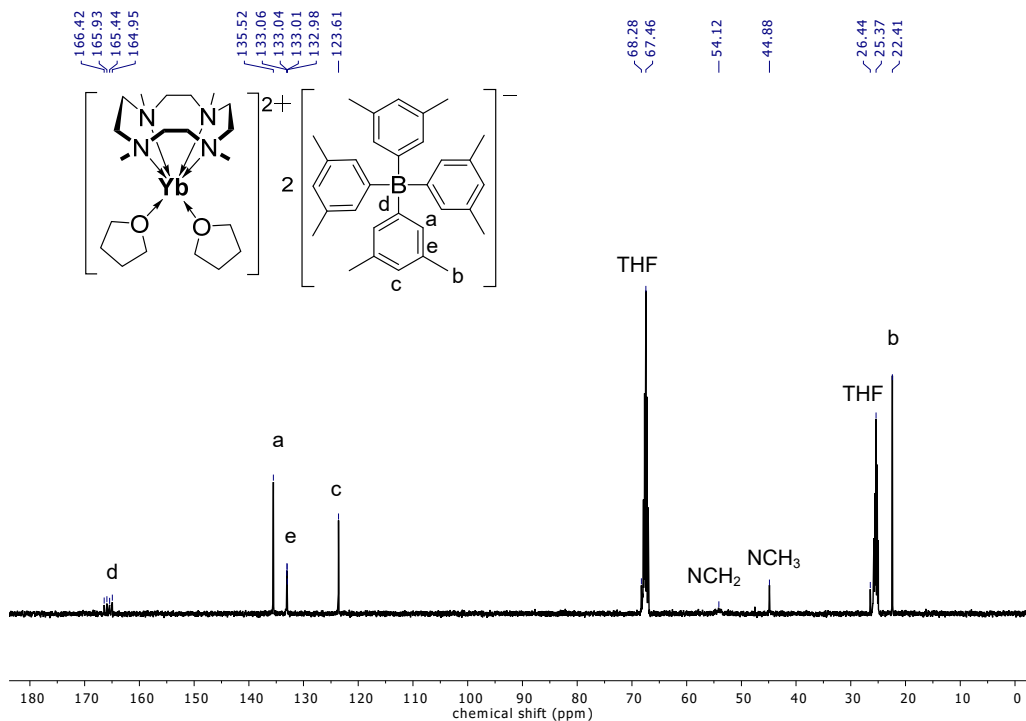


Fig. S41. $^{13}\text{C}\{^1\text{H}\}$ NMR spectrum (101 MHz, $[\text{D}_8]\text{THF}$, 25 °C) of $[(\text{Me}_4\text{TACD})\text{Yb}(\text{thf})_2][\text{B}(\text{C}_6\text{H}_3\text{-3,5-Me}_2)_4]_2$ (**9**).

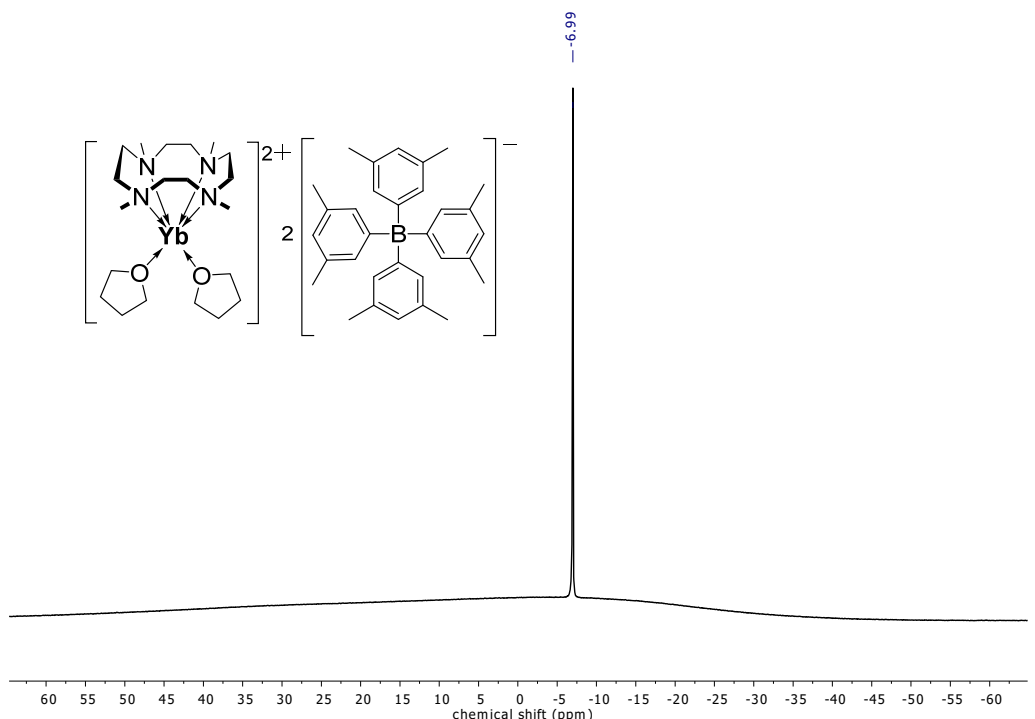


Fig. S42. $^{11}\text{B}\{^1\text{H}\}$ NMR spectrum (128 MHz, $[\text{D}_8]\text{THF}$, 25 °C) of $[(\text{Me}_4\text{TACD})\text{Yb}(\text{thf})_2][\text{B}(\text{C}_6\text{H}_3\text{-}3,5\text{-Me}_2)_4]_2$ (**9**).

3.31. UV-Vis Spectrum of $[(\text{Me}_4\text{TACD})\text{Yb}(\text{thf})_2][\text{B}(\text{C}_6\text{H}_3\text{-}3,5\text{-Me}_2)_4]_2$ (**9**)

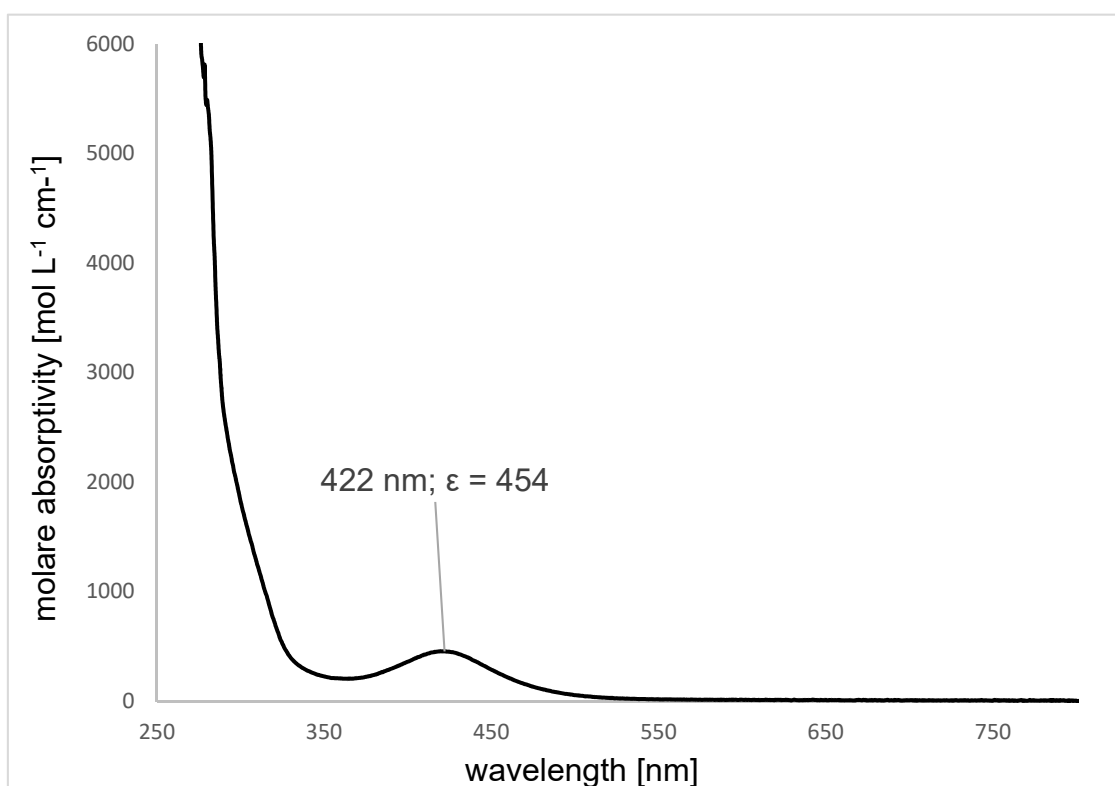


Fig. S43. UV-Vis spectrum (THF, 25 °C) of $[(\text{Me}_4\text{TACD})\text{Yb}(\text{thf})_2][\text{B}(\text{C}_6\text{H}_3\text{-}3,5\text{-Me}_2)_4]_2$ (**9**).

3.32. Deuterolysis of $[(\text{Me}_4\text{TACD})_2\text{Yb}_2(\mu_2\text{-H})_2(\text{thf})][\text{B}(\text{C}_6\text{H}_3\text{-3,5-Me}_2)_4]_2 \bullet 2.5\text{THF}$ (**7**)

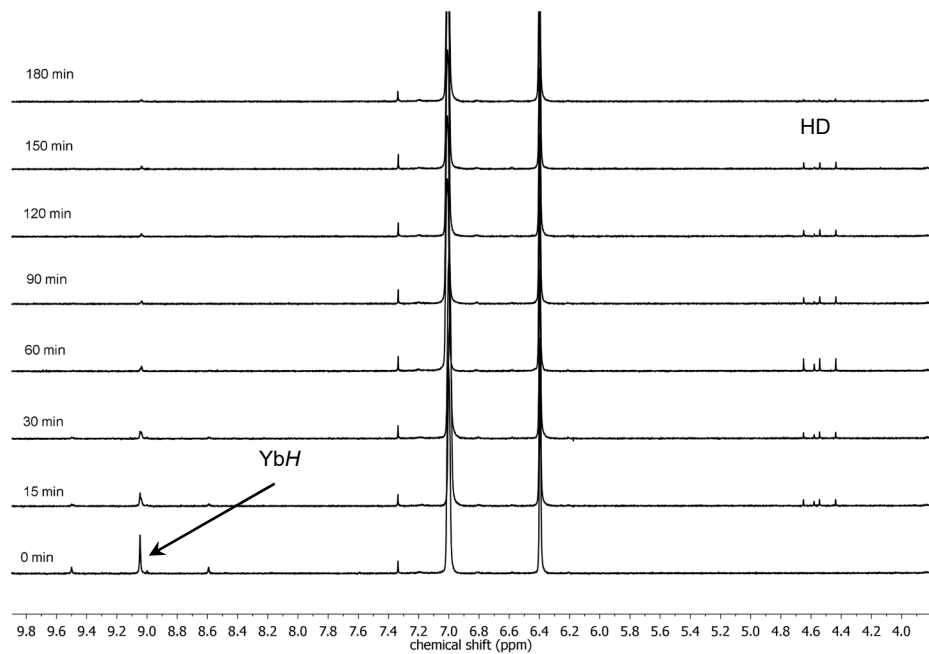


Fig. S44. Deuterolysis of $[(\text{Me}_4\text{TACD})_2\text{Yb}_2(\mu_2\text{-H})_2(\text{thf})][\text{B}(\text{C}_6\text{H}_3\text{-3,5-Me}_2)_4]_2 \bullet 2.5\text{THF}$ (**7**).

3.33. Deuterolysis of $[(\text{Me}_4\text{TACD})_2\text{Yb}_2(\mu_2\text{-H})_3][\text{B}(\text{C}_6\text{H}_3\text{-3,5-Me}_2)_4] \bullet \text{THF}$ (**8**)

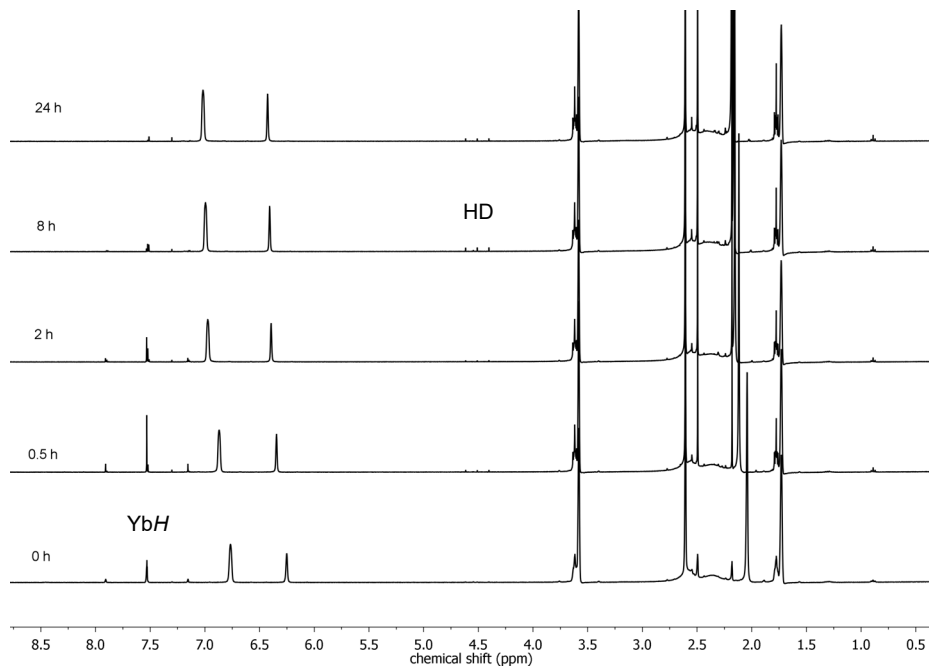


Fig. S45. Deuterolysis of $[(\text{Me}_4\text{TACD})_2\text{Yb}_2(\mu_2\text{-H})_3][\text{B}(\text{C}_6\text{H}_3\text{-3,5-Me}_2)_4] \bullet \text{THF}$ (**8**).

3.34. Scrambling of **7** with $[(\text{Me}_4\text{TACD})_2\text{Ca}_2(\mu_2\text{-H})_2(\text{thf})_x][\text{B}(\text{C}_6\text{H}_3\text{-3,5-Me}_2)_4]_2$

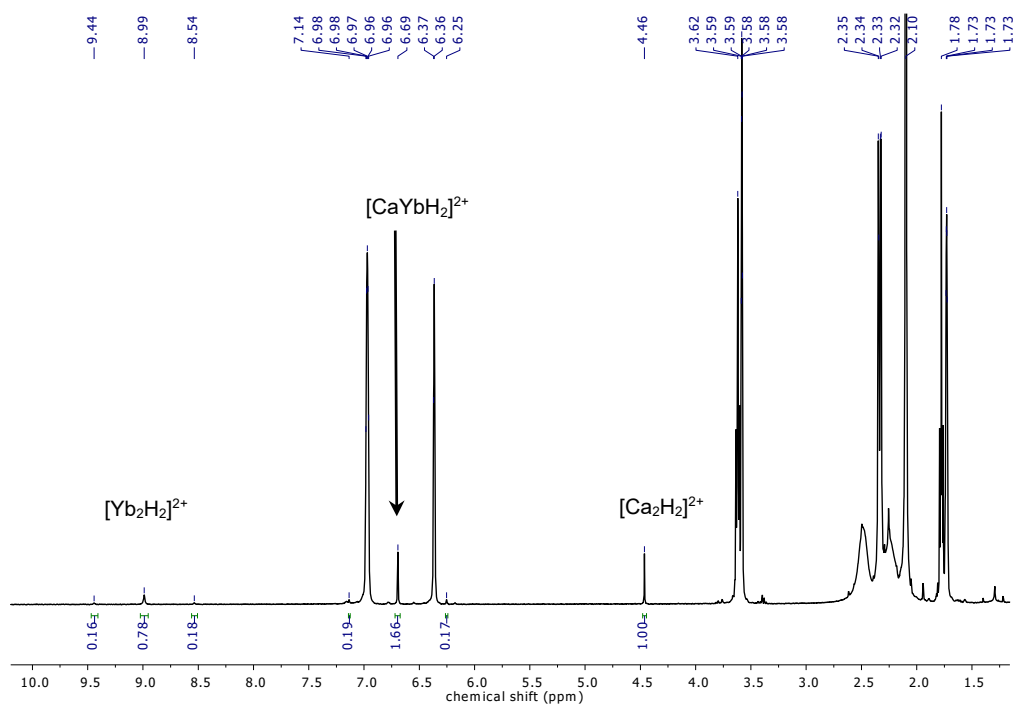


Fig. S46. ^1H NMR spectrum (400 MHz, $[\text{D}_8]\text{THF}$, 25 °C) of an equimolar mixture of $[(\text{Me}_4\text{TACD})_2\text{Ca}_2(\mu_2\text{-H})_2(\text{thf})][\text{B}(\text{C}_6\text{H}_3\text{-3,5-Me}_2)_4]_2$, $[(\text{Me}_4\text{TACD})_2\text{Yb}_2(\mu_2\text{-H})_2(\text{thf})][\text{B}(\text{C}_6\text{H}_3\text{-3,5-Me}_2)_4]_2$ (**7**) and $[(\text{Me}_4\text{TACD})_2\text{CaYb}(\mu_2\text{-H})_2(\text{thf})_x][\text{B}(\text{C}_6\text{H}_3\text{-3,5-Me}_2)_4]_2$.

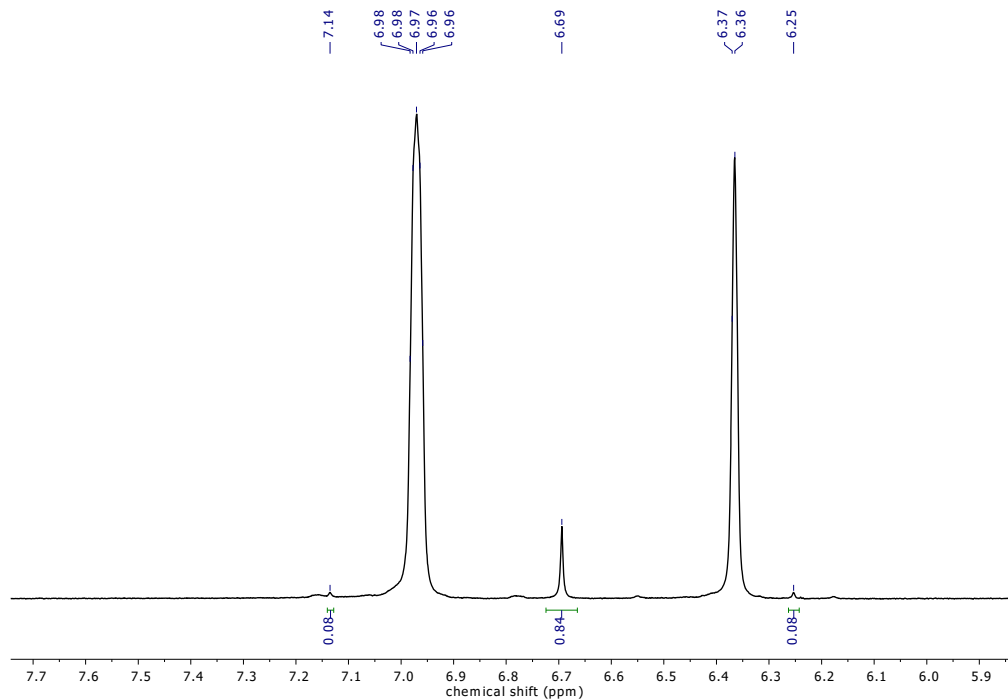


Fig. S47. ^1H NMR spectrum (400 MHz, $[\text{D}_8]\text{THF}$, 25 °C) of the equimolar mixture of $[(\text{Me}_4\text{TACD})_2\text{Ca}_2(\mu_2\text{-H})_2(\text{thf})][\text{B}(\text{C}_6\text{H}_3\text{-3,5-Me}_2)_4]_2$, $[(\text{Me}_4\text{TACD})_2\text{Yb}_2(\mu_2\text{-H})_2(\text{thf})][\text{B}(\text{C}_6\text{H}_3\text{-3,5-Me}_2)_4]_2$ (**7**) and $[(\text{Me}_4\text{TACD})_2\text{CaYb}(\mu_2\text{-H})_2(\text{thf})_x][\text{B}(\text{C}_6\text{H}_3\text{-3,5-Me}_2)_4]_2$ between 5.9 – 7.7 ppm.

3.35. Scrambling of **8** with $[(\text{Me}_4\text{TACD})_2\text{Ca}_2(\mu_2\text{-H})_3(\text{thf})_x][\text{B}(\text{C}_6\text{H}_3\text{-3,5-Me}_2)_4]$

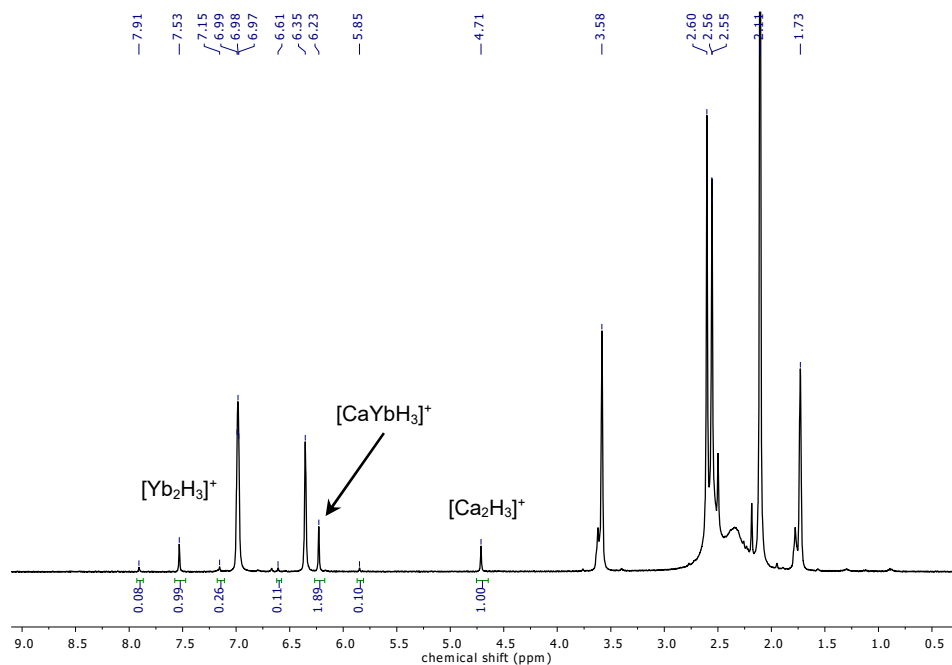


Fig. S48. ^1H NMR spectrum (400 MHz, $[\text{D}_8]\text{THF}$, 25 °C) of an equimolar mixture of $[(\text{Me}_4\text{TACD})_2\text{Ca}_2(\mu_2\text{-H})_3][\text{B}(\text{C}_6\text{H}_3\text{-3,5-Me}_2)_4]$ and $[(\text{Me}_4\text{TACD})_2\text{Yb}_2(\mu_2\text{-H})_3][\text{B}(\text{C}_6\text{H}_3\text{-3,5-Me}_2)_4]$ (**8**) to give $[(\text{Me}_4\text{TACD})_2\text{CaYb}(\mu_2\text{-H})_3][\text{B}(\text{C}_6\text{H}_3\text{-3,5-Me}_2)_4]$.

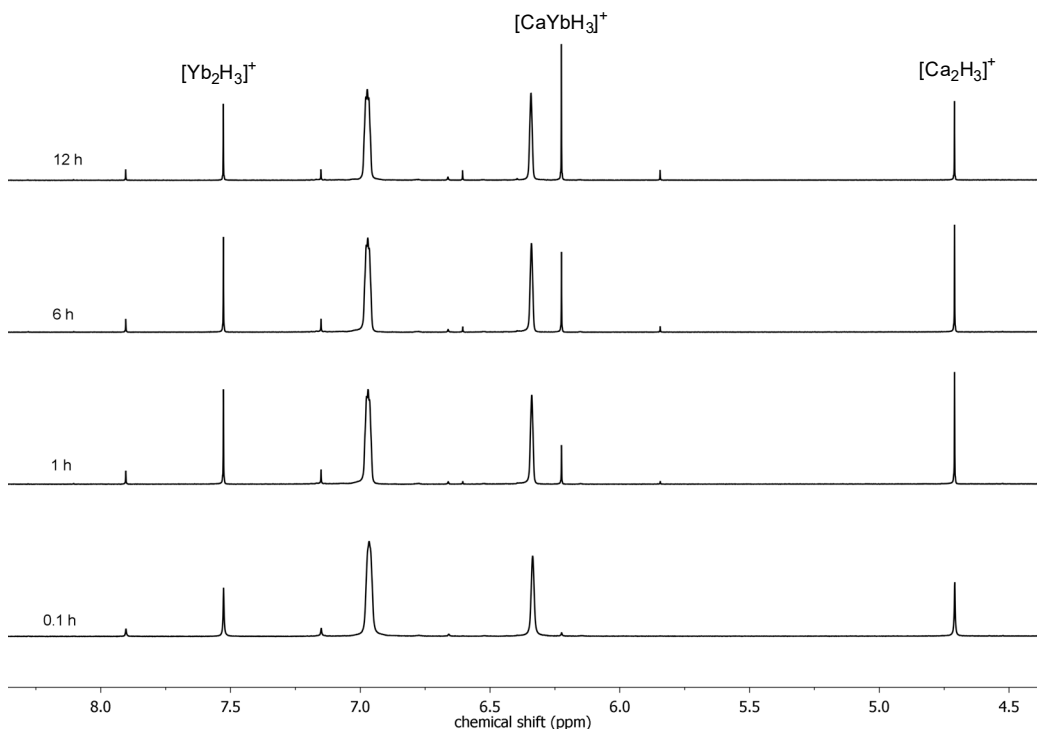


Fig. S49. ^1H NMR spectrum (400 MHz, $[\text{D}_8]\text{THF}$, 25 °C) of an equimolar mixture of $[(\text{Me}_4\text{TACD})_2\text{Yb}_2(\mu_2\text{-H})_3][\text{B}(\text{C}_6\text{H}_3\text{-3,5-Me}_2)_4]$ and $[(\text{Me}_4\text{TACD})_2\text{Ca}_2(\mu_2\text{-H})_3][\text{B}(\text{C}_6\text{H}_3\text{-3,5-Me}_2)_4]$ to give $[(\text{Me}_4\text{TACD})_2\text{CaYb}(\mu_2\text{-H})_3][\text{B}(\text{C}_6\text{H}_3\text{-3,5-Me}_2)_4]$.

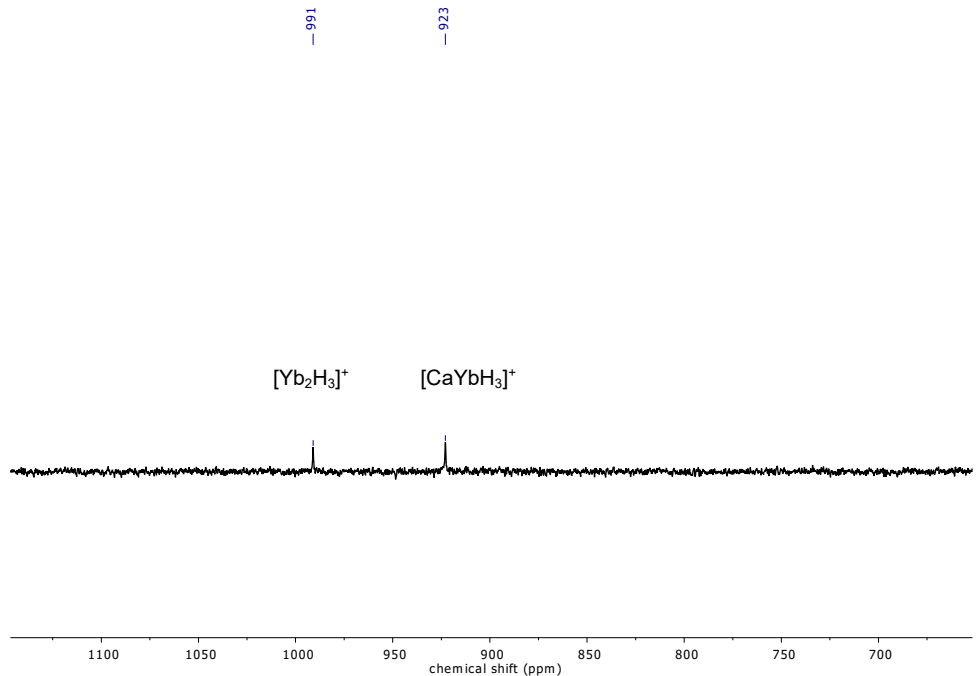


Fig. S50. $^{171}\text{Yb}\{^1\text{H}\}$ NMR spectrum (71 MHz, $[\text{D}_8]\text{THF}$, 25 °C) of an equimolar mixture of $[(\text{Me}_4\text{TACD})_2\text{Ca}_2(\mu_2\text{-H})_3][\text{B}(\text{C}_6\text{H}_3\text{-3,5-Me}_2)_4]$ and $[(\text{Me}_4\text{TACD})_2\text{Yb}_2(\mu_2\text{-H})_3][\text{B}(\text{C}_6\text{H}_3\text{-3,5-Me}_2)_4]$ (**8**) to give $[(\text{Me}_4\text{TACD})_2\text{CaYb}(\mu_2\text{-H})_3][\text{B}(\text{C}_6\text{H}_3\text{-3,5-Me}_2)_4]$.

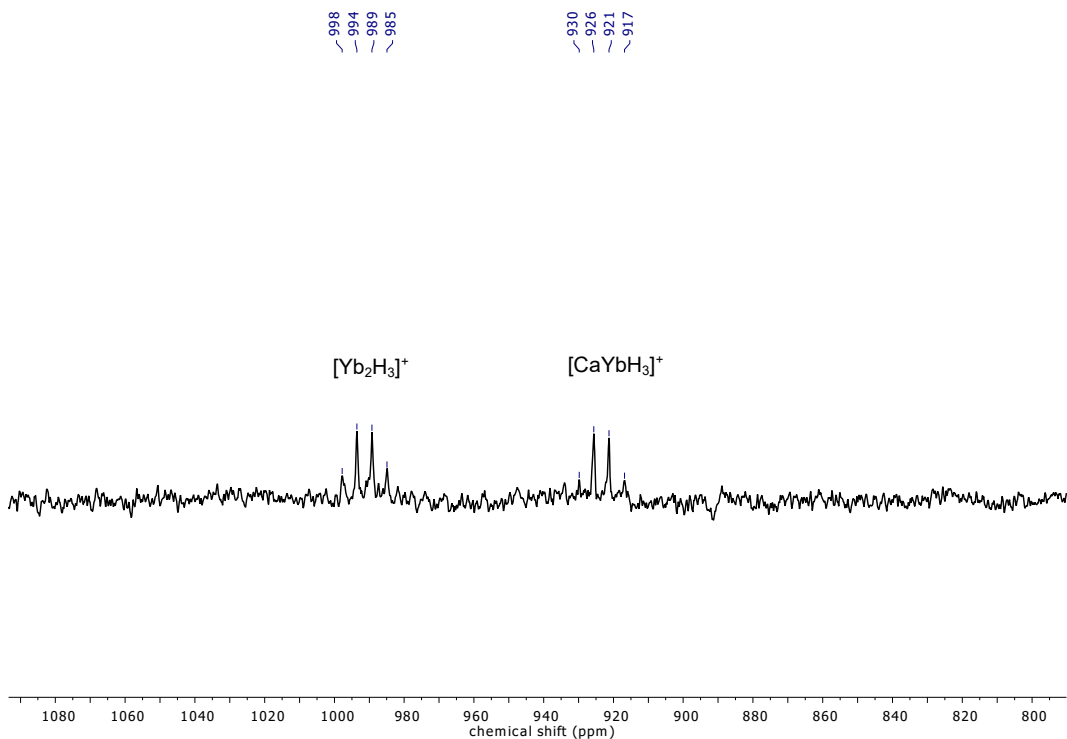


Fig. S51. ^{171}Yb NMR spectrum (71 MHz, $[\text{D}_8]\text{THF}$, 25 °C) of an equimolar mixture of $[(\text{Me}_4\text{TACD})_2\text{Ca}_2(\mu_2\text{-H})_3][\text{B}(\text{C}_6\text{H}_3\text{-3,5-Me}_2)_4]$ and $[(\text{Me}_4\text{TACD})_2\text{Yb}_2(\mu_2\text{-H})_3][\text{B}(\text{C}_6\text{H}_3\text{-3,5-Me}_2)_4]$ (**8**) to give $[(\text{Me}_4\text{TACD})_2\text{CaYb}(\mu_2\text{-H})_3][\text{B}(\text{C}_6\text{H}_3\text{-3,5-Me}_2)_4]$.

4. Catalysis

Hydrogenation of 1-hexene.

In a glass autoclave containing a glass coated stir bar, $[(\text{Me}_4\text{TACD})_2\text{Yb}(\mu_2\text{-H})_2(\text{thf})][\text{B}(\text{C}_6\text{H}_3\text{-3,5-Me}_2)_4]_2\bullet 2.5 \text{ THF}$ (**7**) (9.5 mg, 0.005 mmol) and 1,4-bistrimethylsilylbenzene (11.1 mg, 0.05 mmol) were dissolved in $[\text{D}_8]\text{THF}$ (0.5 mL) and 1-hexene (8.4 mg in 0.1 mL $[\text{D}_8]\text{THF}$, 0.1 mmol) was added. The solution was degassed, pressurized with H_2 (1 bar), stirred for 24 h at 70 °C and analyzed by ^1H NMR spectroscopy.

Hydrosilylation of 1-hexene.

To a solution of $[(\text{Me}_4\text{TACD})_2\text{Yb}(\mu_2\text{-H})_2(\text{thf})][\text{B}(\text{C}_6\text{H}_3\text{-3,5-Me}_2)_4]_2\bullet 2.5 \text{ THF}$ (**7**) (9.5 mg, 0.005 mmol) and 1,4-bistrimethylsilylbenzene (11.1 mg, 0.05 mmol) in $[\text{D}_8]\text{THF}$ (0.5 mL) were added 1-hexene (8.4 mg in 0.1 mL $[\text{D}_8]\text{THF}$, 0.1 mmol) and *n*-hexylSiH₃ (12.2 mg in 0.1 mL $[\text{D}_8]\text{THF}$, 0.105 mmol) or Et₂SiH₂ (9.2 mg in 0.1 mL $[\text{D}_8]\text{THF}$, 0.105 mmol). The mixture was transferred into a J.-Young type NMR tube, heated to 70 °C for 24 h and analyzed by NMR spectroscopy.

$(n\text{-hexyl})_2\text{SiH}_2^{S7}$:

^1H NMR (400 MHz, $[\text{D}_8]\text{THF}$, 25 °C): $\delta = 0.65 - 0.75$ (m, 4 H, H_2SiCH_2), 0.85 – 0.95 (m, 6 H, CH₃), 1.24 – 1.50 (m, 16 H, CH₂), 3.68 (*p*, $^1J = 3.7$ Hz, $H_2\text{Si}$) ppm.

$^{29}\text{Si}\{\text{H}\}$ NMR (79 MHz, $[\text{D}_8]\text{THF}$, 25 °C, dept45): $\delta = -29$ ppm.

GC-MS (EI): *m/z* calc. for $(n\text{-hexyl})_2\text{SiH}^+$ (C₁₂H₂₇Si⁺): 199.19; found: 198.70.

$\text{Et}_2(n\text{-hexyl})\text{SiH}^{S8}$:

^1H NMR (400 MHz, $[\text{D}_8]\text{THF}$, 25 °C): $\delta = 0.56 - 0.71$ (m, 6 H, HSiCH_2), 0.85 – 0.94 (m, 3 H, CH_{3,hexyl}), 0.96 – 1.08 (m, 6 H, CH_{3,ethyl}), 1.25 – 1.43 (m, 8 H, CH₂), 3.69 (m, 1 H, $H\text{Si}$) ppm.

$^{29}\text{Si}\{\text{H}\}$ NMR (79 MHz, $[\text{D}_8]\text{THF}$, 25 °C, dept45): $\delta = -2$ ppm.

GC-MS (EI): *m/z* calc. for Et(*n*-hexyl)SiH⁺ (C₈H₁₉Si⁺): 143.13; found: 143.35.

4.1. Typical NMR spectra of catalytic hydrosilylation

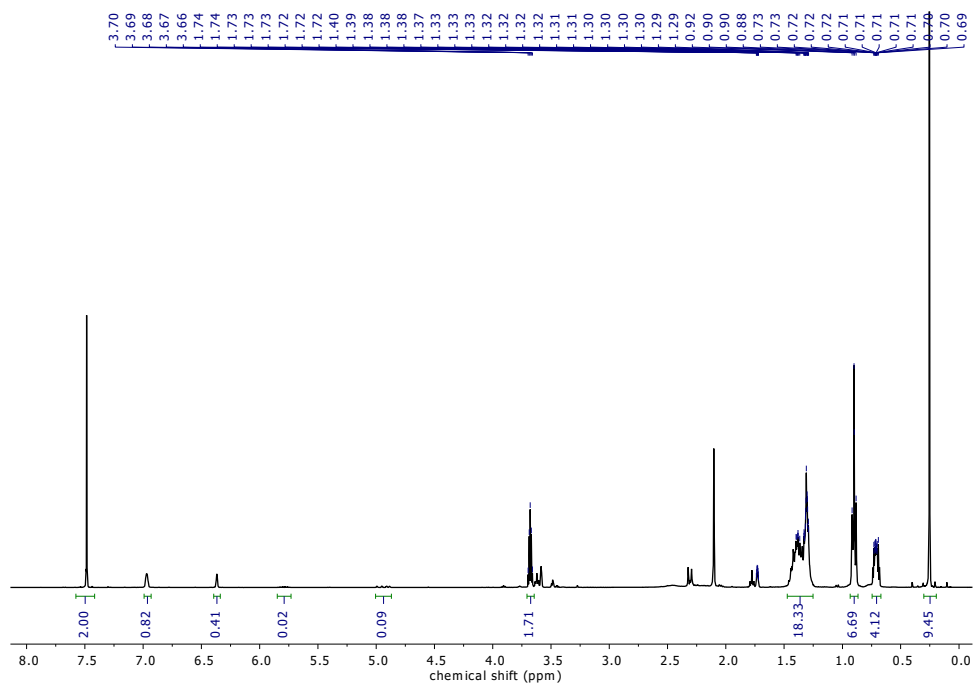


Fig. S52. ¹H NMR spectrum (400 MHz, [D₈]THF, 25 °C) of the hydrosilylation product of *n*-hexene with (*n*-hexyl)SiH₃.

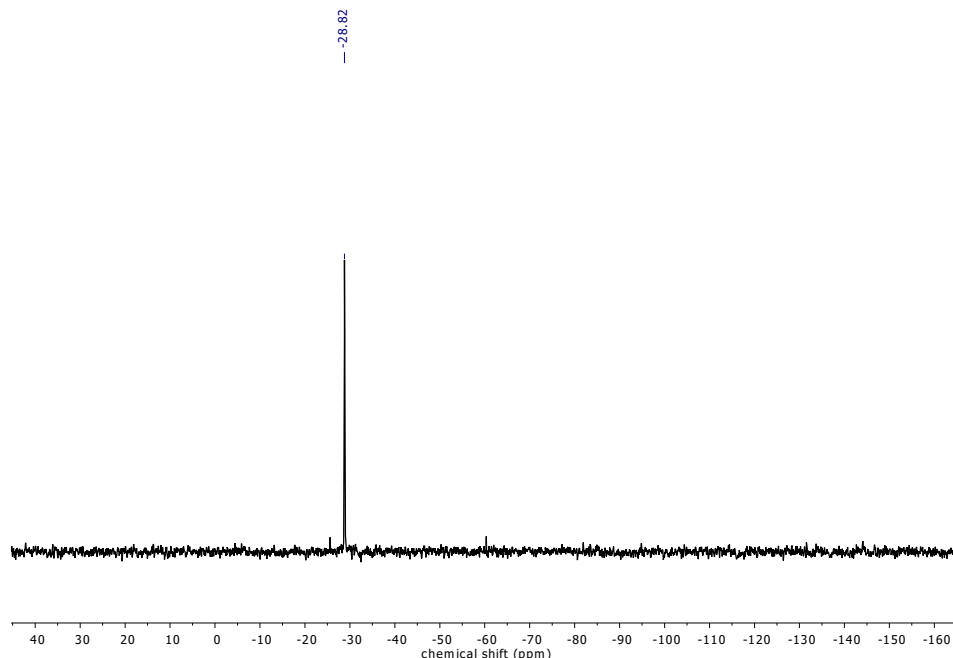


Fig. S53. ²⁹Si{¹H} NMR spectrum (79 MHz, [D₈]THF, 25 °C, dept45) of the hydrosilylation product of *n*-hexene with (*n*-hexyl)SiH₃.

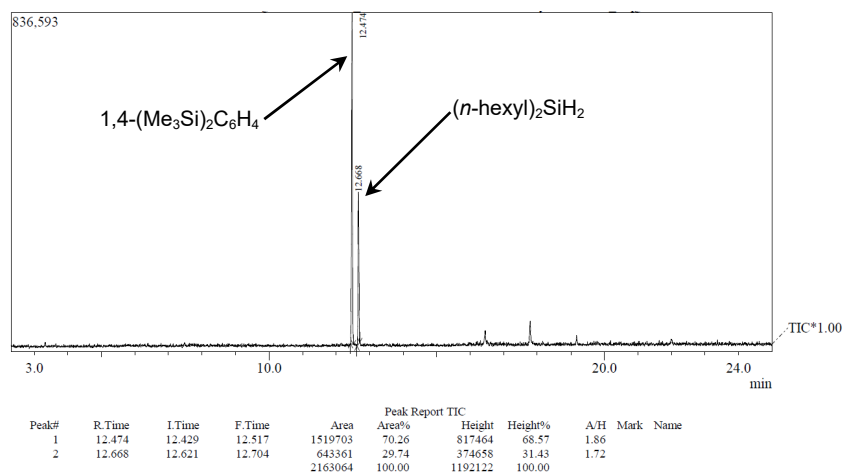


Fig. S54. Gas chromatogram of the reaction mixture of the hydrosilylation of 1-hexene with (n-hexyl)SiH₃.

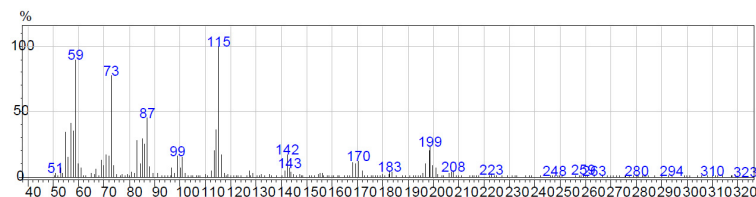


Fig. S55. Mass spectrum of (n-hexyl)₂SiH₂ (peak 2).

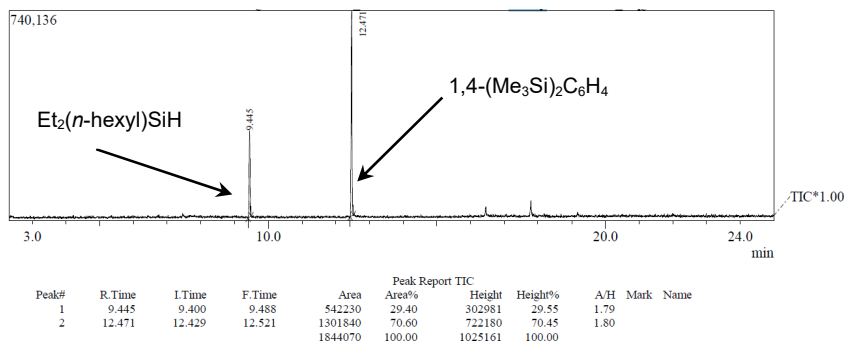


Fig. S56. Gas chromatogram of the reaction mixture of the hydrosilylation of 1-hexene with Et₂SiH₂.

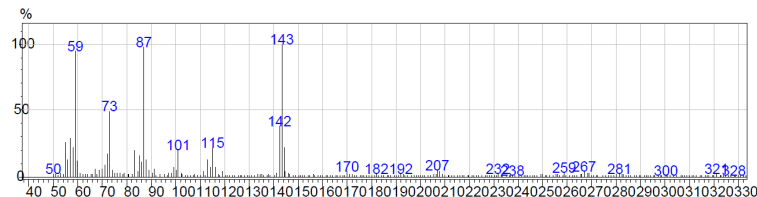


Fig. S57. Mass spectrum of Et₂(n-hexyl)SiH (peak 1).

5. X-Ray Crystallography

X-ray diffraction data of **2**, **6** and **7** were collected at -173°C on a Bruker D8 goniometer with APEX CCD area-detector in ω -scan mode. Mo-K α radiation (multilayer optics, $\lambda = 0.71073\text{\AA}$) from an Incoatec microsource was used. The SMART program package was used for the data collection and unit cell determination; processing of the raw frame data was performed using SAINT;^{S9} absorption corrections were applied with SADABS.^{S10} The structures were solved by direct methods using SHELXS2013.^{S11} Each compound contains co-crystallized THF in the crystal lattice. In **7**, one of the co-crystallized THF molecules is found disordered around a center of symmetry (Wyckoff position $2d$). The refinements were carried out against F^2 with SHELXL-2017/1.^{S11} In the refinement of **2**, the reflections $1\ 0\ 0$, $1\ 1\ 0$, and $-1\ 1\ 1$ were omitted from the refinement because they were most likely affected by the beam stop, as well as $3\ 3\ 0$. The reflections $-1\ 0\ 1$, $0\ -1\ 1$, $1\ 1\ 0$ and $1\ 1\ 1$ in **6** and the reflections $1\ 0\ 0$, $2\ 0\ 0$, $1\ 1\ 0$, $0\ 1\ 1$, $-1\ 1\ 2$ and $2\ 1\ 0$ in **7** were also omitted from the corresponding refinements. The structure of **7** contains a disordered ligand of THF coordinated to the metal center. The disorder could be modelled well with split positions for atoms O1, C25, C26, C27 and C28. All non-hydrogen atoms in **6** and **7** were refined with anisotropic displacement parameters. The hydride atoms H1 and H2 in **7** were located in a Fourier difference map and were refined with isotropic displacement parameters. All remaining hydrogen atoms were included in idealized positions and treated as riding. Repeated attempts to obtain a suitable crystal of the highly sensitive compound **2** only gave a crystal that showed satisfactory diffraction up to a θ value of 20.96° . However, the structure solution unambiguously reveals the molecular connectivity. Due to the low resolution, only the Yb metal atom was refined with anisotropic displacement parameters; the silicon, carbon, oxygen and nitrogen atoms were refined with isotropic displacement parameters. The routine SQUEEZE as implied in the program system PLATON was used in the treatment of **7**.^{S12} Graphical representations were obtained with the program DIAMOND.^{S13}

Table S1. Crystallographic data of compounds **2**, **6** and **7**.

	2	6	7
formula	C ₄₈ H ₅₈ N ₄ Si ₂ Yb, 2(C ₄ H ₈ O)	C ₃₂ H ₃₆ B,C ₁₉ H ₃₅ N ₄ Yb, 3(C ₄ H ₈ O)	2(C ₂₈ H ₆₆ N ₈ OYb ₂), 4(C ₃₂ H ₃₆ B),5(C ₄ H ₈ O)
<i>Mw</i> / g mol ⁻¹	1064.41	1140.27	3840.11
cryst. color, habit	red, rod	red, block	red, rod
crystal size / mm	0.14 × 0.14 × 0.27	0.20 × 0.08 × 0.07	0.14 × 0.14 × 0.18
crystal system	monoclinic	triclinic	monoclinic
space group	<i>P</i> 2 ₁ / <i>c</i>	<i>P</i> 1̄	<i>P</i> 2 ₁ / <i>c</i>
<i>a</i> / Å	15.0291(10)	12.3940(14)	22.3771(9)
<i>b</i> / Å	19.9303(19)	13.0452(16)	12.7674(5)
<i>c</i> / Å	18.7135(17)	19.0172(19)	35.4193(14)
α / °		102.769(5)	
β / °	110.869(5)	92.103(6)	102.0235(7)
γ / °		94.209(5)	
<i>V</i> / Å ³	5237.6(5)	2986.2(6)	9897.2(7)
<i>Z</i>	4	2	2
<i>d</i> _{calc} /Mg·m ⁻³	1.350	1.268	1.289
μ (MoKa)/mm ⁻¹	1.875	1.612	1.930
<i>F</i> (000)	2208	1200	4016
θ range / °	1.55 – 20.96	2.03 – 25.71	1.64 – 26.54
index ranges	-15 ≤ <i>h</i> ≤ 15, -19 ≤ <i>k</i> ≤ 19, -18 ≤ <i>l</i> ≤ 18	-14 ≤ <i>h</i> ≤ 15, -15 ≤ <i>k</i> ≤ 15, -23 ≤ <i>l</i> ≤ 22	-27 ≤ <i>h</i> ≤ 27, -15 ≤ <i>k</i> ≤ 16, -44 ≤ <i>l</i> ≤ 44
refln. (<i>R</i> _{int})	37917 (0.2238)	43760 (0.1157)	119082 (0.0685)
independ. reflns	5518	11108	20477
observed reflns	3395	8550	16685
data/restr./param	5518 / 0 / 273	11108 / 0 / 661	20477 / 18 / 1130
<i>R</i> ₁ , <i>wR</i> 2 [<i>I</i> > 2σ(<i>I</i>)]	0.0770, 0.1842	0.0569, 0.1368	0.0353, 0.0755
<i>R</i> ₁ , <i>wR</i> 2 (all data)	0.1302, 0.2036	0.0865, 0.1515	0.0494, 0.0806
GooF on <i>F</i> ²	1.045	1.004	1.030
largest diff. peak, hole/ e·Å ³	0.937, -1.107	2.052, -3.182	2.296, -0.719
CCDC number	1851362	1851363	1851364

6. Computational Details

Calculations were carried out at the DFT level using the hybrid functional B3PW91^{S14} with the Gaussian 09^{S15} suite of programs. The ytterbium center was treated with a small-core relativistic pseudopotential (RECP) ([Ar] + 3d)^{S16} in combination with its adapted basis set (segmented basis set that includes up to g functions). Polarized all-electron triple-ζ 6-311G(d,p)^{S17} basis sets were used for C, H, O and N. Geometry optimization was carried out without any symmetry restriction. The nature of the extrema (minimum) was verified with analytical frequency calculations. The NBO analysis^{S18} was finally carried out on the optimized geometry.

Geometry optimization of **6** and **7** were carried out at the DFT level without any symmetry constraint on the ytterbium hydride dimer. Bonding analysis was carried out using Molecular

Orbital analysis and NBO. There is no indication of any Yb-Yb interaction in **7**. Geometry optimizations on putative $[(\text{Me}_4\text{TACD})\text{Ca}(\eta^1\text{-CH}_2\text{Ph})(\text{thf})]^+$ and $[(\text{Me}_4\text{TACD})\text{Ca}(\eta^3\text{-CH}_2\text{Ph})]^+$ were carried out on the same level of theory. The enthalpy of THF dissociation is 2.7 kcal/mol, which is in line with the fast removal of coordinated THF under vacuum.

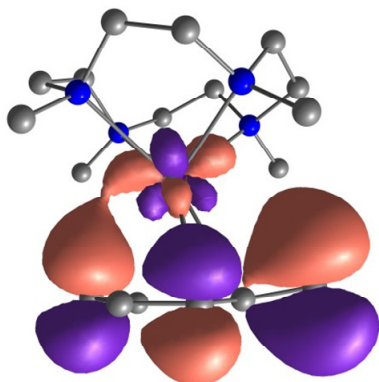


Fig. S58. HOMO of the cation in $[(\text{Me}_4\text{TACD})\text{Yb}(\eta^6\text{-PhCH}_2)][\text{B}(\text{C}_6\text{H}_3\text{-3,5-Me}_2)_4]$ (**6**).

Table S2. Cartesian coordinates of the optimized molecular cation of
 $[(\text{Me}_4\text{TACD})\text{Yb}(\eta^6\text{-PhCH}_2)][\text{B}(\text{C}_6\text{H}_3\text{-3,5-Me}_2)_4]$ (**6**)

Yb	1.929795000	-2.573525000	16.136852000
N	0.570491000	-0.628452000	17.257253000
N	-0.062694000	-1.909868000	14.545485000
N	2.882736000	-1.846853000	13.842842000
N	3.520586000	-0.556634000	16.553964000
C	3.418864000	-4.680133000	16.677753000
C	3.034800000	-4.201660000	18.000718000
C	1.714376000	-4.161798000	18.414209000
C	0.650419000	-4.561205000	17.569553000
C	1.006889000	-5.194822000	16.354702000
C	2.316826000	-5.248383000	15.910681000
C	-0.713410000	-0.512322000	16.532661000
C	1.368652000	0.608261000	17.118974000
C	0.290460000	-0.886638000	18.680908000
C	-0.581243000	-0.608175000	15.016768000
C	0.471329000	-1.791343000	13.170179000
C	-1.144721000	-2.910608000	14.555072000
C	1.837757000	-1.117386000	13.099441000
C	4.048076000	-0.980781000	14.128892000
C	3.340121000	-3.016020000	13.069624000
C	3.802486000	0.044210000	15.231978000
C	2.846343000	0.415176000	17.440371000
C	4.780304000	-1.000560000	17.180938000
C	4.683225000	-4.504751000	16.155417000
H	3.822921000	-3.897615000	18.684762000
H	1.491720000	-3.805746000	19.417825000
H	-0.370929000	-4.586323000	17.932082000
H	0.228934000	-5.649058000	15.744637000

H	2.548269000	-5.749192000	14.974154000
H	-1.220798000	0.434248000	16.781604000
H	-1.364601000	-1.313531000	16.895152000
H	0.966918000	1.401846000	17.769711000
H	1.261897000	0.976757000	16.094933000
H	1.221333000	-0.997626000	19.240923000
H	-0.270751000	-1.817901000	18.781226000
H	-0.291687000	-0.069851000	19.134273000
H	-1.567268000	-0.404411000	14.568618000
H	0.080744000	0.181883000	14.651050000
H	-0.230631000	-1.242510000	12.521684000
H	0.538466000	-2.802291000	12.757253000
H	-1.541563000	-3.034588000	15.564461000
H	-0.754095000	-3.877946000	14.231875000
H	-1.970177000	-2.623049000	13.885945000
H	2.118882000	-1.005627000	12.039639000
H	1.769438000	-0.102158000	13.501257000
H	4.371423000	-0.447468000	13.219922000
H	4.873650000	-1.639038000	14.416060000
H	2.501666000	-3.678272000	12.843411000
H	4.062820000	-3.574173000	13.669459000
H	3.808682000	-2.716074000	12.120037000
H	4.682841000	0.704185000	15.293686000
H	2.963514000	0.691295000	14.958704000
H	3.346616000	1.396540000	17.406953000
H	2.956480000	0.053270000	18.466959000
H	5.243559000	-1.784410000	16.578441000
H	4.568088000	-1.427482000	18.163945000
H	5.487887000	-0.166942000	17.305334000
H	4.961634000	-4.980029000	15.219646000
H	5.497570000	-4.167691000	16.789222000

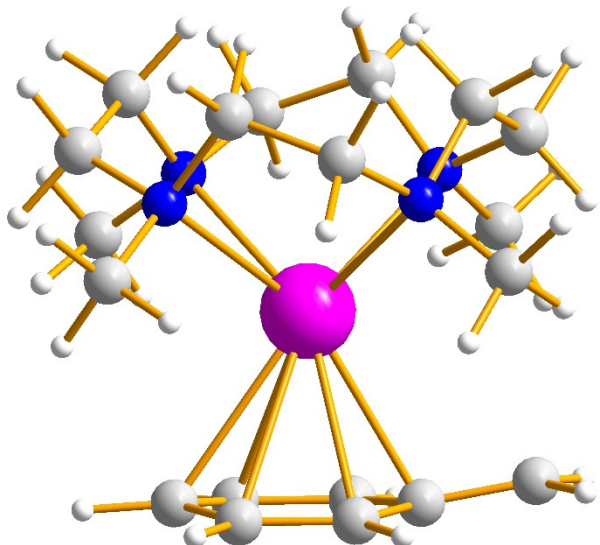


Fig. S59. DIAMOND representation of the optimized molecular cation of **6**.

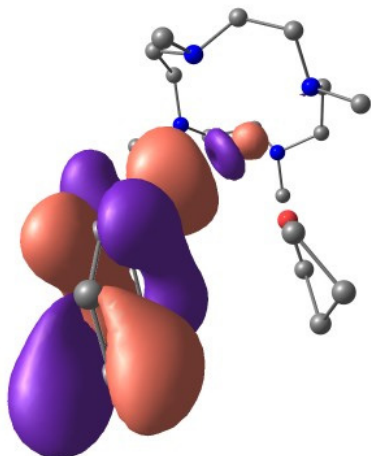


Fig. S60. HOMO of the molecular cation in $[(\text{Me}_4\text{TACD})\text{Ca}(\eta^1\text{-PhCH}_2)(\text{thf})][\text{B}(\text{C}_6\text{H}_3\text{-3,5-Me}_2)_4]$.

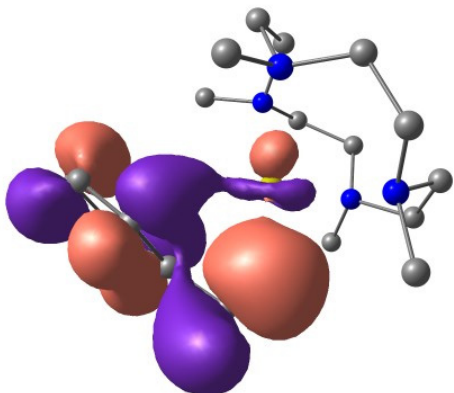


Fig. S61. HOMO of the molecular cation in $[(\text{Me}_4\text{TACD})\text{Ca}(\eta^3\text{-PhCH}_2)][\text{B}(\text{C}_6\text{H}_3\text{-3,5-Me}_2)_4]$.

Table S3. Cartesian coordinates of the optimized molecular cation of $[(\text{Me}_4\text{TACD})\text{Ca}(\eta^1\text{-PhCH}_2)(\text{thf})][\text{B}(\text{C}_6\text{H}_3\text{-3,5-Me}_2)_4]$.

Ca	1.631577000	-2.436278000	16.105024000
O	3.286752000	-2.441975000	17.932421000
N	0.050542000	-0.635630000	17.217304000
N	0.055949000	-1.289172000	14.269386000
N	0.172088000	-4.273652000	15.036072000
N	0.065409000	-3.645238000	17.980873000
C	-1.049246000	-0.298083000	16.289914000
C	-0.993399000	-2.663970000	18.287547000
C	-0.484720000	-1.235830000	18.457873000
C	-0.592361000	-0.099635000	14.851642000
C	-0.942429000	-2.315819000	13.910500000
C	-0.350676000	-3.714769000	13.770178000
C	-0.929877000	-4.692744000	15.922274000
C	-0.508012000	-4.865284000	17.376770000
C	0.757834000	-4.012439000	19.225963000
C	3.406773000	-2.438673000	14.346874000
C	1.042643000	-5.422636000	14.729007000
C	0.789394000	-0.877102000	13.059100000

C	0.798691000	0.586624000	17.555731000
C	4.745935000	-2.905301000	14.738537000
C	3.924096000	-1.266495000	18.494622000
C	5.293125000	-1.713567000	18.997911000
C	5.076385000	-3.202552000	19.271965000
C	4.167754000	-3.589407000	18.119527000
C	5.730740000	-2.017920000	15.231679000
C	6.981752000	-2.461283000	15.653403000
C	7.312086000	-3.817762000	15.609616000
C	6.366748000	-4.714756000	15.109397000
C	5.117647000	-4.268671000	14.683986000
H	-1.114140000	-4.382030000	13.337707000
H	0.480043000	-3.690032000	13.059164000
H	-1.369931000	-5.641257000	15.572920000
H	-1.729476000	-3.950013000	15.856929000
H	1.443069000	-5.858778000	15.647689000
H	1.886843000	-5.089120000	14.121896000
H	0.499764000	-6.211447000	14.186062000
H	-1.440592000	-2.053363000	12.962631000
H	-1.730977000	-2.321611000	14.668635000
H	-1.458611000	0.220261000	14.248654000
H	0.128194000	0.722663000	14.802060000
H	1.293699000	-1.730176000	12.605660000
H	1.560528000	-0.150064000	13.320415000
H	0.113157000	-0.425607000	12.316413000
H	-1.567492000	0.615165000	16.625535000
H	-1.794566000	-1.096372000	16.329019000
H	-1.302104000	-0.618754000	18.866427000
H	0.315066000	-1.218025000	19.204764000
H	1.229761000	1.035147000	16.657246000
H	1.616486000	0.346927000	18.238484000
H	0.157191000	1.339818000	18.038728000
H	-1.526415000	-2.951242000	19.209145000
H	-1.741451000	-2.696323000	17.491232000
H	-1.376031000	-5.225574000	17.953774000
H	0.249352000	-5.651961000	17.448883000
H	1.257876000	-3.144503000	19.657844000
H	1.521864000	-4.763799000	19.017301000
H	0.061853000	-4.428921000	19.971069000
H	3.022056000	-3.039295000	13.507018000
H	3.462728000	-1.399772000	13.989606000
H	3.537669000	-4.458480000	18.327675000
H	6.007389000	-3.773561000	19.264022000
H	6.039766000	-1.589789000	18.209415000
H	3.992583000	-0.494856000	17.720626000
H	4.729890000	-3.755564000	17.196329000
H	4.580069000	-3.359314000	20.236388000
H	5.611781000	-1.150028000	19.878133000
H	3.292277000	-0.900806000	19.314499000
H	5.510285000	-0.950987000	15.252079000
H	7.716383000	-1.736915000	15.999586000
H	8.291064000	-4.162184000	15.928633000
H	6.609658000	-5.772429000	15.035445000
H	4.412509000	-4.990030000	14.272615000

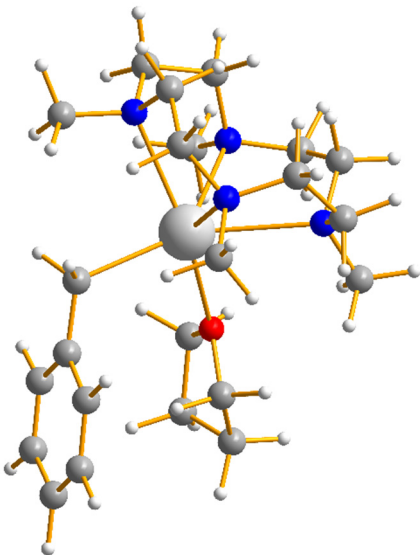


Fig. S62. DIAMOND representation of the optimized molecular cation of
[(Me₄TACD)Ca(η^1 -PhCH₂)(thf)][B(C₆H₃-3,5-Me₂)₄].

Table S4. Cartesian coordinates of the optimized molecular cation of
[(Me₄TACD)Ca(η^3 -PhCH₂)][B(C₆H₃-3,5-Me₂)₄].

Ca	2.380358000	0.536076000	18.556061000
N	4.472088000	-0.246090000	19.756888000
N	2.083314000	1.174106000	21.011443000
N	1.981898000	3.080399000	18.666436000
N	4.390118000	1.655019000	17.420267000
C	1.990073000	-1.689876000	16.033528000
C	1.090130000	-1.111325000	16.980780000
C	0.419270000	0.071083000	16.534533000
C	0.566226000	0.565673000	15.233143000
C	1.424249000	-0.049134000	14.326370000
C	2.130440000	-1.185658000	14.748234000
C	1.015939000	-1.539065000	18.351424000
C	4.776668000	-1.634598000	19.365982000
C	4.183724000	-0.194273000	21.206132000
C	3.417823000	1.054694000	21.635264000
C	1.129568000	0.260678000	21.667774000
C	1.582936000	2.562390000	21.091683000
C	2.219983000	3.495284000	20.065273000
C	0.622362000	3.463585000	18.246435000
C	2.966225000	3.702462000	17.753242000
C	4.357210000	3.076983000	17.818969000
C	4.316446000	1.535381000	15.952324000
C	5.584735000	0.654027000	19.395119000
C	5.621589000	0.997548000	17.907961000
H	5.111946000	-0.259546000	21.796244000
H	3.599437000	-1.085054000	21.453861000
H	6.553218000	0.209434000	19.676199000
H	5.492247000	1.571406000	19.984573000
H	4.989053000	-1.693525000	18.295965000

H	3.909018000	-2.267814000	19.565310000
H	5.646170000	-2.030698000	19.911688000
H	3.330157000	1.049308000	22.733903000
H	3.998172000	1.947723000	21.383795000
H	1.736576000	2.984284000	22.097908000
H	0.499591000	2.531556000	20.940040000
H	1.457602000	-0.774739000	21.561061000
H	0.151285000	0.338202000	21.187558000
H	1.016333000	0.492094000	22.737772000
H	1.842931000	4.516734000	20.235142000
H	3.299836000	3.541223000	20.232753000
H	3.057210000	4.782636000	17.952327000
H	2.571049000	3.611373000	16.736984000
H	-0.123700000	3.012900000	18.905264000
H	0.435254000	3.101194000	17.233040000
H	0.481285000	4.554870000	18.266083000
H	5.032264000	3.670062000	17.180665000
H	4.754141000	3.161550000	18.835122000
H	6.508516000	1.620811000	17.709894000
H	5.757255000	0.083630000	17.322078000
H	3.392279000	1.978062000	15.575980000
H	4.298088000	0.481304000	15.667705000
H	5.169864000	2.026893000	15.460881000
H	1.384175000	-2.545397000	18.553669000
H	0.056718000	-1.347538000	18.841458000
H	-0.341451000	0.510987000	17.183192000
H	-0.024526000	1.425229000	14.922439000
H	1.523999000	0.322138000	13.311630000
H	2.786805000	-1.699100000	14.048947000
H	2.518154000	-2.599798000	16.312100000

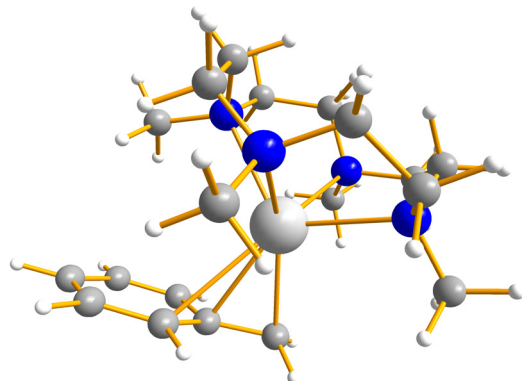


Fig. S63. DIAMOND representation of the optimized molecular cation of $[(\text{Me}_4\text{TACD})\text{Ca}(\eta^3\text{-PhCH}_2)][\text{B}(\text{C}_6\text{H}_3\text{-3,5-Me}_2)_4]$.

Table S4. Cartesian coordinates of the optimized molecular dication of $[(\text{Me}_4\text{TACD})_2\text{Yb}_2\text{H}_2(\text{thf})][\text{B}(\text{C}_6\text{H}_3-3,5-\text{Me}_2)_2]_2 \bullet 2.5\text{THF}$ (**7**).

Yb	-0.021385	2.935662	24.186706
Yb	-0.418759	2.372866	27.906530
N	-2.031591	3.988216	22.646477
N	-0.349914	0.058019	29.263713
N	-2.726241	1.956118	29.243503
N	-0.795758	4.338566	29.679807
N	1.571453	2.438663	29.718889
N	0.854999	3.761091	21.619479
N	0.965979	0.897119	22.694846
N	-1.930326	1.100720	23.667213
O	1.798623	4.639549	24.913620
C	3.057712	6.607924	25.307425
C	1.644462	6.055742	25.179262
C	3.171543	4.243312	25.154525
C	3.816117	5.411889	25.887860
C	-2.795595	4.934375	23.476989
C	-0.450740	-1.075306	28.329678
C	-3.893451	2.246076	28.393839
C	-0.537901	5.634582	29.032068
C	2.876803	2.313623	29.050486
C	1.636891	5.006366	21.620412
C	2.254559	0.505727	23.290253
C	-2.217745	0.361800	24.900808
C	-2.717203	2.870794	30.404948
C	-2.216329	4.277085	30.087429
C	-2.780011	0.546030	29.685306
C	-1.458895	0.018768	30.238398
C	0.103460	4.154155	30.836587
C	1.515242	3.722693	30.449379
C	1.367287	1.299426	30.638689
C	0.962210	0.002022	29.944325
C	1.708725	2.680761	21.083712
C	1.153358	1.275235	21.281378
C	-0.347525	3.944006	20.782884
C	-1.468730	4.703067	21.482895
C	0.017209	-0.228542	22.814195
C	-1.443302	0.173858	22.628066
C	-3.151407	1.814929	23.244154
C	-2.913508	2.892930	22.194819
H	0.776073	1.637482	26.048057
H	-1.299307	3.552193	26.107430
H	-3.025972	-0.374810	24.763452
H	-1.322930	-0.159004	25.247605
H	-2.517662	1.074924	25.674795
H	-0.315957	-2.041626	28.839150
H	-1.431630	-1.085692	27.847750
H	0.309575	-0.978646	27.549453
H	-0.784531	6.480839	29.691285
H	0.517591	5.718373	28.759916
H	-1.129498	5.713305	28.115666
H	3.710150	2.331952	29.769413

H	2.929614	1.383055	28.481600
H	3.012251	3.138046	28.345247
H	2.002007	5.261040	20.613092
H	1.029762	5.841107	21.977251
H	2.495971	4.907516	22.286805
H	2.668131	-0.398638	22.817565
H	2.987026	1.308654	23.171613
H	2.121551	0.329613	24.361103
H	-3.628473	5.389101	22.918246
H	-3.189946	4.431508	24.361632
H	-2.138963	5.735422	23.828305
H	-4.840347	2.118783	28.940473
H	-3.845647	3.267851	28.011759
H	-3.903733	1.572173	27.533290
H	1.830993	0.565541	20.779002
H	0.194189	1.182133	20.765310
H	2.684751	2.763075	21.573707
H	1.898361	2.827964	20.006965
H	-0.093398	4.474445	19.850213
H	-0.711081	2.960094	20.476473
H	-1.097941	5.670669	21.835614
H	-2.254412	4.931958	20.744193
H	-3.892710	3.292781	21.884006
H	-2.479690	2.443560	21.297852
H	-3.583940	2.271091	24.140181
H	-3.906079	1.110314	22.856458
H	-2.059085	-0.740400	22.602158
H	-1.572559	0.648311	21.651870
H	0.156892	-0.667661	23.806621
H	0.258071	-1.023985	22.089696
H	3.155426	3.306064	25.718173
H	3.662144	4.065059	24.188427
H	4.894743	5.462678	25.722718
H	3.644956	5.336609	26.967797
H	3.459551	6.874860	24.324367
H	3.101665	7.497918	25.939455
H	1.073975	6.503501	24.360389
H	1.071976	6.173460	26.106958
H	-3.562193	0.399556	30.447853
H	-3.084214	-0.056060	28.822938
H	-1.620397	-1.008898	30.602065
H	-1.168677	0.602421	31.115872
H	0.980846	-0.810321	30.688955
H	1.710025	-0.261543	29.189756
H	2.284819	1.107014	31.218147
H	0.605529	1.578750	31.371426
H	2.133868	3.687701	31.360959
H	1.969280	4.484827	29.807543
H	0.173371	5.081867	31.427377
H	-0.338092	3.409938	31.504458
H	-2.398516	4.918097	30.965229
H	-2.807557	4.703533	29.271219
H	-3.729695	2.954454	30.832110
H	-2.098692	2.428474	31.190730

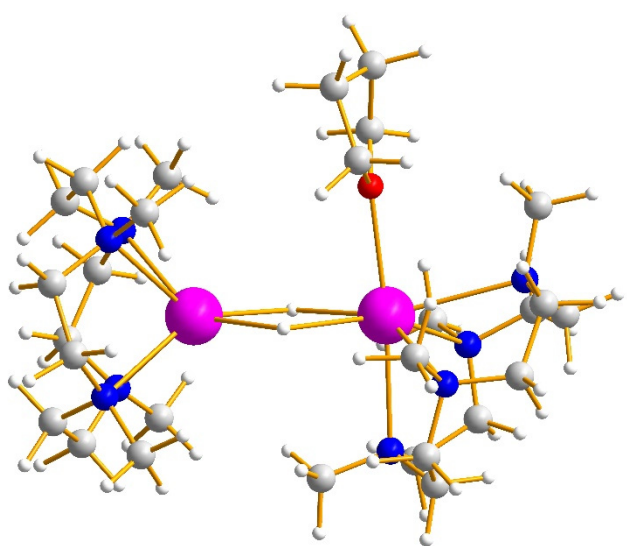


Fig. S64. DIAMOND representation of the optimized molecular dication of **7**.

7. References

- S1 P. L. Watson, T. H. Tulip, I. Williams, *Organometallics* **1990**, *9*, 1999-2009.
- S2 V. Leich, K. Lamberts, T. P. Spaniol, J. Okuda, *Dalton Trans* **2014**, *43*, 14315-14321.
- S3 K. Izod, D. G. Rayner, S. M. El-Hamruni, R. W. Harrington, U. Baisch, *Angew. Chem. Int. Ed.* **2014**, *53*, 3636-3640.
- S4 P. Girard, J. L. Namy, H. B. Kagan, *J. Am. Chem. Soc.* **1980**, *102*, 2693-2698.
- S5 J. H. Coates, D. A. Hadi, S. F. Lincoln, *Aust. J. Chem.* **1982**, *35*, 903.
- S6 D. Vasu, H. Yorimitsu, A. Osuka, *Angew. Chem. Int. Ed.* **2015**, *54*, 7162-7166.
- S7 Y. Shi, J. Li, C. Cui, *Dalton Trans* **2017**, *46*, 10957-10962.
- S8 X. Jia, Z. Huang, *Nat Chem* **2016**, *8*, 157-161.
- S9 Bruker, SAINT+ (Version 7.68), Bruker AXS Inc., Madison, Wisconsin, USA, **2009**.
- S10 Bruker, SADABS (V 2004/1), Bruker AXS Inc., Madison, Wisconsin, USA, **2004**.
- S11 G. M. Sheldrick, *Acta Crystallogr A* **2008**, *64*, 112-122.
- S12 A. L. Spek, *Acta Crystallogr. D* **2009**, *D65*, 148-155.
- S13 H. Putz, K. Brandenburg, DIAMOND Crystal and Molecular Visualization, Version 4, Crystal Impact GbR, Bonn, 2018.
- S14 a) J. P. Perdew, Y. Wang, *Phys. Rev. B* **1992**, *45*, 13244-13249; b) A. D. Becke, *J. Chem. Phys.* **1993**, *98*, 5648-5652.
- S15 M. J. Frisch, G. W. Trucks, H. B. Schlegel, G. E. Scuseria, M. A. Robb, J. R. Cheeseman, V. G. Zakrzewski, J. A. Montgomery, R. E. Stratman, J. C. Burant, S. Dapprich, J. M. Millam, A. D. Daniels, K. N. Kudin, M. C. Strain, O. Farkas, J. Tomasi, V. Barone, M. Cossi, R. Cammi, B. Mennucci, C. Pomelli, C. Adamo, S. Clifford, J. Ochterski, G. A. Petersson, P. Y. Ayala, Q. Cui, K. Morokuma, D. K. Malick, A. D. Rabuck, K. Raghavachari, J. B. Foresman, J. Cioslowski, J. V. Ortiz, A. G. Baboul, B. B. Stefanov, G. Liu, A. Liashenko, P. Piskorz, I. Komaromi, R. Gomperts, R. Martin, D. J. Fox, T. Keith, M. A. AllLaham, C. Y. Peng, A. Nanayakkara, C. Gonzalez, M. Challacombe, P. M. W. Gill, B. Jonhson, W. Chen, M. W. J. Wong, L. Andres, M. Head-Gordon, E. S. Replogle, J. A. Pople, Gaussian 03, Revision E.01, Gaussian, Inc., Wallingford CT, 2004.
- S16 M. Dolg, H. Stoll, H. Preuss, *J. Chem. Phys.* **1989**, *90*, 1730-1734.
- S17 J.-P. Blaudeau, M. P. McGrath, L. A. Curtiss, L. Radom, *J. Chem. Phys.* **1997**, *107*, 5016-5021.
- S18 A. E. Reed, L. A. Curtiss, F. Weinhold, *Chem. Rev.* **1988**, *88*, 899-926.